Table 1
Analytes used for Ratio and deconvolution studies

Analyte	Molar mass (g/mol)	Concentration in PBS buffer (ppm)
Sodium azide[a]	65	2.15
2-Hydroxypyridine[a]	95.1	10.92
Sodium pyruvate[a]	110	2.96
Benzoic acid[b]	122.4	2.38
Phenylalanine[a]	165.2	2.54
Tryptophan[a]	204.2	2.92
Peptide 451, ggyr[a]	451.5	0.94
Peptide 848, WAGGDASGE[a]	848.8	0.83
Peptide 1009, APRLRFYS[a]	1009.2	1.03
Cytochrome *C*[a]	12327	1.1
Myoglobin[a]	16700	0.87
Carbonic anhydrase[a]	29000	0.64
Ovalbumin[a]	43000	0.93
Bovine serum albumin[a]	68000	1.13

[a] Sigma–Aldrich, St. Louis, MO.
[b] Eastman Kodak, Rochester, NY.

FMD30971, Ocean Optics, Dunedin, FL) that was then connected to a dual-channel UV–vis absorbance detector (SD-2000, Ocean Optics, Dunedin, FL) for the absorbance measurements.

The H-Sensor glass-chip was etched in glass using methods previously described [7]. The branches of the H-shaped flow channel are 1 cm long and 250 μm wide. The central H channel is 2 cm long and 500 μm wide. The entire chip was etched to a depth of 200 μm. Holes were bored at the sample and receiving stream inlets and outlets using 0.75 mm diamond tipped drill bits (C.R. Laurence Co., Los Angeles, CA). Nanoport assemblies (N-126S, Upchurch Scientific) were used to connect the H-Sensor micro-fluidic chip to PEEK tubing. For all experiments, both the receiving and sample stream pumps were filled with 10 mM pH 7.4 phosphate buffer solution. All samples were dissolved in the same buffer solution. Each stream had a flow of 2 μL/min, for a total flow through the central channel of the H-Sensor of 4 μL/min. The samples analyzed are shown in Table 1. All samples and buffer chemicals were purchased from either Sigma–Aldrich (St. Louis, MO) or Eastman Kodak (Rochester, NY); see Table 1 for details. Five solution mixtures of benzoic acid and peptide 848 (WAGGSASGE) were also prepared for deconvolution studies. Each sample contained a total injected concentration of 1000 ppm. Two pure samples as well as three mixtures were prepared. The three mixtures had 3:1, 1:1, and 1:3 mass/mass ratios of peptide 848:benzoic acid.

4. Results and discussion

We began by performing proof-of-principle experiments with the absorbance-based H-Sensor coupled to FIA. These early experiments were aimed at obtaining experimental Ratios (Eq. (1)) and comparing them to the theoretical Ratios obtained via Eq. (5). Fig. 3A shows the multi-wavelength sample stream data for benzoic acid. The receiving stream data is not shown for brevity. Initially, for benzoic acid, experimental Ratios were calculated using only the absorbance at 280 nm. Fig. 3B presents the 280 nm data for both the sample and receiving streams for the same benzoic acid analysis. The Ratio for benzoic acid (0.45) was calculated by dividing the area under the receiving stream signal (shown in Fig. 3B) by the area of the sample stream signal (also in Fig. 3B).

In this manner, Ratio values were experimentally determined for all of the analytes in Table 1. For many analytes, it is more informative to relate to molar mass than to diffusion coefficient, since often the diffusion coefficient information is not readily available (as was the case for many of the analytes in this report). Fig. 4 shows the Ratio values for all analytes tested versus each analyte's molar mass. The solid curve in Fig. 4 is the theoretical relationship between the Ratio and molar mass as estimated by Eqs. (5) and (6). The experimentally obtained Ratio values show an adequate agreement with theoretically calculated curve. It is important to note that the curve has been calculated from a general expression (Eq. (6)). The proximity of any one data point to the curve is not as important as the correlation between the experimental data and the theoretical curve.

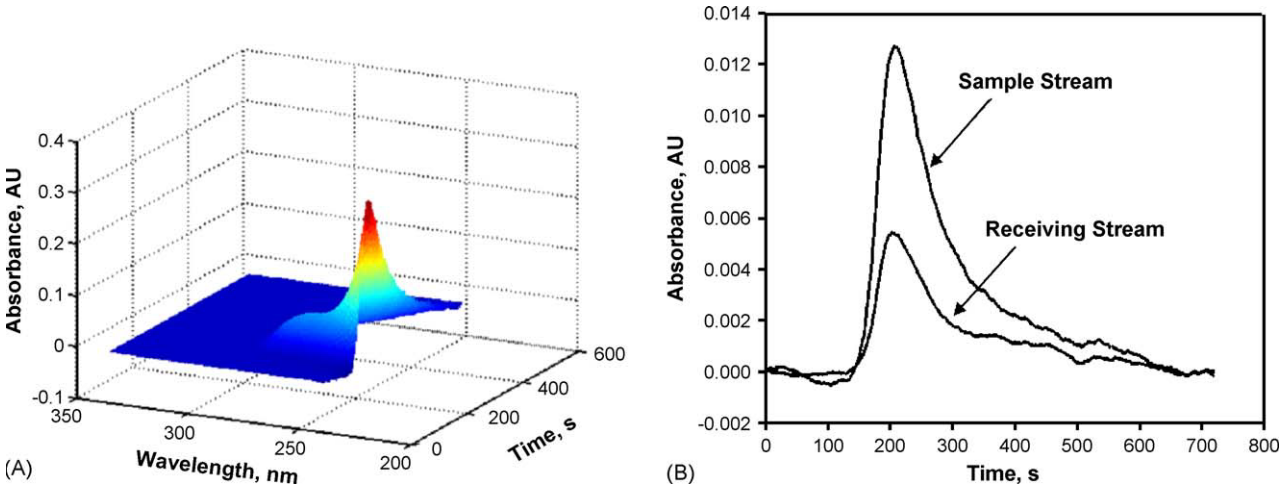

Fig. 3. (A) The sample stream data collected for a single injection of benzoic acid. Note that a similar, yet with a less intense signal, data file is collected for the receiving stream. Each injection results in two data files. (B) Data initially collected as in (A) for benzoic acid with only the absorbance at 280 nm plotted. Both the sample and receiving stream data are shown. The experimental Ratio for benzoic acid is 0.45.

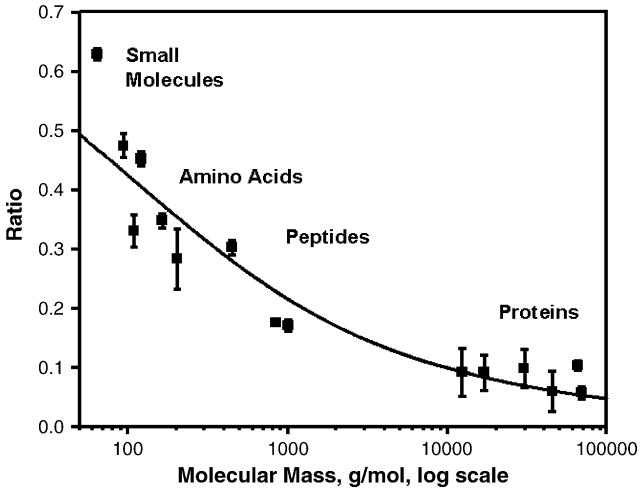

Fig. 4. Comparison between several experimental Ratios (Eq. (1)) plotted along with the theoretical Ratio curve (Eqs. (5) and (6)). The experimental Ratio values plotted as a function of molar mass. The theoretical conversion between diffusion coefficient and molar mass was performed using Eq. (6).

The correlation between the experimental and theoretical Ratio values was reassuring as we began investigating the analytical utility of the multi-wavelength features of the H-Sensor. Thus, our next step was to investigate the deconvolution of individual analyte signals from mixtures using the multi-wavelength information provided by this absorbance-based H-Sensor. A series of binary mixtures were created to test the applicability of a classic least squares (CLS) deconvolution of H-Sensor data. Five solutions of benzoic acid and peptide 848 (mixture details given in the Section 3) were prepared and injected into the H-Sensor. Fig. 5A presents the sample stream signal for a mixture of 250 ppm benzoic acid and 750 ppm peptide 848. Note that Fig. 5A is only one-half of the data acquired from a single analyte injection. There is also a unique signal detected for the receiving stream. For ease of analysis, the absorbance at each wavelength was summed along the time axis, thus removing the time dependence at this juncture, leaving two (both receiving and sample stream) two-dimensional data sets.

With the data reduced to absorbance versus wavelength, the classical least squares method was used to find the contribution of each analyte in the mixtures for both the sample and receiving streams, and thus, be able to determine the Ratio values of each deconvoluted analyte. The CLS method assumes that the mixture spectrum was due to a linear combination of the pure components of the mixture. Both the mixture and the pure component sample stream spectra are shown in Fig. 5B. Each pure spectrum is then multiplied by a factor and summed with the other pure spectrum. This process is repeated until the summed pure spectra match, as closely as possible, the mixture spectrum. The concentration of each analyte in the mixture is calculated by multiplying the concentration of the pure spectrum by the same factor that yielded the best-matched spectrum (minimizing the error of the CLS fit). Lastly, Fig. 5B also shows a plot of the difference (i.e., the minimized error of the fit) between the predicted mixture spectrum as compared to the experimentally measured mixture spectrum. The intensity of the difference plot is less than one order of magnitude of the original spectra. This suggests a reasonable CLS fit, albeit with some run-to-run variation from the individual standards and the mixture.

We now turn our attention to investigate the utility of the CLS deconvolution of the receiving and sample stream signals for several mixtures of benzoic acid and peptide 848, in order to provide consistent Ratio values. The theory above assumes that diffusion, and therefore the Ratio value, is independent of analyte concentration. CLS deconvolution provides a receiving and sample stream concentration for each analyte in the mixture. If the assumption is correct, the Ratio value for each analyte should be constant across all mixtures, suitably near infinite dilution conditions, which is often the case for many analyses. Recall

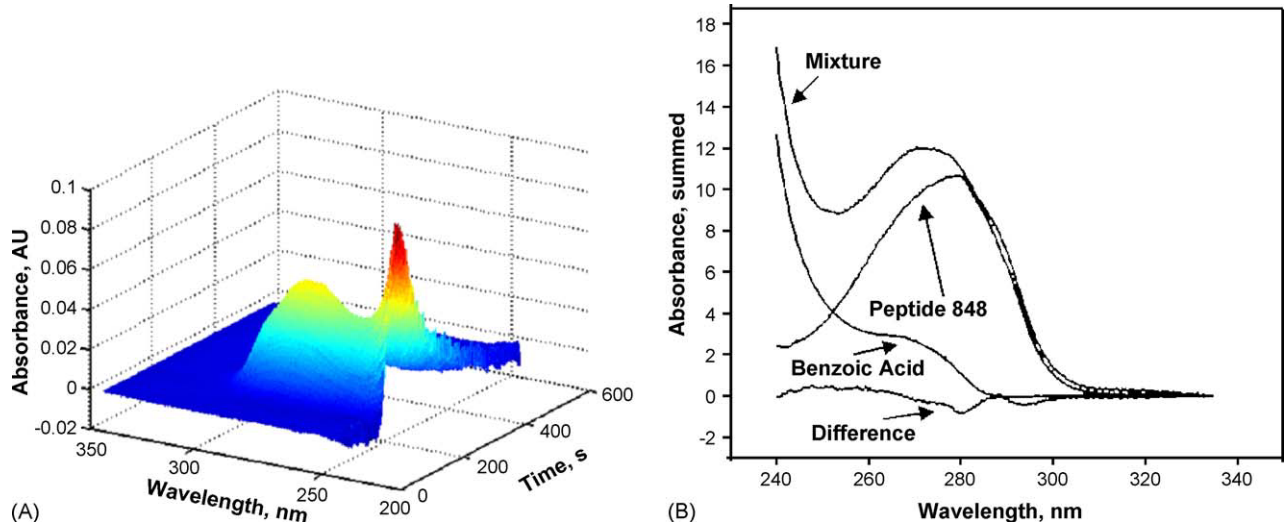

Fig. 5. (A) Sample stream signal for a mixture of 250 ppm benzoic acid and 750 ppm peptide 848. Five mixtures were created and analyzed via CLS. (B) Pure and mixture sample stream spectra of benzoic acid and peptide 848 used for CLS deconvolution. The absorbance values were summed across all time points to yield the two-dimensional representation. Also shown is the difference plot. The difference plot was generated by subtracting the summed deconvolved spectra from the mixture spectrum. This mixture data was from the 1:3 mass:mass mixture of benzoic acid and peptide 848.

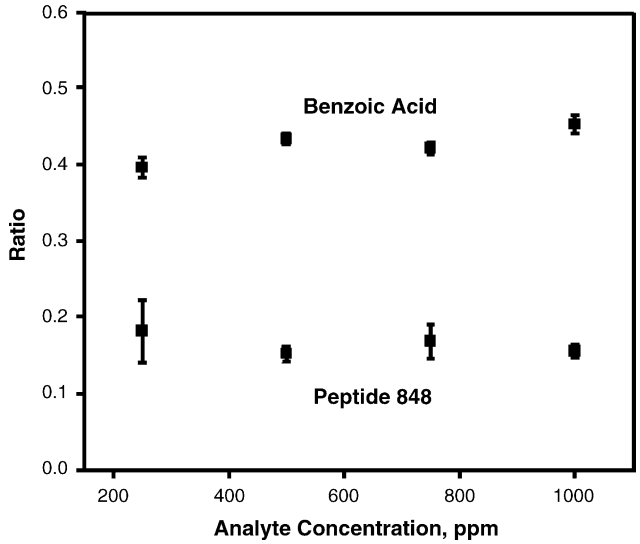

Fig. 6. The Ratio values calculated from the CLS fit. The Ratios for benzoic acid and peptide 848 remain relatively independent of concentration.

from the Section 3, two pure samples as well as three mixtures were prepared, at 3:1, 1:1, and 1:3 mass/mass ratios of peptide 848:benzoic acid. For example, the 1:3 mixture was 750 ppm benzoic acid to 250 ppm peptide 848. After CLS deconvolution, a Ratio value for each analyte in the mixture can be easily found by dividing the calculated receiving stream concentration by the calculated sample stream concentration. Fig. 6 shows the Ratio values for both benzoic acid and peptide 848 calculated in this manner. The Ratio values are relatively constant, regardless of the concentration of each analyte in the mixture. This fact supports the assumption made above that we are operating sufficiently within the infinite dilution regime, where the diffusion of an analyte is independent of analyte concentration. Working within the infinite dilution range also insures that the sample stream viscosity will not increase significantly due to the analyte presence. If this were to occur the merge point on-chip would shift, artificially increasing the receiving stream signal intensity. For more information concerning viscosity-induced flow changes, readers are referred to two previous publications [7,9]. In this regard, a more thorough quantitative study specifically for the H-Sensor is warranted after the success of this proof-of-principle study.

The final portion of the current study involved simulating chromatographic data using actual experimental H-Sensor data to determine the applicability of the generalized rank annihilation method deconvolution of H-Sensor data [11,12]. Overlapped HPLC peaks were simulated by offsetting the pure peptide 848 FIA signal by varying lengths of time from the pure benzoic acid FIA signal. The length of the offset was such that the chromatographic resolution between the peaks ranged from 0 to 1, equating to a retention time difference of 0–300 s. The time axis of the peptide 848 data was changed by adding the desired offset (in seconds) to each time point. The two data sets were then added together to create the simulated chromatographic data set. In this manner, several simulated chromatographic separations of benzoic acid and peptide 848 mixtures were generated, each with a different resolution. The simulated separations are chemometrically defined as second order for either the receiving or sample stream signals when considered separately (simulated HPLC/multi-wavelength absorbance). However, the separations are third order when the receiving and sample stream data are considered jointly. The three axes of interest are simulated separation time, spectral selectivity, and analyte diffusion coefficient selectivity.

To successfully deconvolute the individual analytes of a co-eluting mixture, GRAM requires knowledge of how many analytes are in the mixture, as well as two second-order data files (a ‘standard’ and an ‘unknown’) of the co-eluting mixture. Arbitrarily, the sample stream was used as the standard, and the receiving stream was used as the unknown. No alignment was performed on the two data sets, as great care was taken to experimentally ensure equal flow rates (i.e., residence times from the chip to the two detectors) in both streams to preserve the original analyte peak profile. In principle, one could also image the absorbance on-chip in order to obtain the diffusion coefficient information, thus circumventing the issue of requiring equal flow paths following the chip to both detectors. Application of GRAM for this data returns the individual pure analyte chromatographic concentration profiles in time, their absorbance spectra, and the Ratio of each analyte between the standard and unknown chromatograms (thus diffusion coefficient information as well). Generally, the success of applying GRAM to chromatographic data is typically determined by the amount of retention time shifting between the two separately injected chromatograms. The difficulty of averting or correcting the retention time shifting problems before performing GRAM has been the subject of previous study [15,16]. However, in principle, retention time reproducibility is averted with the H-Sensor, as a chromatographic detector, since all of the necessary data for a successful GRAM deconvolution is provided with one injection. This is a result of the H-Sensor producing both a sample stream and a receiving stream chromatogram upon each injection. The two chromatograms can serve as the ‘standard’ and ‘unknown’ chromatogram as long as the chromatographically overlapped components have sufficiently unique diffusion coefficients. Unique diffusion coefficients ensure that the receiving stream chromatogram’s composition is not co-linear to the sample stream chromatogram for the overlapped components. If the chromatographic separation were based on size or diffusion coefficient, co-eluting analytes would have very similar diffusion coefficients, thus, adversely effecting GRAM deconvolution.

Demonstration of this concept is shown in Fig. 7. The sample and receiving stream chromatograms with a resolution of 0.3 are presented in Fig. 7A and B, respectively. The chromatograms are shown as a contour plot to allow for easier visualization of the change in relative signal intensity between the two. If the two analytes’ diffusion coefficients were similar the receiving stream signal would look like a less intense sample stream signal, and GRAM would be less successful. GRAM was run on each of the simulated chromatograms, the pure component peaks were shown in time, the pure component spectra were provided, and a Ratio for each analyte in the simulated chromatographic peak

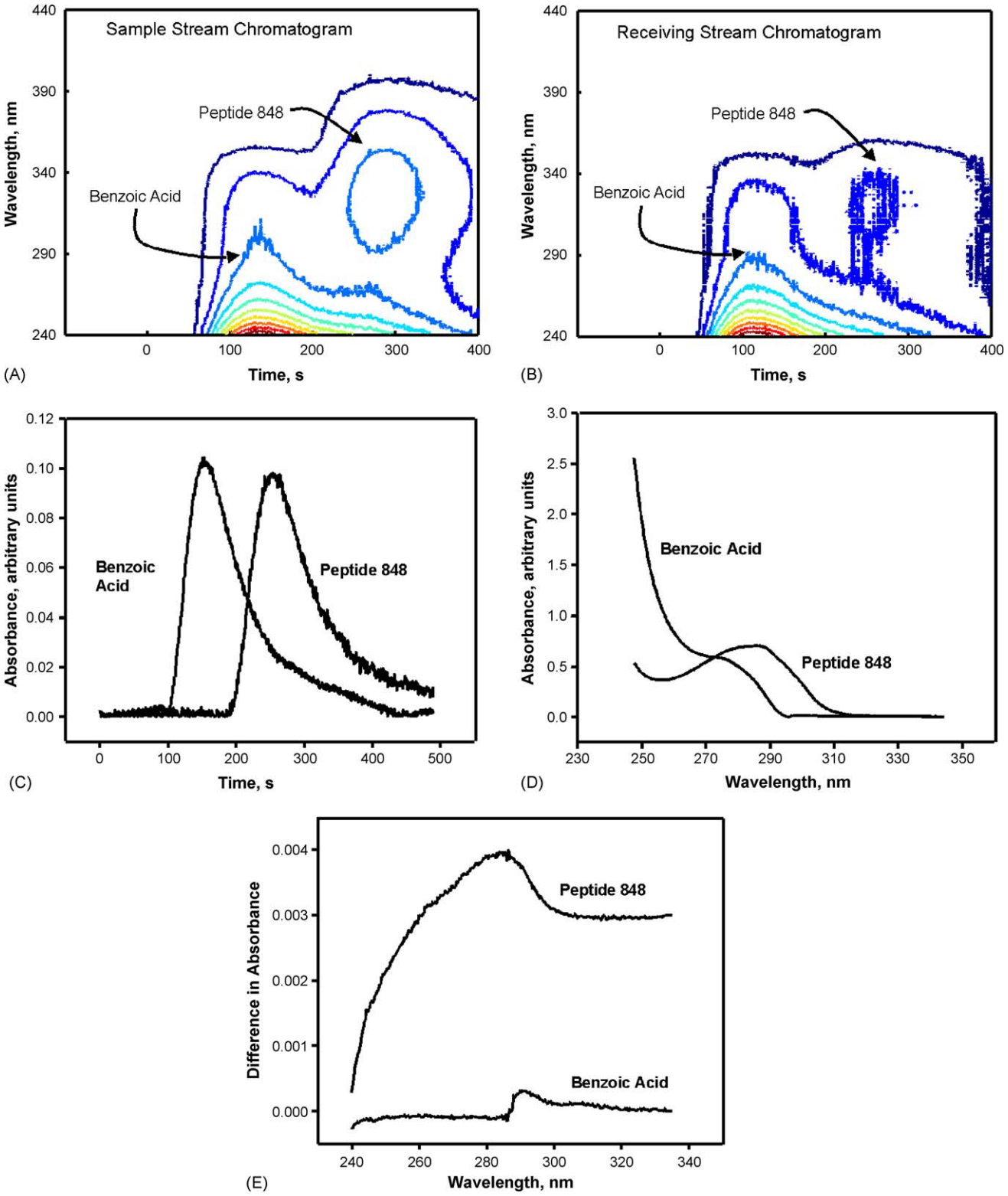

Fig. 7. (A) Contour plot of the simulated sample stream chromatogram used for GRAM. Experimental FIA sample stream peaks for 3000 ppm peptide 848 and 1000 ppm benzoic acid were offset 150 data points (90 s), giving a resolution of 0.3. The data files were then summed to yield simulated chromatograms. (B) The contour plot of the simulated receiving stream chromatogram used for GRAM. Note the different relative intensities of benzoic acid and peptide 848 in (A) and (B). (C) The GRAM provided chromatographic concentration traces of each deconvolved analyte in the mixture. (D) The spectroscopic deconvolution results of GRAM for the 0.3 resolution chromatogram for both 3000 ppm peptide 848 and 1000 ppm benzoic acid. (E) The difference between FIA obtained pure spectra for 1000 ppm benzoic acid and 3000 ppm peptide 848 spectra and the deconvolved spectra provided by GRAM. The differences are very small. Absorbance units in (E) are quantitatively relative to (D). The peptide 848 plot is offset by +0.003 for clarity.

was determined. Fig. 7C and D, shows the GRAM results for the simulated chromatogram with a resolution of 0.3. Fig. 7C shows the deconvolved concentration traces for each component in the mixture. Fig. 7D shows the deconvolved absorbance spectra for each component. Fig. 7E presents one method for evaluating the success of the GRAM deconvolution. Fig. 7E shows the two difference plots between each of the deconvolved component absorbance spectra (provided by GRAM) and the pure spectra. The peptide 848 difference plot has been offset +0.003 units for clarity. Note that the intensity of the difference plots is approximately two orders of magnitude smaller than that of the absorbance spectra provided by GRAM (Fig. 7D), indicating successful deconvolution. The results of GRAM were also evaluated by determining the percent error in the GRAM Ratio of benzoic acid and peptide 848 as resolution varies. The GRAM Ratio at a resolution of 1.0 was used as the known value. The percent error was therefore the GRAM Ratio at each resolution divided by the GRAM Ratio at a resolution of 1.0 multiplied by 100%. At all resolutions above approximately 0.25, the percent error for both analytes was less than 10%, which is consistent with previously published work [17,18]. In a worst-case scenario the flow rates between streams would not be the same and the resulting receiving and sample stream data would need to be aligned before application of GRAM. Fig. 7D and the low percent error in the GRAM Ratio provide evidence that the flow rates are very similar. However, that is not to say that flow rate fluctuations are completely unavoidable. Flow rate fluctuations could result from pump malfunction, unequal backpressure on the exit streams, or large changes in relative stream viscosity. Current and future work will entail new H-Sensor experimental designs to dampen the effect of flow rate fluctuations. However, the initial proof-of-principle GRAM results are very promising. Assuming the overlapped analytes have distinct diffusion coefficients the results show that the H-Sensor does provide all of the information for successful application of GRAM to HPLC/multi-wavelength absorbance data without the need for a second injection, or, in principle, retention time alignment.

5. Conclusions

The absorbance based H-Sensor has been introduced as a novel FIA detector. An H-Sensor model has been developed that relates an experimentally determined Ratio value to analyte diffusion coefficient and therefore molar mass. The theory adequately describes the experimental Ratio molar mass trend. The multi-dimensionality of H-Sensor data allows successful implementation of CLS methods of FIA data. CLS deconvolution of benzoic acid and peptide 848 mixtures are reported. When combined with a simulated chromatographic time axis, H-Sensor data can be analyzed with GRAM, thus providing the Ratio of each deconvoluted analyte. The H-Sensor produces two non-colinear chromatograms with each analysis. These chromatograms can serve as both the standard and the unknown in GRAM. The GRAM results show great promise in deconvolving overlapping analytes in future studies with actual chromatographic separations.

Acknowledgments

R.C. thanks the Commission on Higher Education in Thailand for financial support for her visit to the University of Washington.

References

[1] T. Hirschfeld, Anal. Chem. 52 (1980) 297A.
[2] K.S. Booksh, B.R. Kowalski, Anal. Chem. 66 (1994) 782A.
[3] J. Blomberg, P.J. Schoenmakers, U.A.Th. Brinkman, J. Chromatogr. A 972 (2002) 137.
[4] J.P. Brody, A.E. Kamholz, P. Yager, Proc. Micro. Nano-Fabricated Electro-Opt. Mech. Syst. Biomed. Environ. Appl. (1997) 103.
[5] A.E. Kamholz, B.H. Weigl, B.A. Finlayson, P. Yager, Anal. Chem. 71 (1999) 5340.
[6] A.E. Kamholz, P. Yager, Biophys. J. 80 (2001) 155.
[7] C.D. Costin, A.D. McBrady, M.E. McDonnell, R.E. Synovec, Anal. Chem. 76 (2004) 2725.
[8] C.D. Costin, R.E. Synovec, Anal. Chem. 74 (2002) 4558.
[9] A.D. McBrady, R.E. Synovec, J. Chromatogr. A 1105 (2006) 2.
[10] P. Jandik, B.H. Weigl, N. Kessler, J. Cheng, C.J. Morris, T. Schulte, N. Avdalovic, J. Chromatogr. A 954 (2002) 33.
[11] E. Sanchez, L.S. Ramos, B.R. Kowalski, J. Chromatogr. 385 (1987) 151.
[12] B.E. Wilson, E. Sanchez, B.R. Kowalski, J. Chemom. 3 (1989) 493.
[13] J. Crank, The Mathematics of Diffusion, Clarendon Press, Oxford, UK, 1975.
[14] J. Brandrup, E.H. Immergut, Polymer Handbook, John Wiley & Sons, New York, 1975.
[15] E. Comas, A.R. Gimero, J. Ferre, R.M. Marce, F. Borrull, F.X. Rius, Anal. Chim. Acta 470 (2002) 163.
[16] B.J. Prazen, R.E. Synovec, B.R. Kowalski, Anal. Chem. 70 (1998) 218.
[17] C.A. Bruckner, B.J. Prazen, R.E. Synovec, Anal. Chem. 70 (1998) 2796.
[18] C.G. Fraga, B.J. Prazen, R.E. Synovec, Anal. Chem. 73 (2001) 5833.

Available online at www.sciencedirect.com
ScienceDirect
Microchemical Journal 86 (2007) 195–203
MICROCHEMICAL JOURNAL
www.elsevier.com/locate/microc

Enhancing chemical analysis with signal derivatization using simple available software packages

Kritsana Jitmanee [a,b], Jaroon Jakmunee [a,b], Somchai Lapanantnoppakhun [a,b], Sunanta Wangkarn [a,b], Norio Teshima [c,*], Tadao Sakai [c], Gary D. Christian [d,*], Kate Grudpan [a,b,*]

[a] Department of Chemistry, Faculty of Science, Chiang Mai University, Chiang Mai 50200, Thailand
[b] Institute for Science and Technology Research and Development, Chiang Mai University, Chiang Mai 50200, Thailand
[c] Department of Applied Chemistry, Aichi Institute of Technology, 1247 Yachigusa, Yakusa-cho, Toyota 470-0392, Japan
[d] Department of Chemistry, University of Washington, Seattle, WA 98195-1700, USA

Received 19 February 2007; received in revised form 19 March 2007; accepted 20 March 2007
Available online 31 March 2007

Abstract

Derivative techniques for analytical signal processing are useful for solving some noise and signal resolution problems in various fields of study such as titrimetry, spectrophotometry, chromatography and electrochemistry. The broad use of these techniques, however, is often limited by costly inflexible built-in software packages in commercial analytical instruments. We propose here the application of commercial simple software packages such as Microsoft® Excel and Microcal Origin for signal smoothing and fitting, and for obtaining derivative analytical signals in batch and flow-based analyses, including potentiometric titration, spectrophotometry, chromatography, voltammetry and sequential injection analysis (SIA). The worldwide (especially Excel) software packages are easy-to-use for less experienced users and have also capabilities for advanced users, and therefore employing such packages can result in expansion of useful derivative techniques. We demonstrate application of the available package-aided derivative capabilities for enhancing some chemical analyses, including potentiometric acid–base titration, Bradford assay of protein, chromatographic separation of ajmaline and reserpine and anodic stripping voltammetry of copper. The derivative signals from smoothed and fitted curves offer better accuracy and precision, even for non-resolving peaks and tailing peaks. In some cases, the optimization of experimental conditions is not further required, which can lead to fast method development.

Keywords: Signal derivatization; Microsoft Excel; Microcal Origin; Enhancement of chemical analyses

1. Introduction

Derivative spectrophotometry was introduced in the early stage by Giese and French [1] to identify low intensity bands overlapped by bands of higher intensity. Afterwards, with the rapid development of data processing techniques, a great number of works on mathematical derivatization of analytical signals have been reported in many fields of study, *e.g.* spectrophotometry [2], atomic absorption spectrometry [3], voltammetry [4], and chromatography [5,6] to overcome the signal overlapping of analyte with matrices and to improve the S/N ratio. Some applications have been reported, such as, illicit drugs [7], biomedical [8], pharmaceutical, clinical and environmental analyses [9].

Derivative signals can be obtained by using hardware [5,6] and software [10–13]. Hardware derivatization has been carried out with laboratory-made electronic circuits or a derivatization unit which accompanies an analytical instrument, so that the derivative signal(s) are automatically obtained. However, the typical drawback is that the shape of the derivative signal strongly depends on the resistor–capacitor (RC) time constant of the circuit. Software derivatization may be accomplished by built-in software or by a derivatization algorithm written using the software package. Modern and costly instruments may

* Corresponding authors. K. Grudpan is to be contacted at Department of Chemistry, Faculty of Science, Chiang Mai University, Chiang Mai 50200, Thailand. Tel.: +66 53 943341; fax: +66 53 222268.
E-mail addresses: teshima@aitech.ac.jp (N. Teshima), christian@chem.washington.edu (G.D. Christian), kate@chiangmai.ac.th (K. Grudpan).

0026-265X/$ - see front matter © 2007 Published by Elsevier B.V.
doi:10.1016/j.microc.2007.03.005

possess a derivative function provided by built-in controlled-software for performing derivatization of signals. However, the function is usually inflexible and limited. Most general-purpose instruments or measuring devices, *e.g.* ultraviolet-visible spectrometers, fluorescent spectrometers, etc., usually do not possess a derivative function. In addition, to write software for calculating derivatives requires user's skill in programming and mathematics, which is difficult for many users.

Usually in chemometrics, one uses complicated software, but we are interested in using simple software packages as derivatization tools. They include Microsoft® Excel [14] and Microcal Origin [15]. Excel is very familiar to almost all computer users and does not require skill of programming. Hence, in many works, Excel (usually with Visual Basic) has been exploited for non-linear curve fitting [16–18], for calculating equilibrium gas speciation [19] and for estimation of pharmacokinetic parameters [20]. Origin is a very useful software package for scientific graphing and data analysis with C programming capabilities. Both software packages can be used, not only for computing derivatives of signals, but also for other data evaluation.

The aim of this work is to use such readily available software packages for derivatization of analytical signals to solve some analytical problems, so that cost-effective batch and/or flow-based chemical analyses [21] can be achieved. The application of signal derivatization for solving analytical problems such as titrimetric end point detection, separation of overlapping signals, and peak tailing is discussed.

2. Experimental

In order to perform derivatization of analytical signals with the software packages of Excel and Origin, it is necessary to obtain a digital file of the *X*–*Y* data set. The file extensions should be available for the two packages before data processing of derivatization.

Continuous flow acid–base potentiometric titration (titrant was continuously added to titrand in a vessel at a constant flow rate of 2 ml/min) was performed with a home-made flow system. The potential during the titration was recorded by a lab-made electronic unit and the data was saved as Excel files (xls).

The batchwise and SIA methods for determination of protein content by the Bradford assay [22,23] were performed using a fiber optic based spectrophotometer for detection (Ocean Optics, Inc.). The analytical signals were recorded via FIALab software [24] and were saved as DAT files (dat).

Chromatographic determination of ajmaline and reserpine was performed with an Agilent HPLC-UV model 100 at 280 nm. The absorbance–time data was recorded and saved as CSV file (csv).

To determine Cu by anodic stripping voltammetry, a 757 VA Computrace voltammetric system (Metrohm, Switzerland) was used. The voltammetric measurement was performed by using a glassy carbon-disc working electrode, a carbon auxiliary electrode and an Ag/AgCl reference electrode. The 757 PC

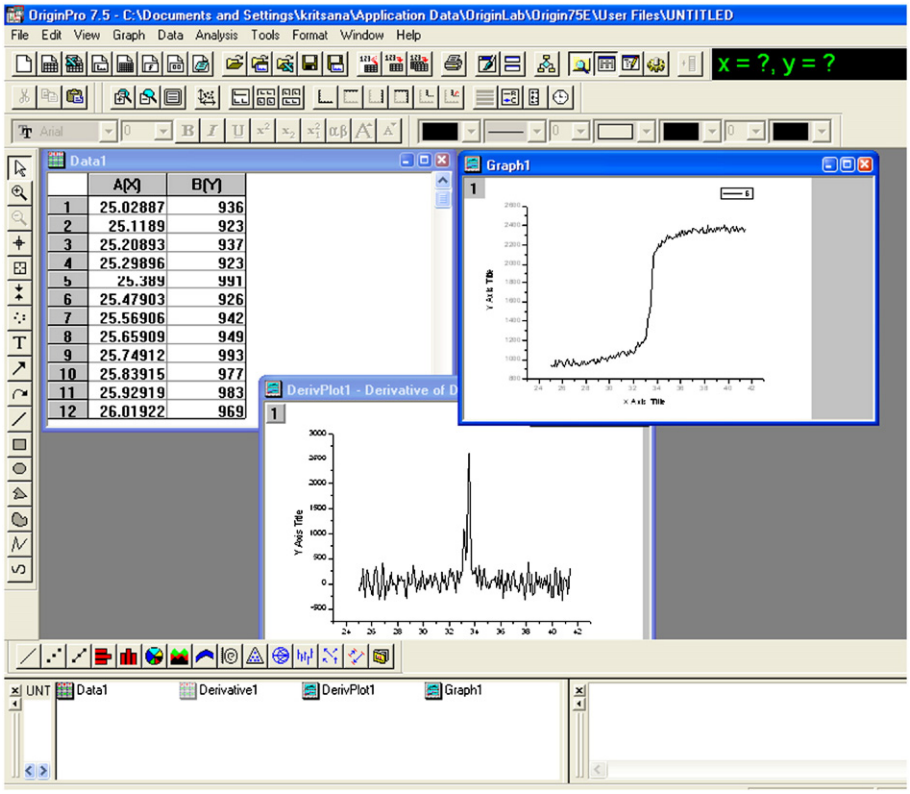

Fig. 1. Working windows of Origin.

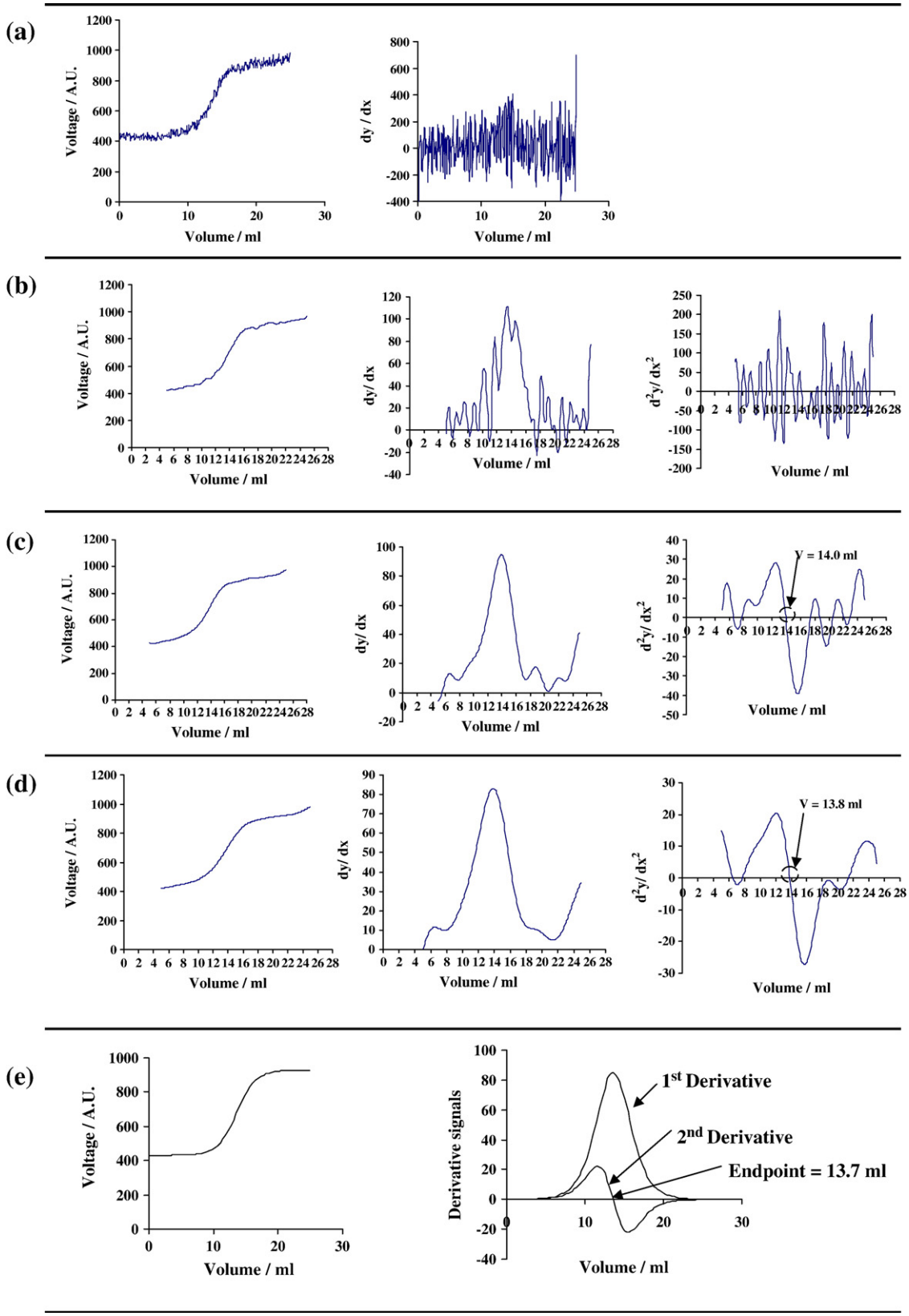

Fig. 2. Titration curve of 25.0 ml of 0.10 M HCl–0.15 M CH_3COOH mixture with 0.19 M NaOH (only the first potential break for HCl is shown here). (a), raw titration curve and its first derivative; (b), 5 data points Fast Fourier Transform (FFT) smoothing curve and its first and second derivatives; (c), 15 data points FFT smoothing curve and its first and second derivatives; (d), 25 data points FFT smoothing curve and its first and second derivatives; (e) sigmoidal-fitting curve and its first and second derivatives.

software version 2.0 with 757 VA Computrace was used to control the system. The resulting measurements were exported as TEXT files (txt).

These obtained DAT, CSV, TEXT files were able to be opened with both Excel and Origin for derivatization of signals and other data processing as well. The first derivative of analytical signals was computed by using the following equation:

$$dy/dx = 0.5^{*}\{[(y_{i+1} - y_i)/(x_{i+1} - x_i)] + [(y_{i+2} - y_{i+1})/(x_{i+2} - x_{i+1})]\} \quad (1)$$

where dy/dx is the first derivative data, and x_i and y_i are the ith data point. The first derivative graph was the plot of dy/dx against x. The second derivative and other derivative orders were computed by successive derivatization from the first derivative data.

Once a set of data is imported to Origin worksheet as shown in Fig. 1, we can easily plot the graph of the raw data, and also can simply click for signal derivatization to obtain simultaneously the derivative data and its graph by the built-in derivative software. Origin could perform successive signal derivatization up to the second derivative in an active working window.

Calculation of derivative data set in Excel could be also simply performed by using equation (1) in an Excel worksheet window. In this work, Excel was used for calculation of derivatization rather than using Origin because in the case of Excel, just by copying a raw data set to the pre-loaded derivative function's worksheet, the derivative data was readily obtained. These can be done several worksheets simultaneously. Therefore, it was very fast and simple to obtain derivative data if there were many raw data sets to deal with.

Excel, to our knowledge, can not be used for peak area integration and peak height measurement whereas Origin can do so simply. Hence, Origin was used for such data processing throughout this work.

3. Results and discussion

3.1. General discussion

3.1.1. Smoothing of signal: The importance of number of data points

A sigmoid titration curve is often differentiated to detect the end point. However, a noisy sigmoid titration curve obtained by titration of a HCl–CH_3COOH mixture with NaOH could not define its end point because of the noisy first derivative curve as shown in Fig. 2(a) (in Fig. 2, the second potential breaks for CH_3COOH are not shown). Therefore, signal de-noising of the original titration curves must be considered before derivatization. We have used two approaches to signal de-noising, *i.e.,* smoothing and fitting. There are several smoothing algorithms in Origin, *i.e.,* Fast Fourier Transform (FFT), Savitsky–Golay, Moving average, etc. Among them, FFT was used for smoothing of the signal depicted in Fig. 2(a) before derivatization. For smoothing, the number of data points to be considered in the calculation is important. Generally, the larger the number of data points, the smoother the signal obtained, as depicted in Fig. 2(b)–(d). As a result, the clearer derivative signals were obtained, so that the end point detection was improved. However, too large a number of data points for the calculation resulted in distortion of the shape of titration curve from the original one (Fig. 2(a)). This led to an error in the end point detection, *i.e.,* the end points obtained from the second derivative signal with 15-points (Fig. 2(c)), 25-points (Fig. 2(d)) and 45-points (not shown) are 14.0, 13.8 and 13.3 ml, respectively. The variation in the end points (*ca* 0.7 ml) was caused by the distortion of the shape of titration curve.

However, it was found that the use of sigmoidal-fitting could perform de-noising more simply and conveniently than the use of smoothing. The resulting smoothed curve and its first and second derivative curves are shown in Fig. 2(e). A very clear derivative signal was obtained, and the end point of 13.7 ml was well-defined. As advantages, Origin, allows simple "click" to adjust and change smoothing parameters, compared with the tedious manual adjustment in conventional smoothing methods. And the resulting smoothed signals are simultaneous and graphically shown. However, it should be noted that this sigmoidal-fitting algorithm should be suitable for only sigmoid-shape signals (unsuitable for non-sigmoid-shape signals).

3.1.2. Derivatization of signal: spacing of derivative

It is known that the spacing between data points used for calculation of derivatives is also important to consider since it affects the shape of the derivative signal. Large spacing causes distortion of the derivative signal. We used the pre-smoothed signal with 15 data points FFT (Fig. 2(c)) as a model of signal to be differentiated. The effect of spacing of dx is shown in Fig. 3. When the space of dx increased, the shape of the second derivative signal became broader and its amplitude decreased as well. Although the end point tended to decrease with increasing the space of dx in the range from 1 to 30, the variation of end point was not significantly large. Since the data was originally

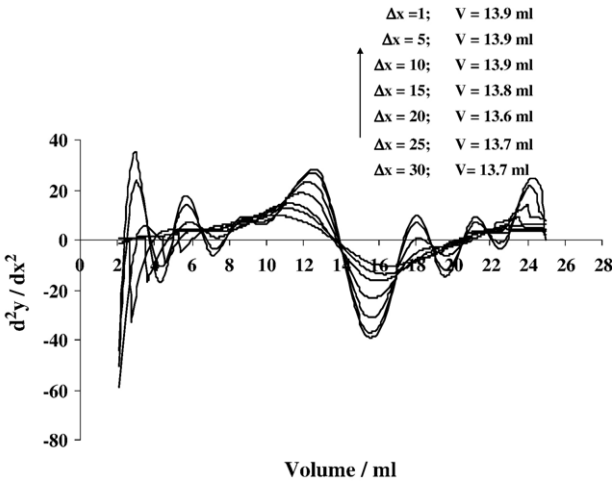

Fig. 3. Effect of spacing of dx for derivatization. The original data to be differentiated is the pre-smoothed signal with 15 data points FFT shown in Fig. 2(c).

smoothed or in some cases was de-noised, dx of 1 was used throughout for the application of derivatization.

One can set various dx values easily and simultaneously according to one's desire by using Excel, and therefore the calculation of derivatization could be performed more simply and quickly. Unlike Excel, the spacing of dx for signal derivatization calculation in Origin was fixed at 1 and could not be changed. The details for using the software packages may be obtained via their website homepages [14,15].

3.2. Detection of end point for titration

A titration curve of HCl with NaOH was performed by batchwise titration, and the first and second derivative titration curves were obtained by means of the derivative calculation mentioned above. The well-defined end point was given from the second derivative signal where it was located at the point of intersection between the second derivative signal and X-axis (became zero). The utilization of Excel for such data processing has been reported and discussed in the literature [25–27].

In the continuous flow potentiometric titration of mixture of HCl and CH_3COOH with NaOH, the titration curve is shown in Fig. 4(a) (the first potential break is shown in Fig. 2(a)). However, the titration curve was noisy, and hence the application of differentiation calculation to this signal was not feasible for obtaining the correct end points, as shown in Fig 4 (b), especially the first end point for HCl could never be found. As discussed in Section 3.1, the sigmoidal-fitting was therefore applied for de-noising. However, a limitation was encountered with performing sigmoidal-fitting over the whole curve by Origin. So, the titration curve was divided into two parts indicated by 1 and 2 in Fig. 4 before performing fitting, so that the two parts of curve could be subjected to de-noising by using Origin. The fitted curves are shown in Fig. 4(c) and (d), where their first and second derivative curves are also shown. It can be seen that the first and second derivative signals were clarified, which resulted in the easy detection of two end points. The end points for HCl and CH_3COOH were located at 13.7 ml and 33.4 ml, respectively, and those values were in good agreement with equivalence points.

3.3. Not well-resolved peaks

3.3.1. Batchwise Bradford assay for protein

Protein content was assayed by the Bradford method. The method involved the association of dye (Coomassie Brilliant Blue G-250) with protein, giving an absorption maximum at 595 nm. Under set conditions, the absorption spectra are shown

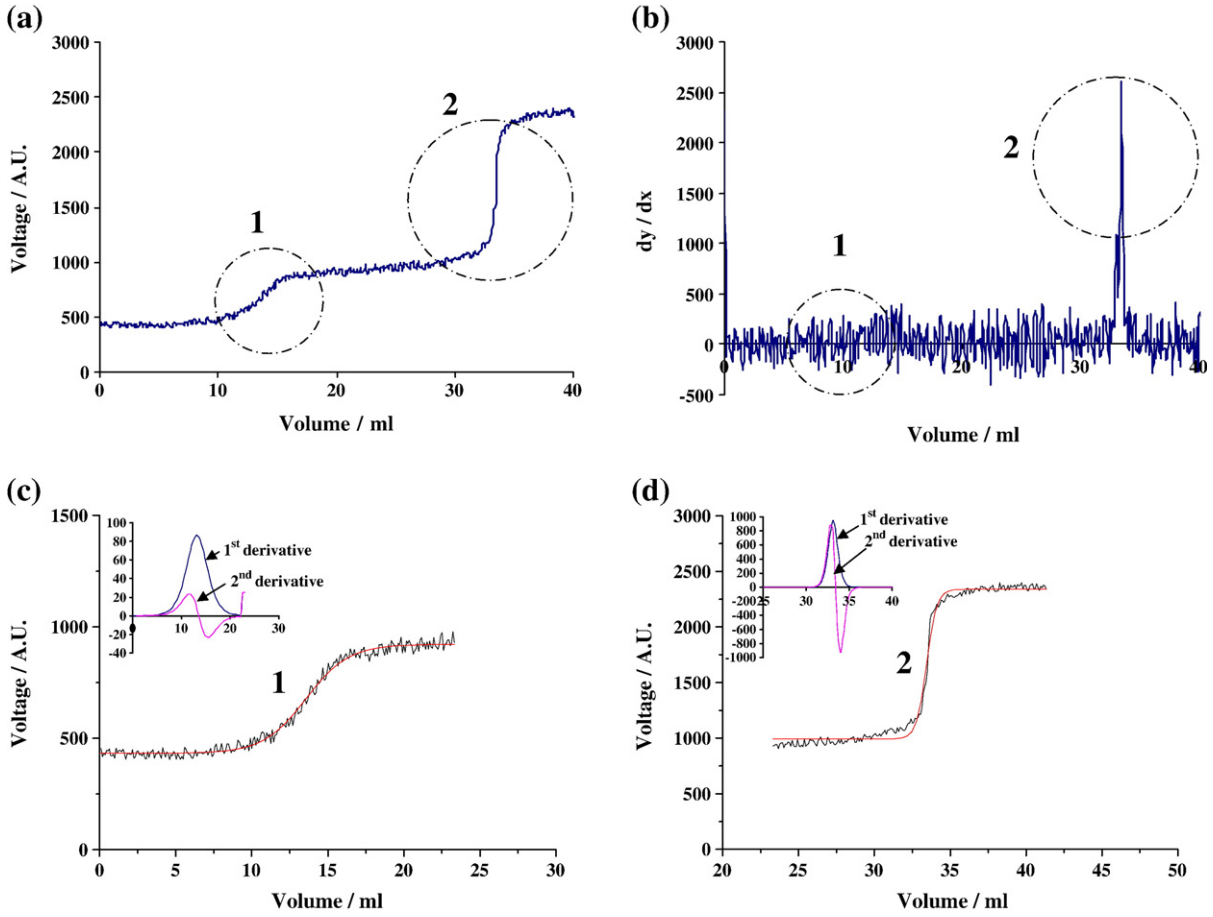

Fig. 4. Continuous flow potentiometric titration of HCl–CH_3COOH mixture with NaOH (concentration and volume as stated in Fig. 2). 1 and 2 denote the end points for HCl and CH_3COOH, respectively. Concentrations and volumes as in Fig. 2. (a), raw data of titration curve; (b) the first derivative signal; (c) sigmoidal-fitting of the first potential break and its first and second derivatives; (d), sigmoidal-fitting of the second potential break and its first and second derivatives.

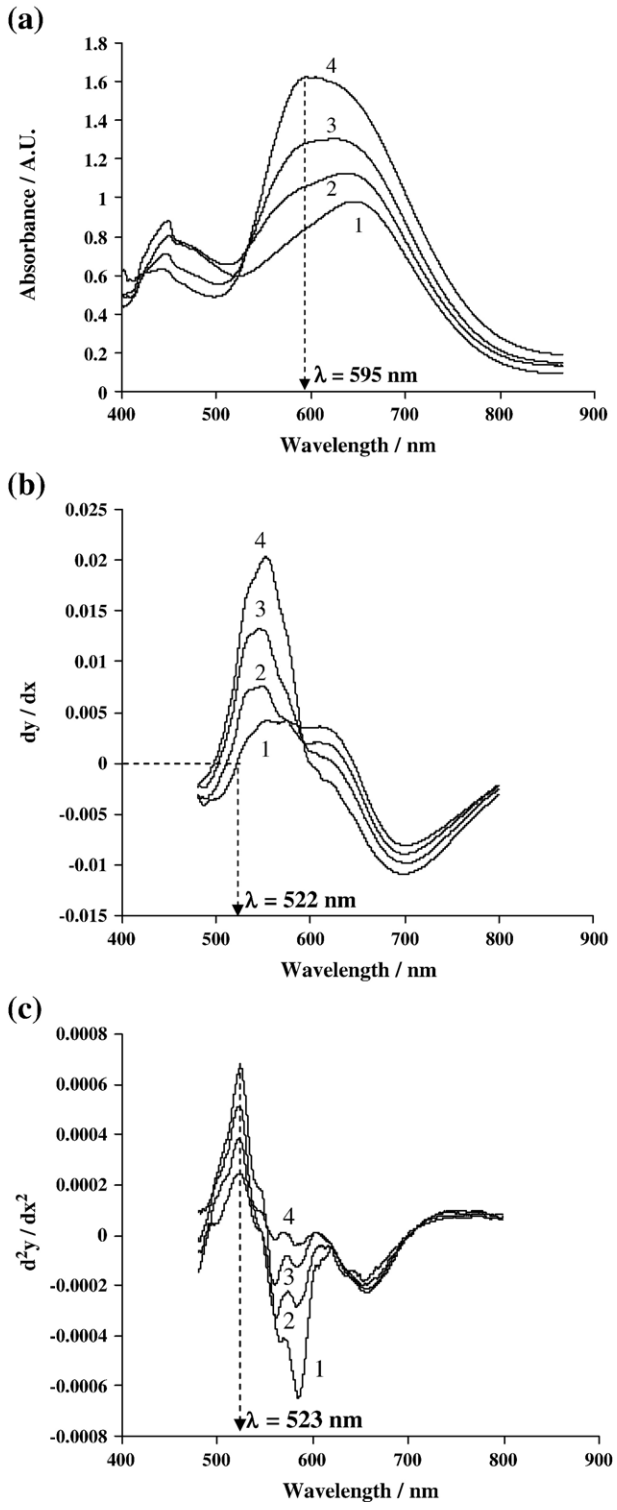

Fig. 5. Batchwise spectrophotometric determination of protein. (a), absorbance spectra; (b), the first derivative spectra; (c), the second derivative spectra. Bradford reagent: 5 ml of 0.1 g/l. Concentrations of bovine serum albumin as protein standard (mg/ml), (1), 0; (2), 0.2; (3), 0.4; (4), 0.6.

in Fig. 5(a). The absorption maximum for reagent blank was 646 nm, and that for the protein-dye ion association was 595 nm. By plotting the absorbance at 595 nm versus protein concentration, the calibration graph equation in the range of 0–0.4 mg/ml protein was $Y=1.10X+0.84$ ($r^2=0.9999$), where Y and X are absorbance and protein concentration (mg/ml), respectively. However, the dynamic range was quite short, because the analyte peak was interfered from the blank absorbance. Therefore the signal derivatization was attempted to reduce or eliminate the blank problem.

Fig. 5(b) depicts the first derivative signals. We exploited the conventional zero-crossing method which used the point

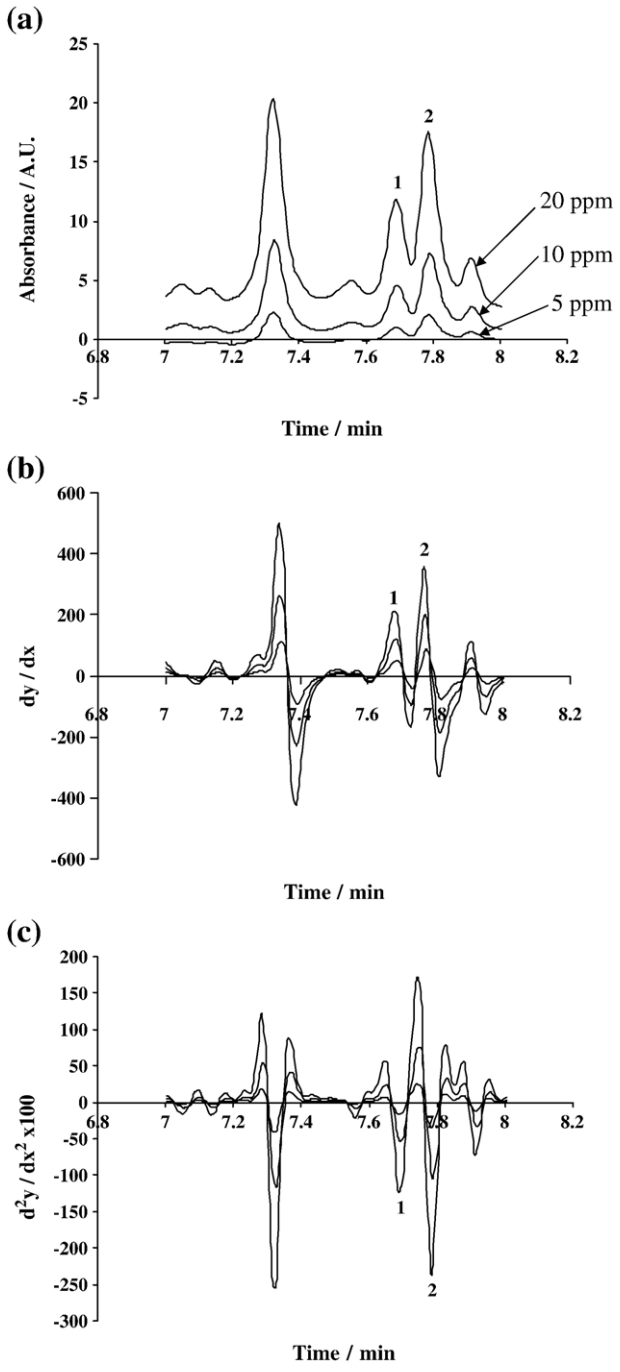

Fig. 6. Chromatographic separation of ajmaline (peak 1) and reserpine (peak 2). (a), original chromatograms; (b) the first derivatives; (c) the second derivatives. Analytical column, Luna C18 column (150×4.6 mm, 5 μm); mobile phase, 0.1% TFA and acetonitrile (gradient elution); flow rate, 1.0 ml/min; detection wavelength, 280 nm.

where blank signal becomes zero. In this case, the wavelength was at 522 nm. The calibration graph for 0–0.4 mg/ml protein was plotted by using the amplitude at this wavelength: $Y=0.0187X-8.97\times10^{-5}$ ($r^2=0.9994$), where Y and X are the first derivative amplitude and protein concentration (mg/ml), respectively. The dynamic range was not improved by using the first derivative signal. We tried to exploit the second derivative signal as another approach (Fig. 5(c)). The second derivative amplitude at 523 nm was plotted against protein concentration, and the calibration equation was $Y=0.000686X-0.000243$ ($r^2=0.9992$), where Y and X are amplitude and protein concentration (mg/ml), respectively. The dynamic range was improved to be in the range of 0–0.6 mg/ml.

3.3.2. Chromatographic separation of ajmaline and reserpine

The application of derivatives to chromatographic analysis of multicomponents was reported in the literature [28], but without any detailed information. We demonstrate here the application of a simple signal derivative procedure for chromatographic analysis of ajmaline and reserpine. These two compounds (peaks 1 and 2 in Fig. 6) were not well-resolved under the set of conditions. Quantitative analysis optimally requires good separation of the two chromatographic curves. However, optimization procedures are usually time consuming and waste many chemicals. The derivatization of the chromatogram was attempted for resolving both peaks. The relative standard deviations of peak area and peak height of derivative signals for the first and second derivatives were comparable. However, the calibration graph from the second derivative signals was more sensitive than that from the first derivative by about 50 fold. The calibration equations using the second derivative peak area and height were $Y=-21.7X+61.2$ ($r^2=0.9999$) and $Y=-720X+2.00\times10^3$ ($r^2=0.9999$) for ajmaline and $Y=-37.0X+88.3$ ($r^2=0.9999$) and $Y=-1.35\times10^3X+3.13\times10^3$ ($r^2=0.9999$) for reserpine, where Y is the peak area or height and X is the analyte concentration (ppm), respectively. The relative standard deviations of peak areas were 1.4% and 1.9% for analyzing 20 ppm ($n=3$) of ajmaline and reserpine, respectively.

Quantification of both species was feasible without further optimization of experimental conditions for resolving both species. This is very useful for fast method development. Also

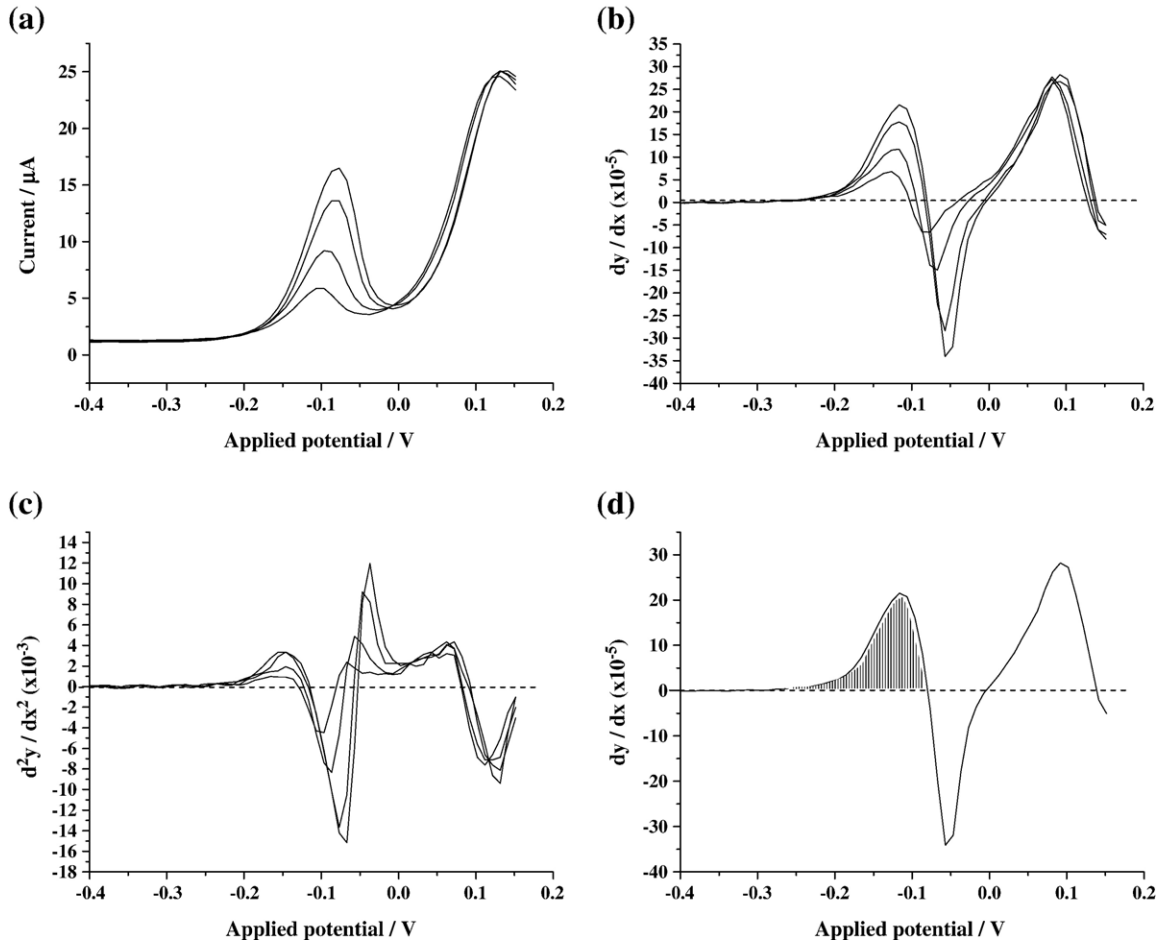

Fig. 7. Anodic stripping voltammograms for determination of Cu. (a), original; (b), the first derivatives; (c) the second derivatives; (d) the shade area denotes the peak integration area from the first derivative. Supporting electrolyte, 0.6 M acetate buffer pH 4.6; deposition potential/time, −0.8 V/87 s; scan potential, −0.9 to 0.15 V; sweep mode, square wave; step, 0.01 V; amplitude, 0.04 V; frequency, 50 Hz; sweep rate, 0.5 V/s; cleaning potential/time, 0.2 V/20 s. Cu amount (µg/ml), 0; 0.05; 0.10; 0.12.

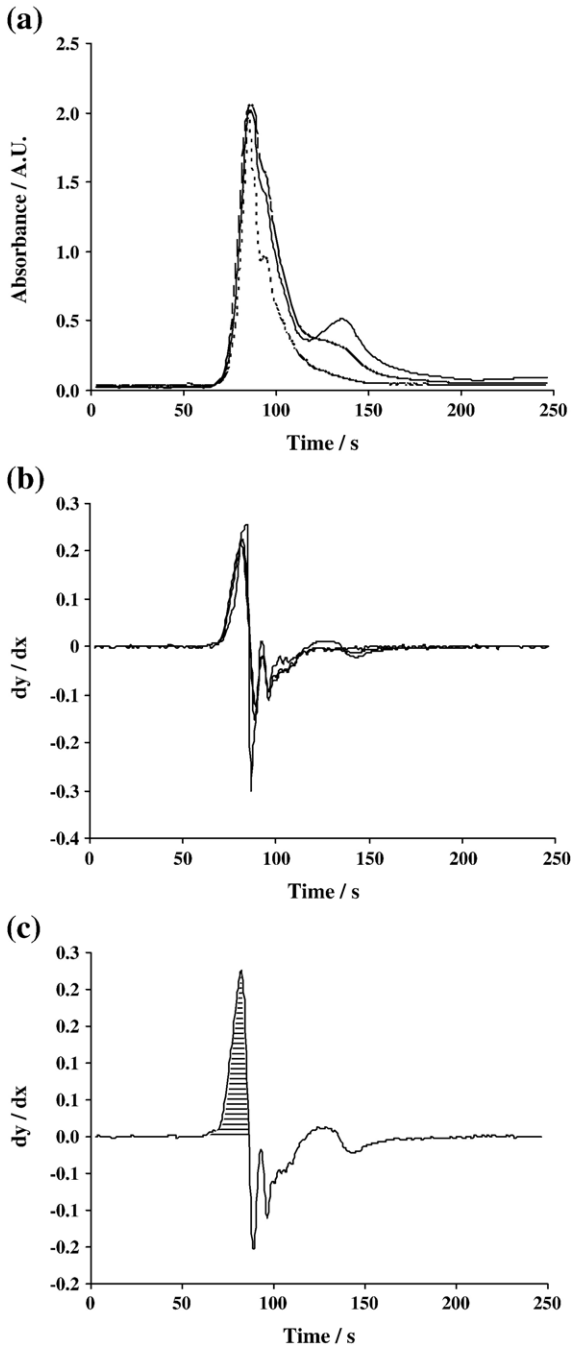

Fig. 8. SIA-grams of Bradford assay for protein (triplicate analysis). (a), original; (b), the first derivative; (c), the shade area denotes the peak integration area. Bradford reagent, 100 µl of 0.25 g/l; BSA, 100 µl (0.4 mg/ml); Carrier, 10 % (v/v) H_3PO_4/5 % (v/v) ethanol.

by applying the signal derivatization procedure, the analysis time under conditions for unwell-resolved peaks can be shortened compared with those for well-resolved peak profiles.

3.4. Unprecise peak area due to peak tailing

3.4.1. Anodic stripping voltammetric determination of Cu

The voltammogram obtained by analyzing Cu under a set of conditions is depicted in Fig. 7(a). One encounters difficulty in the selection of integration window for such a tailing peak. In this work, the voltammograms were computed to their first and second derivative signals (Fig. 7(b) and (c)). The integration window was simply defined by selecting the two outermost data points of the interested peak where the derivative signals was close to zero. An example of integration area is depicted in Fig. 7(d). The relative standard deviations of peak area and height for the first and second derivatives were comparable. However, the calibration graphs using the first derivative were better in linearity than those using the second derivative. The calibration equations from the first derivative were $Y=(8.49\times10^{-5})X+4.13\times10^{-6}$ ($r^2=0.9971$) for peak area and $Y=(1.21\times10^{-3})X+6.54\times10^{-5}$ ($r^2=0.9972$) for peak height. The relative standard deviations for sample analyses were 1.6% and 4.5% for peak area and peak height, respectively.

3.4.2. Sequential injection analysis of protein content by Bradford assay

A flow injection method using Bradford assay was proposed for the determination of protein in spiked human urine and rat liver microsome samples [29]. The recovery ranged from 89.3 to 91.9%. The results were not satisfactory for precise analysis, and Bradford assay has not been introduced to the SIA method so far. Fig. 8(a) shows the SIA-grams obtained by triplicate analysis of a standard BSA solution under a set of conditions. It can be seen that the three SIA-grams exhibit peak tailing which was caused by possibly refractive index effects. The relative standard deviation ($n=3$) in peak area was as high as *ca* 50%. Generally, this situation requires optimization of experimental conditions to reduce or eliminated the tailing of peaks. However, we adopted signal derivatization for solving such a problem. The first derivative SIA-grams are shown in Fig. 8(b). The peak area was integrated as in the shade area in Fig. 8(c). The relative standard deviation ($n=3$) of peak areas was greatly improved to as low as 3.4%. In addition, the application of derivatization to such SIA-grams was very useful because the optimization of experimental conditions for solving the problem was unnecessary, which led to fast method development similar to the discussion in Section 3.3.2.

4. Conclusion

The derivatization of signals using two commercial software packages, namely Excel and Origin, has been successfully applied to the solving of analytical problems in batch and flow-based methods such as titrimetry, spectrophotometry, chromatography, voltammetry and sequential injection spectrophotometry. Resulting derivative analytical signals by using such simple and flexible packages resulted in easy and accurate end point detection for noisy sigmoid titration curves, well-resolved absorbance spectra and chromatograms and no tailing effect in voltammograms and SIA-grams. Such signal derivatization should be attractive for not only enhancement of many chemical analyses, but also fast method development since the optimization of experimental conditions could be minimized.

Acknowledgements

The authors would like to thank The Thailand Research Fund (TRF) and The Postgraduate Education and Research Program in Chemistry (PERCH) for financial support. Also, the present work was partly supported by a grant of the Frontier Research Project "Materials for the 21st Century — Materials Development for Environment, Energy, and Information" (for 2002–2006 fiscal years) from the Japanese Ministry of Education, Culture, Sports, Science and Technology.

References

[1] A.T. Giese, C.S. French, Appl. Spectrosc. 9 (1955) 78.
[2] A. Savitzky, M.J.E. Golay, Anal. Chem. 36 (1964) 1627.
[3] H.W. Sun, J. Ha, D.Q. Zhang, L.L. Yang, J.M. Sun, Anal. Sci. 18 (2002) 603.
[4] C. Zhao, Y. Pan, C. He, Z. Guo, L. Sun, Anal. Sci. 19 (2003) 607.
[5] V. Such, J. Traveset, R. Gonzalo, J. Chromatogr. 234 (1982) 77.
[6] D.T. Zelt, J.A. Owen, G.S. Marks, J. Chromatogr. 189 (1980) 209.
[7] A.H. Lawrence, Trends Anal. Chem. 2 (1983) V.
[8] A.F. Fell, Trends Anal. Chem. 2 (1983) 63.
[9] J. Karinska, Talanta 64 (2004) 801.
[10] A.F. Fell, H.P. Scott, R. Gill, A.C. Moffat, J. Chromatogr. 282 (1983) 123.
[11] G. Vivo-Truyols, J.R. Torres-Lapasio, A.M. van Nederkassel, Y.V. Heyden, D.L. Massart, J. Chromatogr. A 1096 (2005) 133.
[12] G. Vivo-Truyols, J.R. Torres-Lapasio, A.M. van Nederkassel, Y.V. Heyden, D.L. Massart, J. Chromatogr. A 1096 (2005) 146.
[13] J.-S. Yu, Z.-X. Zhang, J. Electroanal. Chem. 403 (1996) 1.
[14] http://www.microsoft.com/, last accessed December 20, 2006
[15] http://www.originlab.com/, last accessed December 20, 2006
[16] S. Walsh, D. Diamond, Talanta 42 (1995) 561.
[17] N. Maleki, B. Haghighi, A. Safavi, Microchem. J. 62 (1999) 229.
[18] R.C. Eanes, R.K. Marcus, Spectrochim. Acta, Part B: Atom. Spectrosc. 55 (2000) 403.
[19] V.C. Kress, M.S. Ghiorso, C. Lastuka, Comp. Geosci. 30 (2004) 211.
[20] C. Dansirikul, M. Choi, S.B. Duffull, Comp. Bio. Med. 35 (2005) 389.
[21] K. Grudpan, Talanta 64 (2004) 1084.
[22] M. Bradford, Anal. Biochem. 72 (1976) 248.
[23] J.J. Sedmak, S.E. Grossberg, Anal. Biochem. 79 (1977) 544.
[24] http://www.fialab.com/, last accessed December 20, 2006
[25] G.D. Christian, Analytical Chemistry, 6th ed, John Wiley and Sons, New York, 2004.
[26] S.R. Crouch, F.J. Holler, Applications of Microsoft Excel in Analytical Chemistry, 8th ed, Brooks/Cole-Thomson Learning, Belmont, USA, 2004.
[27] D.A. Skoog, D.M. West, F.J. Holler, S.R. Crouch, Fundamentals of Analytical Chemistry, 8th ed, Brooks/Cole-Thomson Learning, Belmont, USA, 2004.
[28] S. Liu, X. Tian, X. Chen, Z. Hu, J. Chromatogr A 928 (2001) 109.
[29] T. Shuto, M. Koga, I. Tanaka, T. Akiyama, H. Igisu, Bunseki Kagaku 36 (1987) 256.

Available online at www.sciencedirect.com
ScienceDirect
Microchemical Journal 86 (2007) 209–215
MICROCHEMICAL JOURNAL
www.elsevier.com/locate/microc

Field-amplified sample injection and in-capillary derivatization for capillary electrophoretic analysis of metal ions in local wines

Apichai Santalad [a], Rodjana Burakham [a], Supalax Srijaranai [a,*], Kate Grudpan [b]

[a] Department of Chemistry, Faculty of Science, Khon Kaen University, Khon Kaen 40002, Thailand
[b] Department of Chemistry, Faculty of Science, Chiang Mai University, Chiang Mai 50200, Thailand

Received 21 March 2007; received in revised form 27 March 2007; accepted 27 March 2007
Available online 1 April 2007

Abstract

In-capillary derivatization and field-amplified sample injection (FASI) coupled to capillary zone electrophoresis (CZE) was evaluated for the analysis of metals (Co(II), Cu(II), Ni(II), and Fe(II)) using 2-(5-Nitro-2-Pyridylazo)-5-(*N*-Propyl-*N*-Sulfopropylamino)Phenol (Nitro-PAPS) as the derivatizing agent. For FASI, the optimum conditions were water as sample solvent, 1 s hydrodynamic injection (0.1 psi) of a water plug, 5 s of electrokinetic introduction (10 kV) of the sample. The in-capillary derivatization was successfully achieved with zone-passing strategy in order tandem injection of Nitro-PAPS reagent (0.5 psi, 7 s), a small water plug (0.1 psi, 1 s), and metal ion introduction (10 kV, 5 s). The solution of 45 mmol L^{-1} borate pH 9.7 and 1.0×10^{-5} mol L^{-1} Nitro-PAPS containing 20% acetonitrile was used as the running buffer. The limit of detection obtained by the proposed method was lower than those from pre-capillary derivatization about 3–28 times. The recovery of the method was comparable to pre-capillary derivatization method. In-capillary derivatization-FASI-CZE was applied to analysis of metals in wine samples. The results were compared with those obtained by CZE with pre-capillary derivatization method and atomic absorption spectrometry (AAS).

Keywords: Capillary zone electrophoresis; Field-amplified sample injection; In-capillary derivatization; Metal ions; Nitro-PAPS; Wines

1. Introduction

The analysis of heavy metals in a range of substances is of considerable interest due to potential human toxicities. There is increasing demand for simple and reliable methods for the simultaneous detection of several metal ions with low detection limits and low sample/reagent consumption. Atomic absorption spectrometry (AAS) is the most widely used method for metal analysis but simultaneous multi-element analysis is not possible. Inductively coupled plasma atomic emission spectrometry (ICP-AES) is capable of multi-element analysis, but the instrumentation is relatively expensive. The simultaneous determination of metal ions with conventional high performance liquid chromatography (HPLC) and ion chromatography (IC) have several disadvantages, such as long analysis times and consumption of large volumes of reagents. Recently, capillary electrophoresis (CE) has been shown to be a powerful separation technique for the analysis of metals in a wide variety of sample matrices [1–8] because of the significant advantages of resolution, speed, simplicity and lower sample/reagent consumption. The electrophoretic determination of metals can be easily achieved by indirect detection through the addition of appropriate species to the background electrolyte to produce UV-absorbing species [9,10], but the number of appropriate compounds for this environment is limited. The pyridylazo reagent, 2-(5-Nitro-2-Pyridylazo)-5-(*N*-Propyl-*N*-Sulfopropylamino) Phenol (Nitro-PAPS) is a synthesized chromogenic reagent which forms water-soluble chelates with giving high molar absorptivities of ca. 10^4–10^5 L mol^{-1} cm^{-1} [11–13]. Nitro-PAPS has been used as a chromogenic reagent in various analytical techniques for the determination of various metal ions. Flow-injection spectrophotometry for the determination of Fe(II) in purified salts [13] and the trace analysis of V(V) in river water [14] using Nitro-PAPS have been demonstrated. The HPLC-based determination of Cu(II), Co(II), Ni (II) and Fe(II) in rain and river waters using Nitro-PAPS has

* Corresponding author. Tel. +66 4320 2222 41x12243; fax: +66 4320 2373.
E-mail address: supalax@kku.ac.th (S. Srijaranai).

0026-265X/$ - see front matter © 2007 Elsevier B.V. All rights reserved.
doi:10.1016/j.microc.2007.03.006

been reported [11]. The use of Nitro-PAPS chelates incorporating pre-capillary derivatization in CE for the determination of trace metal impurities in nickel and iron salts has been described [15].

In CE, derivatization has been accomplished by either pre-capillary [16,17], post-capillary [18] and in-capillary [1,2,19–21] methods. Pre-capillary derivatization requires large amounts of derivatization ligand, whereas post-capillary derivatization requires significant post-capillary hardware modification, and loss of efficiency during separation and peak broadening has been noted [18,22,23]. The increased popularity of in-capillary derivatization takes advantage of the fact that there is minimal sample dilution compared to pre-capillary and post-capillary derivatization. In-capillary derivatization can be performed by three modes: zone-passing, at-inlet and throughout-capillary [24–26]. Among these strategies, zone-passing is appropriate for the Nitro-PAPS derivatization since the formation of the metal complex occurs within seconds.

In order to increase the sensitivity of detection in CE, the on-line preconcentration methods have been developed with different strategies, such as large volume sample stacking [27], sweeping [28], dynamic pH junction-sweeping [29], and field-amplified sample injection (FASI) [8,30–35]. FASI is very popular since it is quite simple, requiring only the electrokinetic injection of the sample after the introduction of a small plug of high-resistivity solvent (mainly water). In FASI, samples are normally prepared in a low conductivity buffer and injected electrokinetically into a capillary containing a high-conductivity running buffer.

In this work, the feasibility of combining FASI with in-capillary derivatization of metal ions (Co(II), Cu(II), Ni(II), and Fe(II)) with Nitro-PAPS before their analysis by capillary zone electrophoresis (CZE) is demonstrated. The combination of electrokinetic injection and water or organic solvent field-amplified sample stacking is investigated. Studies of effects of diluents (aqueous versus organic) on the stacking by the electroinjection under FASI are performed. Finally, in-capillary derivatization-FASI-CZE is applied to the analysis of these metal ions in local wine samples.

2. Materials and methods

2.1. Chemicals and reagents

All the reagents used in this work were of analytical reagent grade. Nitro-PAPS was obtained from Dojindo (Japan). A 1×10^{-3} mol L^{-1} stock solution of Nitro-PAPS was prepared in deionized water. The 1000 mg L^{-1} stock atomic absorption standard solutions of metal ions including Co(II), Cu(II), Ni(II) and Fe(II), was purchased from Ajax Finechem (Australia). The working solutions of each metal were daily prepared in deionized water except for Fe(II) was prepared in acidic medium of HCl (1% v/v). Sodium tetraborate was purchased from Univar-Ajak (Australia). Water for preparation of samples and buffer solution was the deionized water obtained from a RiO_s™ Type I Simplicity 185 (Millipore-Waters, U.S.A.) with the resistivity of 18.2 MΩ cm.

2.2. Instrumentation

Experiments were performed on a Beckman P/ACE MDQ capillary electrophoresis instrument (Fullerton, CA, U.S.A.) equipped with a photodiode array detection system. The 32 Karat software version 5.0 (Beckman) was used for instrument control, data acquisition and data analyses. Electrophoretic separations were carried out using uncoated fused-silica capillaries (Beckman) with a total length of 60.2 cm (50.0 cm effective length) and 75 μm I.D. On-capillary detections were performed at either selected wavelengths (200, 214, 250 and 570 nm) or in the scanning mode (190–600 nm). All CZE experiments were thermostated at 25 °C.

A Perkin-Elmer Instruments AAnalyst 100 atomic absorption spectrometer (U.S.A.) equipped with Perkin-Elmer single element hollow cathode lamps and an air–acetylene flame with air and acetylene flow rates of 10 and 3 mL min^{-1} was used for the determination of metals. The wavelengths (nm) selected for the determination of the analytes were as follows: Co 240.7, Cu 324.8, Ni 232.0, and Fe 248.3.

2.3. Pre-capillary derivatization (as a reference method)

The working solutions of metal ions were mixed with Nitro-PAPS solution (1×10^{-3} mol L^{-1}) in the mole ratio of ligand: metal of 2:1 at pH 6.0 at room temperature. The sample solution was introduced into the electrophoretic system by hydrodynamic injection at 0.5 psi (1 psi=6895 Pa) for 5 s before separation. The absorbance was detected at 250 nm.

2.4. In-capillary derivatization and FASI

In-capillary derivatization of metals and Nitro-PAPS was performed by zone-passing option in the tandem mode. Briefly, the capillary was first filled with the carrier electrolyte and then a plug of Nitro-PAPS solution was introduced at 0.5 psi for 7 s. After that, FASI was performed by an introduction of a small water plug (0.5 psi, 1 s) and then the sample was introduced into the capillary with electrokinetic injection at 10 kV for 5 s. Subsequently, the separation voltage of 20 kV was applied through the capillary and the on-line reaction occurred inside the capillary when the metals mixed with the Nitro-PAPS. The complexing reaction occurs during the separation to obtain the corresponding metal-Nitro-PAPS chelates and subjected to spectrometric detection.

2.5. Electrophoretic separation

Prior to use, all new capillaries were initially pretreated with the following cycles: methanol, 0.1 mol L^{-1} HCl and 0.1 mol L^{-1} NaOH for 10 min each and deionized water for 5 min between each rinse and finally equilibrated with the buffer solution for 10 min before applying voltage of 10 kV across the capillary for 5 min. To maintain reproducible migration times, the capillary was pre-conditioned with the running buffer for 3 min before each run. After completing the separation session, the capillary was flushed with 0.1 mol L^{-1}

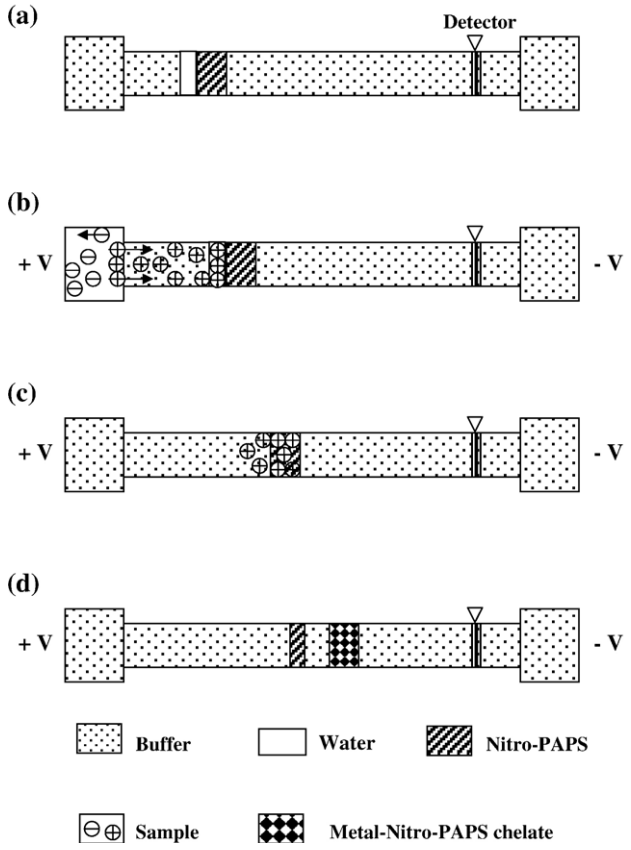

Fig. 1. The schematic reaction of metal ions and Nitro-PAPS based on in-capillary derivatization. (a) Hydrodynamic introduction of buffer, Nitro-PAPS and water plug, (b) electrokinetic injection of the sample, (c) mixing and reaction of metals with Nitro-PAPS, and (d) separation of the metal-Nitro-PAPS chelates.

NaOH for 5 min and then washed with deionized water for 3 min. The running buffer used throughout the separation was 45 mmol L^{-1} borate buffer pH 9.7 and 1.0×10^{-5} mol L^{-1} Nitro-PAPS containing 20% acetonitrile. All running buffers were filtered through a 0.45 μm membrane filter (Nylon, Chrom Tech) and degassed by sonication before use.

2.6. Wine samples

The wine samples studied included a variety of homemade red and white wines from a variety different fruits. The samples were purchased from the local supermarkets in Khon Kaen Province in Northeastern Thailand. The wines were filtered through a 0.45 μm membrane filter and were appropriately diluted about 10 times with water before derivatization and analysis. All analyses were performed in triplicate.

The AAS determinations of metals in wines were performed on standard calibration curves. The calibration curves were constructed in range 0–5 mg L^{-1} with obtained correlation coefficients higher than 0.999 for all studied metals. To obtain the results in line with the calibration curves, wine samples were appropriately diluted with water before directly analyses.

3. Results and discussion

3.1. Spectrometric properties

Although the metal ion-Nitro-PAPS complexes are normally detected at visible wavelengths, higher sensitivity and good signal-to-noise ratios were achieved with detection at 250 nm. Using Job's method, the ligand-to-metal ratio of 2:1 was found for the Co(II), Ni(II) and Fe(II) complexes, and 1:1 for the Cu (II) complex.

3.2. In-capillary derivatization and FASI

In-capillary derivatization can be achieved by successive introductions of a sample solution and the reagent solution followed by application of the specified voltages. Reaction occurs while both zones are overlapping each other in the capillary. In the present study, in-capillary derivatization of metal ions and Nitro-PAPS reagent was performed based on the zone-passing strategy. The Nitro-PAPS reagent was first introduced into the capillary by the hydrodynamic injection mode, followed by hydrodynamic injection of a small water plug and then the metal ions were injected using the electrokinetic mode. All solutions were successively introduced at the anodic end of the capillary. After the specified voltage was applied, the metal ions as positively charged species zones migrated faster than the Nitro-PAPS reagent zone toward the cathode, whereas the negatively charged Nitro-PAPS species migrated to the anode. Thus, the metal ions moved into the reagent zone and reacted to form the metal-Nitro-PAPS chelates. The mixing scheme is illustrated in Fig. 1. The parameters affecting FASI such as injection voltage and sample matrix were investigated and optimized. Preliminary studies involving metal

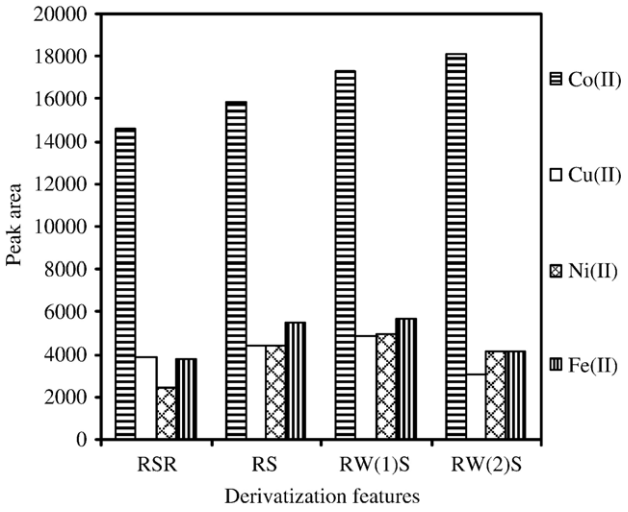

Fig. 2. Comparison of introduction order for in-capillary derivatization based on zone-passing. Conditions: metal ion standards = 3.0 mg L^{-1} each, reagent solution = 1.0×10^{-3} mol L^{-1}, reagent injection time = 7 s at 0.5 psi; sample introduction = 10 kV for 5 s; water injection time = 1 s at 0.1 psi; running buffer = 45 mmol L^{-1} borate pH 9.7 and 1.0×10^{-5} mol L^{-1} Nitro-PAPS containing 20% acetonitrile, potential = 20 kV. Segment assignment: S, Sample; R, reagent; W, water.

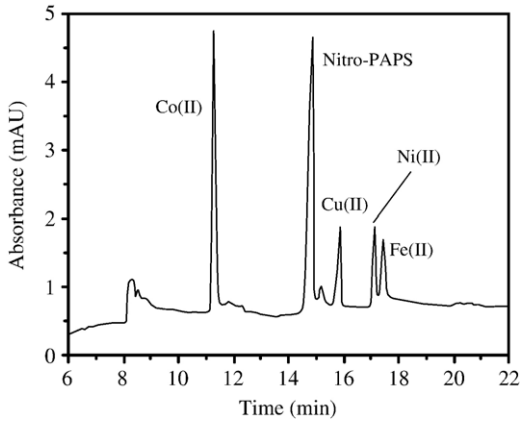

Fig. 3. Electropherogram of metal ion standards (3.0 mg L^{-1} each) obtained from in-capillary derivatization and FASI under the optimum condition as followed: 45 mmol L^{-1} borate pH 9.7 and 1.0×10^{-5} mol L^{-1} Nitro-PAPS containing 20% acetonitrile, applied voltage of 20 kV, temperature of 25 °C and on-capillary detection at 250 nm.

ions dissolved in different solvents such as 10% acetonitrile, water, and 0.4 mol L^{-1} sodium chloride showed that metal ions prepared in water gave the highest peaks for all the chelates. Although metal ions in acetonitrile provided good peak shape, the migration times of the analytes were shifted to longer times. Thus, aqueous solutions of metal ions were used for further studies.

The effect of injection voltage was studied by introducing metal ions dissolved in water at different applied voltages (7–15 kV) with a constant time interval (5 s). The peak areas increased up to 10 kV and remained nearly constant thereafter, possibly due to the competing migration directions and rates that affect local concentrations. Thus, an injection voltage of 10 kV for 5 s was chosen. Fig. 2 summarizes the results corresponding to each derivatization strategy; R, S, and W refer to the reagent, sample, and water, respectively. Among the various zone-passing introduction modes, the R-S-R configuration gave the lowest responses, except for Co(II). The R-S tandem mode gave higher sensitivities for all metal ions, compared to RSR. If the R-S tandem mode was carried out by introduction of a small water plug (at 0.1 psi for 1 s) before electrokinetic metal introduction, RW(1)S, increasing responses were observed. While a time of 2 s, designated RW(2)S, produced an increase for Co(II), the responses for other metals decreased significantly, possibly due to dilution in the reaction zone. The optimum condition is, therefore, represented by RW(1)S.

3.3. The optimization of CZE conditions

In order to achieve complete separation of metal-Nitro-PAPS chelates, the crucial parameters affecting the separation were: buffer pH, concentration of buffers, organic modifier, and separation voltage. Preliminary experiments with three common buffers, acetate (near pH 5.0), phosphate (near pH 7.0), and borate (near pH 9.0) buffers showed that acetate and phosphate did not lead to complete separation due to overlap of peaks from some metals and Nitro-PAPS, whereas borate buffer provided successful separation. Borate buffer was then investigated at the pH ranges of 9.0–10.5. Co(II), Cu(II) and excess Nitro-PAPS were well separated, but by increasing of pH, increased the resolution of Ni(II)- and Fe(II)-Nitro-PAPS could be achieved. At pH values higher than pH 10.5, excess Nitro-PAPS and Cu (II)-Nitro-PAPS peaks co-eluted. The best separation was obtained at pH 9.7.

The effect of borate concentration was then evaluated ranging from 35 to 55 mmol L^{-1}. Increasing the borate concentration resulted in decreased mobility and better resolution. However, high current in the capillary system was observed at high concentrations, so 45 mmol L^{-1} was chosen as the optimum value.

The type and concentration of organic modifier are other parameters that can improve resolution and selectivity in separations [17,20]. For the present study, acetonitrile was selected and varied over the range of 10–25% (v/v). The chelates of metals were completely separated with the running buffer containing 20% acetonitrile, so this was selected for subsequent runs.

In this study, voltages over the range of 15–22 kV showed little effect on separation. However, a poor baseline was observed when the separation was performed at the highest applied voltages, so the optimum of 20 kV was used throughout.

In all the studies, Nitro-PAPS (1.0×10^{-5} mol L^{-1}) was added into the running buffer in order to prevent the dissociation of metal-Nitro-PAPS chelates during the separation and provided good baselines [36]. No effects of Nitro-PAPS concentration changes were observed other than some baseline drift at higher values.

In summary, the optimum running buffer was 45 mmol L^{-1} borate pH 9.7 and 20% acetonitrile containing 1.0×10^{-5} mol L^{-1} Nitro-PAPS. The separation voltage was 20 kV and on-capillary detection was carried out at 250 nm. Under the optimum CZE conditions, the four metal ions was completely separated within 20 min (Fig. 3) with the migration order of Co(II)-, unreacted Nitro-PAPS, Cu(II)-, Ni(II)- and Fe(II)-Nitro-PAPS, respectively.

Table 1
The analytical characteristics of the proposed method

Complex	Linear equation, $y=ax+b$		Linearity (mg L^{-1})	R^2	Intra-day precision, RSD(%), $n=6$		Inter-day precision, RSD(%), $n=4\times3$	
	a	b			t_M	Peak area	t_M	Peak area
Co(II)-Nitro-PAPS	27032.0	−87.0	0.05–3.00	0.9982	0.28	2.00	0.35	4.00
Cu(II)-Nitro-PAPS	1476.7	472.5	0.10–3.00	0.9989	0.38	2.43	0.51	4.20
Ni(II)-Nitro-PAPS	1769.1	537.4	0.05–5.00	0.9953	0.42	2.75	0.67	3.85
Fe(II)-Nitro-PAPS	4384.0	−524.6	0.20–5.00	0.9996	0.25	2.55	0.32	4.36

Table 2
The limit of detection (LOD) and recovery for in-capillary and pre-capillary methods

Complex	LOD (mg L^{-1})			LOD factor		Recovery [b] (%), n=3	
	Pre-capillary [a]	In-capillary					
		Electrokinetic injection [c]	Pressure injection [d]	Pre-capillary/electrokinetic	Pressure/electrokinetic	Pre-capillary	In-capillary
Co(II)-Nitro-PAPS	0.20	0.025	0.30	8.0	12.0	80–102	80–95
Cu(II)-Nitro-PAPS	0.20	0.080	0.50	2.5	6.2	83–104	85–102
Ni(II)-Nitro-PAPS	0.70	0.025	1.00	28.0	40.0	80–103	82–97
Fe(II)-Nitro-PAPS	0.70	0.100	0.50	7.0	5.0	82–94	87–103

[a] Injection of complexes at 0.5 psi for 5 s.
[b] Reported as mean values for the twelve studied wine samples.
[c] Metal ion injection at 10 kV for 5 s.
[d] Metal ion injection at 0.5 psi for 5 s.

The peak of excess Nitro-PAPS (migration time 15 min) was close to the Cu(II) peak (16.0 min).

3.4. Analytical validations

To validate the quantitative aspects of the proposed method using FASI combined with in-capillary derivatization method, quality and quantity parameters using the optimized CZE method were evaluated and the results are shown in Table 1. Calibration curves based on the peak area at concentrations between 0.05 mg L^{-1} and 5.00 mg L^{-1} exhibited good linearity was obtained with R^2 values higher than 0.995. The reproducibility of the method was reported in terms of relative standard deviation (RSD) using six repeat determinations for intra-day precision and four replicate injections for inter-day comparisons. The RSD obtained from both of intra-day and inter-day precisions were lower than 0.5% and 0.7%, respectively, for migration time (t_M) whereas 3.0% and 4.5% for peak area. Limit of detection (LOD) was estimated based on signal-to-noise ratio (S/N) of 3:1 for both pre-capillary and in-capillary methods. The results are shown in Table 2. Co(II)-Nitro-PAPS has larger molar absorptivity (ε) than the other studied metal ions about 1 order of magnitude (i.e. 10^5 L mol^{-1} cm^{-1} for Co(II)-Nitro-PAPS whereas the other metal ions have ε about 10^4 L mol^{-1} cm^{-1}). Thus, a larger signal of Co(II)-Nitro-PAPS as well as its low LOD is obtained. Similar result was observed [11]. The in-capillary method with the electrokinetic injection (10 kV, 5 s) gives lower concentration detection than pre-capillary approach by a factor of 3–28. Whereas the in-capillary method with the electrokinetic injection produced lower LODs in the range of 5–40 times when compared to pressure injection (0.5 psi, 5 s). The results obtained by the proposed method can be used for the analysis of metals in sub-ppm level as lower or similar to those obtained by others [9,10,19]. To ensure that the present method can be used for the analysis of metals in real samples, the recovery was studied by spiking the metal ion standard solutions at 2.0 mg L^{-1} each into all samples and analyzed in triplicate. As shown in Table 2, the recovery obtained from in-capillary method was comparable to the pre-capillary method. The recovery ranges showed dependence on the origin of the sample and the sample matrix.

3.5. Application

The analysis of 12 wine samples was performed following the procedure described in Section 2.6. Fig. 4 shows the typical electropherograms obtained by the proposed method of Emblic fruit wine and white grape wine samples, respectively. The identification of peaks was carried out by comparing the migration time of known metal ions in a standard containing only a single metal ion with those in a metal mixture and by spiking with known metals and looking for increases in peak height. The contents of metals present in all studied wines are

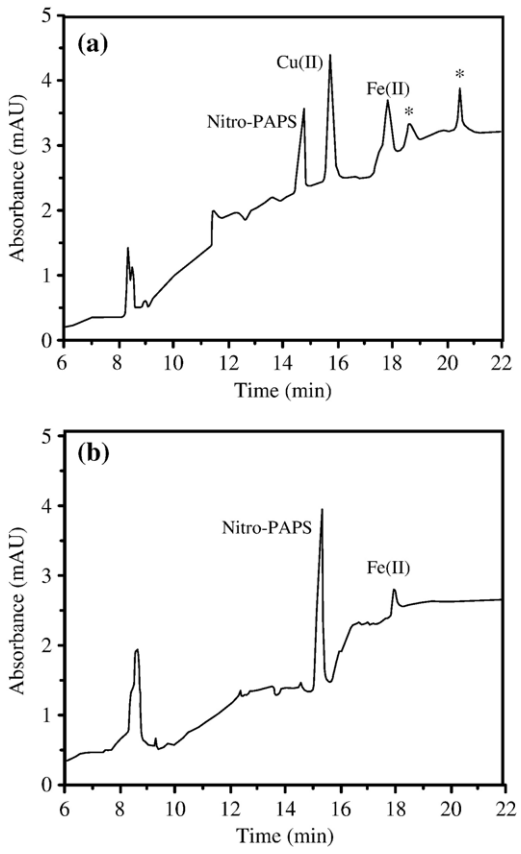

Fig. 4. Electropherograms of wine samples under the optimum conditions: (a) Emblic fruit wine and (b) white grape wine. Remarkable with asterisks (*) are unknown peaks.

Table 3
The content of metals in wine samples (mean, $n=3$)

Wine	Copper(II), mg L^{-1}			Iron(II), mg L^{-1}		
	In-capillary	Pre-capillary	AAS	In-capillary	Pre-capillary	AAS, total iron
Emblic fruit	19.53	19.96	20.36	50.89	51.37	51.80
Mangosteen	n.d.	n.d.	n.d.	7.78	7.36	7.54
Jambolan	n.d.	n.d.	n.d.	11.17	11.95	13.84
Star gooseberry	n.d.	n.d.	n.d.	12.29	12.59	11.26
Organic fruit	n.d.	n.d.	n.d.	10.03	10.28	11.30
Black galingale	5.37	5.52	5.46	15.25	15.73	15.78
Roselle	n.d.	n.d.	n.d.	19.09	20.69	19.60
Longan	n.d.	n.d.	n.d.	34.49	35.38	39.40
Bel fruit	n.d.	n.d.	n.d.	14.18	15.67	13.30
Strawberry	n.d.	n.d.	n.d.	15.86	16.71	14.52
White grape	n.d.	n.d.	n.d.	15.26	15.78	14.34
Red grape	n.d.	n.d.	n.d.	13.03	13.89	12.90

n.d.: not detected.

listed in Table 3. Only Cu(II) and Fe(II) were found in the studied wine samples whereas Co(II) and Ni(II) were not detected. Cu(II) was found in Emblic fruit and Black Galingale wines with a high level about 20 mg L^{-1} for the first sample. The levels of copper in various beverages (e.g. wines, tea, fruit juices, etc.) from some other countries have been reviewed [37]. In wines, the copper concentration was found to be less than 2 mg L^{-1}. Although copper was classified as an essential metal, excessive levels in wines are potentially toxic. The maximum acceptable level of copper in wine as established by the Office International de la Vigne et du Vin (OIV) is 1 mg L^{-1} [38]. Iron is usually present in musts and wines at a concentration range varying from 0.5 up to 20 mg L^{-1} [39]. The highest permissible concentration of iron in table wines set by the official national legislation has been determined to be 10 mg L^{-1}. Iron contents higher than 8–10 mg L^{-1} may result in turbidity and color changes [40]. In the present study, Fe(II) was found at different amounts in all wine samples. The highest value (~51 mg L^{-1}) of Fe(II) was found in Emblic fruit wine which also has the highest content of Cu(II). The Longan wine contained Fe(II) at a level of 34 mg L^{-1} and Fe(II) in Roselle wine at 19 mg L^{-1}. Fe(II) was also detected in other wine samples at levels of 16 mg L^{-1} or lower. The presence of copper and iron at these levels suggest that all wines may be at risk of cloudiness and lack of stability. To establish the reliability of the proposed method for analysis of metals in wine samples, the results obtained using the CZE method with in-capillary derivatization and FASI method have been compared to those using pre-capillary derivatization method and AAS (Table 3). The statistical significant as determined by the *t*-test at 95% confidence level showed no significant difference in the results obtained by the three methods. Comparisons presented here suggest that rapid and reliable results can be obtained in a highly automated process to establish the quality of wines. Iron contamination in homemade preparations is of particular interest.

4. Conclusion

The method and results described here demonstrate that FASI in combination with in-capillary derivatization is a useful technique for CZE determination of cobalt(II), copper(II), nickel(II), and iron(II) using Nitro-PAPS as the complexing agent. FASI of metal ions and in-capillary mixing with Nitro-PAPS were successfully obtained with zone-passing strategies using tandem injection order of Nitro-PAPS, a small water plug, and metal ions. Under the optimum condition, the separation of four metals can be achieved within 20 min. Limit of detections obtained from in-capillary derivatization with electrokinetic injection were 3–28 folds higher than those obtained from the pre-capillary method. The successful application of this method for the determination of metals in wines has been demonstrated. Only copper and iron were found at high levels in wine samples and these may influence on color and stability of the homemade wines. In-capillary derivatization and FASI were superior in terms of simplicity and ease of automation when compared to pre-capillary derivatization. Moreover, small quantities (~nL level) of reagent and sample were required. Thus, the method can be considered to be an alternative to other more complicated methods for analysis of metals in wines.

Acknowledgements

We are grateful to the Center for Innovation in Chemistry: Postgraduate Education and Research Program in Chemistry (PERCH-CIC) and the Thailand Research Fund (TRF) for the financial support. We wish to thank Prof. Richard L. Deming (Department of Chemistry and Biochemistry, California State University Fullerton, Fullerton, U.S.A.) for his kind comments.

References

[1] Z.L. Chen, R. Naidu, J. Chromatogr. A 1023 (2004) 151.
[2] F. Priego-Capote, M.D. Luque de Castro, J. Chromatogr. A 1113 (2006) 244.
[3] C. Ortega, S. Cerutti, R.A. Olsina, L.D. Martínez, M.F. Silva, J. Pharm. Biomed. Anal. 36 (2004) 721.
[4] F. Qu, J.-M. Lin, J. Chromatogr. A 1068 (2005) 169.
[5] A.-N. Tang, D.-Q. Jiang, X.-P. Yan, Anal. Chim. Acta 507 (2004) 199.
[6] M. Übner, M. Kaljurand, M. Lopp, J. Chromatogr. A 1057 (2004) 253.
[7] S. Suárez-Luque, I. Mato, J.F. Huidobro, J. Simal-Lozano, Talanta 68 (2006) 1143.

[8] Z.L. Chen, J.-M. Lin, R. Naidu, Anal. Bioanal. Chem. 375 (2003) 679.
[9] Y.S. Fung, K.M. Lau, J. Chromatogr. A 1118 (2006) 144.
[10] N. Shakulashvili, T. Faller, H. Engelhardt, J. Chromatogr. A 895 (2000) 205.
[11] T. Okutani, Y. Tsukada, A. Sakuragawa, T. Yamaji, S. Morita, J. Chromatogr. A 788 (1997) 113.
[12] T. Yamane, Y. Yamaguchi, Anal. Chim. Acta 345 (1997) 139.
[13] T. Yamane, H. Yamada, Anal. Chim. Acta 308 (1995) 433.
[14] T. Yamane, Y. Yamaguchi, Microkim. Acta 130 (1998) 111.
[15] T. Kagawa, T. Takayanagi, M. Oshima, S. Motomizu, Bunseki Kagaku 51 (2002) 791.
[16] B.-F. Liu, L.-B. Liu, J.-K. Cheng, J. Chromatogr. A 848 (1999) 473.
[17] B.-F. Liu, L.-B. Liu, H. Chen, J.-K. Cheng, Anal. Chim. Acta 434 (2001) 309.
[18] S. Hardy, P. Jones, J.M. Riviello, N. Avdalovic, J. Chromatogr. A 834 (1999) 309.
[19] M. Wang, J.-M. Lin, F. Qu, X. Shan, Z. Chen, J. Chromatogr. A 1029 (2004) 249.
[20] E. Naujalis, A. Padarauskas, J. Chromatogr. A 977 (2002) 135.
[21] W.-P. Yang, Z.-J. Zhang, W. Deng, J. Chromatogr. A 1014 (2003) 203.
[22] H.A. Bardelmeijer, H. Lingeman, C. De Ruiter, W.J.M. Underberg, J. Chromatogr. A 807 (1998) 3.
[23] R. Zhu, W.T. Kok, J. Pharm. Biomed. Anal. 17 (1998) 985.
[24] R.M. Latorre, S. Hernández-Cassou, J. Saurina, J. Chromatogr. A 934 (2001) 105.
[25] G. Jankovskiene, Z. Daunoravicius, A. Padarauskas, J. Chromatogr. A 934 (2001) 67.
[26] A. Taga, A. Nishino, S. Honda, J. Chromatogr. A 822 (1998) 271.
[27] E. Bermudo, O. Núñez, L. Puignou, M.T. Galceran, J. Chromatogr. A 1129 (2006) 129.
[28] J.F. Palmer, J. Chromatogr. A 1036 (2004) 95.
[29] P. Britz-McKibbin, T. Ichihashi, K. Tsubota, D.D.Y. Chen, S. Terabe, J. Chromatogr. A 1013 (2003) 65.
[30] S.-W. Sun, H.-M. Tseng, J. Pharm. Biomed. Anal. 36 (2004) 43.
[31] Q. Weng, G. Xu, K. Yuan, P. Tang, J. Chromatogr. B 835 (2006) 55.
[32] Y. Xu, Y. Gao, H. Wei, Y. Du, E. Wang, J. Chromatogr. A 1115 (2006) 260.
[33] C. Chen, S.-M. Wu, Y.-H. Huang, W.-K. Ko, H.-S. Kou, H.-L. Wu, Anal. Chim. Acta 517 (2004) 103.
[34] L.-Y. Zhang, M.-X. Sun, J. Chromatogr. A 1100 (2005) 230.
[35] N. García-Villar, J. Saurina, S. Hernández-Cassou, Electrophoresis 27 (2006) 474.
[36] D.A. Oxspring, T.J. Maxwell, W.F. Smyth, Anal. Chim. Acta 323 (1996) 97.
[37] P.C. Onianwa, I.G. Adetola, C.M.A. Iwegbue, M.F. Ojo, O.O. Tella, Food Chem. 66 (1999) 275.
[38] S. Galani-Nikolakaki, N. Kallithrakas-Kontos, A.A. Katsanos, Sci. Total Environ. 285 (2002) 155.
[39] K.A. Riganakos, P.G. Veltsistas, Food Chem. 82 (2003) 637.
[40] C.M. Garcia-Jahres, M.A. Lage-Yusty, J. Simal-Lozano, Fresenius J. Anal. Chem. 338 (1990) 703.

ANALYTICA CHIMICA ACTA 600 (2007) 188–193

available at www.sciencedirect.com

ScienceDirect

journal homepage: www.elsevier.com/locate/aca

Online assay of bone specific alkaline phosphatase with a flow injection-bead injection system☆

Supaporn Kradtap Hartwell[a,*], *Duangporn Somprayoon*[a], *Prachya Kongtawelert*[b], *Siriwan Ongchai*[b], *Olarn Arpornchayanon*[c], *Lucksagoon Ganranoo*[a], *Somchai Lapanantnoppakhun*[a], *Kate Grudpan*[a,*]

[a] *Department of Chemistry, Faculty of Science and Institute for Science and Technology Research and Development, Chiang Mai University, Chiang Mai 50200, Thailand*

[b] *Thailand Excellence Center for Tissue Engineering, Department of Biochemistry, Faculty of Medicine, Chiang Mai University, Chiang Mai 50200, Thailand*

[c] *Department of Orthopedic Surgery, Faculty of Medicine, Chiang Mai University, Chiang Mai 50200, Thailand*

ARTICLE INFO

Article history:
Received 4 October 2006
Received in revised form
20 December 2006
Accepted 31 December 2006
Published on line 13 January 2007

Keywords:
Bone alkaline phosphatase
Wheat germ
Flow injection
Bead injection

ABSTRACT

Alkaline phosphatase (ALP) has been used as one of the biomarkers for bone resorption and liver diseases. Normally, total alkaline phosphatase is quantified along with other symptoms to determine the releasing source of the alkaline phosphatase. A semi-automated flow injection-bead injection system was proposed to conveniently and selectively assay bone alkaline phosphatase (BALP) based on its specific binding to wheat germ coated beads. Amount of BALP in serum was determined from the intensity of the yellow product produced from bound BALP on the retained beads and its substrate pNPP. The used beads were discarded and the fresh ones were introduced for the next analysis. The reaction cell was designed to be opened and closed using a computer controlled solenoid valve for a precise incubation time. The performance of the proposed system was evaluated by using it to assay BALP in human serum. The results were compared to those obtained by using a commercial ELISA kit. The system is proposed to be an easy and cost effective system for quantification of BALP as an alternative to batch wise wheat germ specific binding technique.

1. Introduction

Alkaline phosphatase (ALP) is an enzyme primarily produced in liver and bone. It is also produced in lesser amount by the placenta, intestines and kidneys. Some conditions such as bone disease, liver damage and bile duct blockage can cause the release of high amount of ALP into the bloodstream [1–3]. The chemical structures of ALP from different sources are slightly different. Therefore, the isoenzyme test of ALP can reveal its origin which relates to the malfunctioning organ. The assay of ALP in serum is normally part of a routine blood test used mainly for the diagnosis of liver and bone disorders [4]. However, the primary screening value of blood ALP is the total ALP which cannot differentiate between each isoenzyme. To make a full use of any ALP isoenzyme as a marker of a particular disease, the assay technique has to be specific for that isoenzyme. Bone alkaline phosphatase (BALP) would be a very useful biomarker because the diagnosis of most bone diseases needs a long term monitoring of bone mass which may be too late for the effective treatment.

There are a few techniques that have been used to differentiate the two main isoenzymes, bone and liver ALPs,

☆ Presented in the Flow Analysis X.

* *Corresponding authors*. Tel.: +66 53 941910; fax: +66 53 941910.
E-mail addresses: kradtas@yahoo.com (S.K. Hartwell), kate@chiangmai.ac.th (K. Grudpan).

0003-2670/$ – see front matter © 2007 Elsevier B.V. All rights reserved.
doi:10.1016/j.aca.2006.12.056

from each other and from other isoenzymes. Some conventional techniques such as heat activation [5–7] and chemical inhibition [5,6] are simple but the assay of enzyme activity after heat and chemical exposure would not be practical for quantitative analysis for diagnosis of disease. Some other techniques require either high performance instrumentation (such as HPLC and electrophoresis) [8–11] or skilled personnel (such as immunoassay) [12,13], both of which are not always available in the regions where funding are limited and standard facilities are non-existant. Another interesting technique is called wheat germ lectin precipitation. The lectin isolated from *Triticum vulgaris* (wheat germ) is known to selectively bind to *N*-acetylglucosamine and *N*-acetylneuraminic acid residues of BALP [14–16]. This precipitation technique involves few chemicals and simple apparatus. However, BALP activity has to be measured from the precipitate which is not so convenient. Well trained personnel are still needed to perform the experiment and analyze the results. Incorporation of this specific interaction between wheat germ lectin and BALP into a more automated yet simple and cost effective system should be useful in providing health care to people living in areas located far from a modern hospital.

Flow injection-bead injection (FI-BI) is a combination of online chemical mixing and product detecting process with the use of reactive solid bead surfaces that can be introduced into and removed from the system with a flowing stream of solution. The injected beads are retained in the cell that can be designed and adapted as needed. FI-BI has been reported as an alternative to a more sophisticated sequential injection-bead injection (SI-BI). FI-BI offers some degrees of automation and improvement of precision as compared to batch wise process while minimizing the operation expense. Moreover, the closed system of FI helps to reduce the risk of direct contact between an operator and blood samples [17–19].

By employing the wheat germ coated beads with a FI-BI system, an online highly specific assay of BALP can be done easily. Reactive beads are injected into the system and trapped in place. Sample containing BALP is then passed through the bead retention cell. BALP that is captured by wheat germ on the beads can be detected with a suitable substrate. A computer controlled system for bead injection and incubation timing should help to improve the precision and reduce personal errors as compared to the batch wise wheat germ specific binding process.

As in the use of any biomarkers, an elevated BALP almost always requires other complementary testing for the decision of treatment. Therefore, the assay of BALP itself is just one of the aids in the diagnosis of bone disease or the elimination of other ALPs-related disorders. The first generation FI system is simple to set up and is cost effective. It is suitable for such tasks as the quantitative screening of BALP to aid in the prediction of bone disease or to monitor the progress of treatment. A simple spectrophotometer can be used as a detector to quantify the amount of enzyme–substrate product. The performance of the proposed system was evaluated by using it to assay BALP in human serum.

2. Experimental

2.1. Apparatus

The FI-BI system design is as shown in Fig. 1. It is composed of two peristaltic pumps (FIA Lab, USA); one for introduction of beads and carrier solution and another one for controlling the flow of buffer, sample and substrate solutions via 3-way switching valves. BALP standards or serum samples and substrate solution were injected into the system by means of

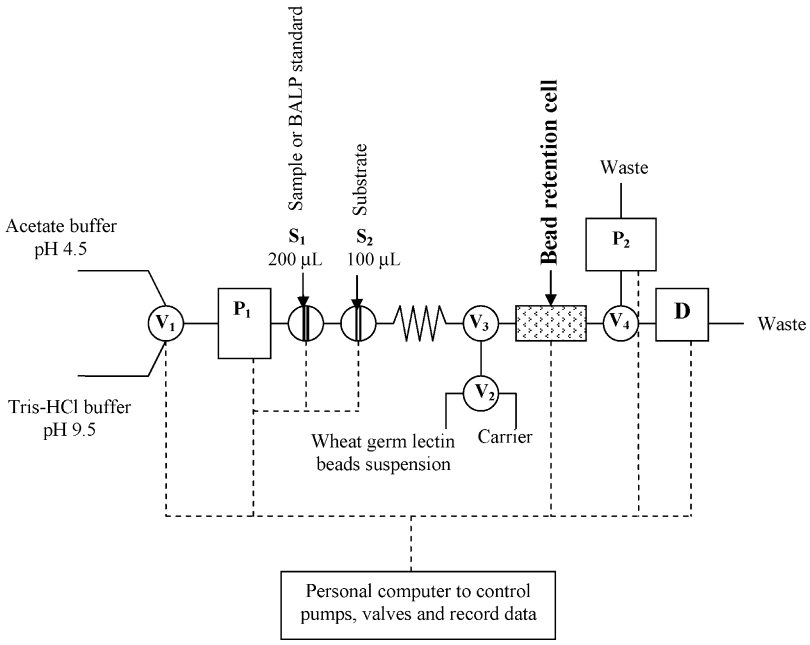

Fig. 1 – The FI-BI system for the assay of BALP. V_1, V_2, V_3 and V_4 are 3-way switching valves, S_1 and S_2 are 6-port injection valves, P_1 and P_2 are peristaltic pumps, D is a Spectronic 21, carrier is DI water and substrate is pNPP.

six-port injection valves (Pittman, USA and Metrohm, Germany). A Spectronic 21 (Spectronic Instrument, USA) with a flow through cell 1 cm, 80 μL (HELLMA, Germany) is for the detection. Two designs of bead retention cells, one based on a two-way pinch valve (Cole-Parmer, USA) and another of Perspex glass cell with solenoid valve (Guardian Electric, USA), were investigated. The pump, valves and the data were controlled and recorded via a computer with an in-house written software using LabVIEW® and Origin (Northampton, USA). The results obtained from the assay of serum samples using the FI-BI system were compared to those obtained by using the commercial 96 well BALP ELISA kit (Metra BAP EIA kit, Cat. No. 8012, Quidel, USA) [20].

2.2. Reagents and samples

Wheat germ lectin beads (size 200–300 μm diameter) were purchased from Sigma (Product No. L1394). Acetate buffer solution pH 4.5, 50 mM was used for bead conditioning. Tris–HCl buffer pH 9.5, 100 mM was used to create an alkaline working condition for enzyme–substrate reaction. As suggested by the manufacturer, triethanolamine pH 7.6, 0.1 M was used as a solvent for preparation of standard BALP solution from solid BALP. BALP stock standard solution was prepared at the concentration of 20,000 U L^{-1}. A liver ALP (LALP) stock standard solution of the same concentration was prepared and stored similarly to the BALP standard solution. *p*-nitrophenol phosphate (pNPP) working solution of 5 mM was prepared in Tris–HCl buffer solution. Bovine serum albumin (BSA, Sigma) was used to dilute the human serum samples that were obtained from the hospital to the required dilution factor. Fetal bovine serum (Lot. No. CN J0094, HyClone Laboratories, Inc.) was used for optimization study of the FI-BI system. Blood samples were collected at the Orthopedics Surgery Department, Maharaj Nakorn Chiang Mai Hospital, Chiang Mai University, Thailand. Details of preparation of each reagent, serum samples and dilution of serum are available in ESI.

3. Results and discussion

3.1. Bead retention cell

Two main purposes of the bead retention cells are the accommodation of the chemical reaction and retention of the analyte.

The first design based on a two-way pinch valve, see ESI, has limited use because of tubing deformation due to pinching pressure.

For the second bead retention cell design, the straight channel of 1/16 in. diameter was created in a Perspex glass piece. Another channel was created at 45° to the straight channel as shown in Fig. 2 to perfectly fit the solid rod (PEEK tubing) which is attached to the metal rod of a solenoid valve. When the valve was switched on, the solid rod was inserted into the flow path of beads in the straight channel, leaving the channel length of 3 cm for bead retention space. The positions of the cell and the valve were adjusted in the way that the tiny space between the cell surface and the solid rod was suitable to retain beads while the solution could flow through. By mounting the cell and the solenoid valve in place, the small space between the cell surface and solid rod can be kept unchanged. After analysis, the solid rod was pulled back and beads were pushed out with a flowing stream of solution. The movement of solid rod was controlled electronically using the LabVIEW® software for applying the voltage to the solenoid valve. There was no problem of back pressure using this cell and therefore, it was chosen for further experiments.

3.2. The FI-BI operation

Operation steps of the FI-BI system (Fig. 1) with the Perspex-solenoid valve bead retention cell were as follows. First, wheat germ lectin coated beads were loaded into the flow cell with a peristaltic pump P_2 through valves V_2, V_3 and V_4 out to waste. Then deionized (DI) water was pumped into the system to pack beads in the bead retention cell by switching valve V_2 to the carrier line. After that, the pump P_2 was stopped and by switching the valves V_3 and V_4, the acetate buffer pH 4.5 was allowed to flow into the system by the peristaltic pump P_1.

A BALP standard or serum sample was injected into the acetate buffer stream via the injection valve S_1 and passed into the bead retention cell. Then the pump P_1 was stopped to allow incubation of BALP with wheat germ lectin coated beads for a desired period of time. Specific lectin on the bead surfaces interacted and separated BALP isoform from human serum sample. After that, the Tris–HCl buffer pH 9.5 was pumped through the system via an operation of the valve V_1 to remove unbound species and to adjust the condition to be alkaline. pNPP was injected into the buffer stream by means of the injection valve S_2. It passed through the bead retention cell and out through the flow cell. The baseline signal of pNPP solution was recorded. Then the pump was stopped for incu-

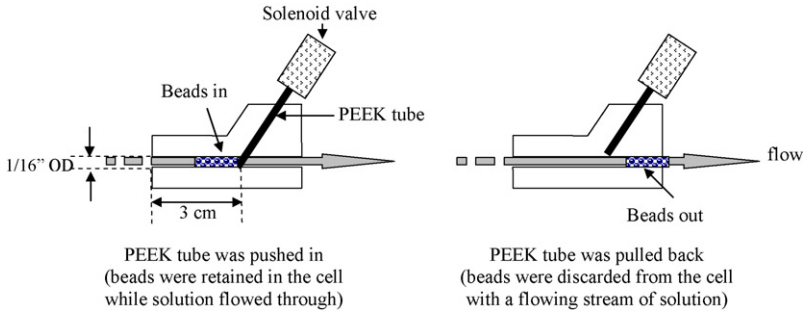

Fig. 2 – The bead retention cell based on a solenoid valve.

Table 1 – The operational conditions of the flow injection-bead injection system for the assay of BALP in human serum samples

Parameters	Selected conditions
Bead suspension	0.25 mL beads in 4 mL acetate buffer pH 4.5
Flow rate (P_2)	3.0 mL min^{-1}
Bead loading time	10 s (Approximately 30 μL of bead volume)
Bead packing	DI water 2 min
Flow rate (P_1)	1.8 mL min^{-1}
Bead conditioning	Acetate buffer 2 min
Sample volume	200 μL
Sample-bead incubation	5 min
Washing step	Tris–HCl buffer 3 min
Substrate volume	100 μL 5 mM pNPP
Enzyme-substrate incubation	5 min
Detection wavelength	405 nm

bation. The sample (200 μL) and a substrate (100 μL) would be stopped at the bead retention cell adequately, which could be controlled by the flow rate of carrier solution and the time when the pump stopped. Finally, the enzyme–substrate product, p-nitrophenol (pNP) was pushed into the flow through cell and was detected at 405 nm by pumping the buffer solution through detection unit. Used beads were discarded and replaced by fresh ones. This helps to reduce the risk of bead contamination, bead surface deterioration and to cut down the analysis time by eliminating the bead regeneration step.

3.3. *Operational conditions*

Various parameters such as sample volume, flow rate, incubation time and concentration of substrate were optimized to obtain the most suitable operational conditions. Since human serum samples were limited, all experiments in this section employed fetal bovine serum as a source of BALP to mimic matrices of real serum samples which will be used in the future.

The summarization of the selected operational conditions of the FI-BI system is shown in Table 1. It should be noted that after incubation of BALP with pNPP, enzyme–substrate product pNP was pushed into the detector. Two repeated enzyme–substrate incubation and detection steps were able to be performed for each sample on the same injected beads. Therefore, the total analytical time for the assay of BALP was approximately 30 min for 2 replicated enzyme–substrate product measurements.

A 5 min incubation time was chosen to shorten the assay process. Although it may not reach equilibrium, the advantage of the FI enables the reproduced timing for the measurement. Sample throughput may be improved by flowing the solution through the reactor slowly rather than stopping it during incubation steps. A more sensitive detector such as fiber optic may be needed to improve performance.

3.4. *Calibration curve*

The selected operational conditions of the FI-BI system were employed to obtain a calibration graph. The BALP activities

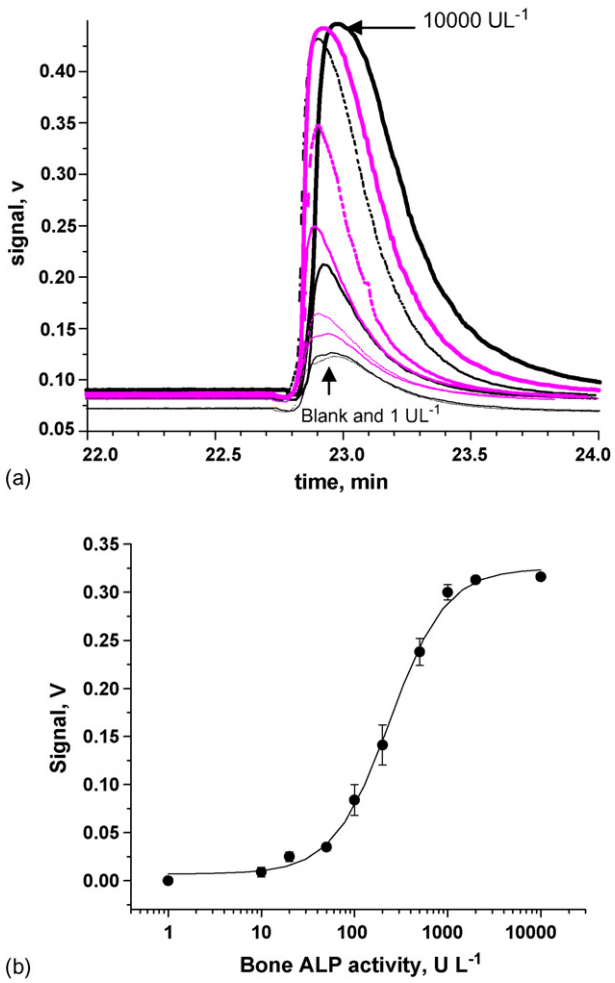

Fig. 3 – (a) The profile of the analytical signals of standard BALP at various concentrations and blank. Peak heights are increased in order with the increase of the BALP activities that are varied from 1 to 10, 20, 50, 100, 200, 500, 1000, 2000 and 10,000 U L^{-1}. (b) Calibration curve of the BALP activities.

were investigated in the range of 1–10,000 U L^{-1} to cover the amount of BALP usually found both in healthy people and bone disease patients. The profile of the analytical signals of BALP activities is shown in Fig. 3(a). The blank signal was found to be the same as and superimposed with the signal obtained from BALP of 1 U L^{-1}. The corresponding calibration curve, plotted between the differences of analytical signals from the background signal and concentrations of BALP, is presented in Fig. 3(b). The calibration curve is the sigmoidal (logistic) fit, see ESI. From this calibration curve, the working range was estimated to be 10–1000 U L^{-1}. This can cover the range of BALP levels reported to be found in healthy people (35–95 U L^{-1}) [16] and at various elevated levels in patients with bone diseases such as osteoporosis.

3.5. *Precision and accuracy*

Within-run precision or repeatability [21] was determined by repeated assaying BALP in a single fetal bovine serum 10 times within one day. The percentage of relative standard deviation

Table 2 – Percent differences of spiked BALP in normal serum samples

Sample	Found BALP ($U\,L^{-1}$)	Expected BALP ($U\,L^{-1}$)	%Difference[a]
Normal serum	16	–	–
Normal serum + 20 $U\,L^{-1}$ std. BALP	43 ± 5	36	19 ± 16
Normal serum + 100 $U\,L^{-1}$ std. BALP	94 ± 7	116	19 ± 6
Normal serum + 500 $U\,L^{-1}$ std. BALP	379 ± 16	516	27 ± 3
Normal Serum + 1000 $U\,L^{-1}$ std. BALP	687 ± 79	1016	32 ± 8

[a] Accuracy was expressed as the percentage of difference between the calculated activities of spiked BALP (expected value) and the measured amount of BALP found by using the FI-BI system: %Difference = [(found value − expected value)/(expected value)] × 100.

(%R.S.D.) was 6. Between-run precision or reproducibility [21] was determined by 10 assays of BALP of a single fetal bovine serum on different days (1 run per day) and the R.S.D. was found to be 5%.

Accuracy of the method and working range of the calibration curve were investigated by spiking various BALP activities (100, 500 and 1000 $U\,L^{-1}$) into a normal serum sample. The results in Table 2 indicate that accuracy of working range (10–1000 $U\,L^{-1}$) of the calibration curve is decreased when BALP activity is higher than 100 $U\,L^{-1}$ (more than 20% difference). This may be due to limited bead surfaces available for accommodation of high amount of BALP. The practical working range should actually be in the range of 10–100 $U\,L^{-1}$ (less than 20% difference). Therefore, dilution of serum sample is necessary for the serum sample with BALP activity near or higher than 100 $U\,L^{-1}$.

3.6. Cross reaction

Because both BALP and LALP exist in the tissue-nonspecific ALP gene locus, they have similar structures. Even though wheat germ lectin has been reported to be 90% specific toward BALP [22], the LALP which is an abundant isoenzyme of ALP in human serum may have cross-reactivity with the wheat germ lectin. From the experiment, see ESI, it was found that low amount of LALP (50–100 $U\,L^{-1}$) does not have detectable cross reactivity with the wheat germ lectin. LALP at 200 $U\,L^{-1}$ showed 3% cross reactivity while 500 and 1000 $U\,L^{-1}$ showed the same level of cross reactivity of 7%. These results are similar to those reported by the commercial BALP ELISA kit (5–8% cross reactivity with LALP). This low cross activity of LALP should not interfere with the assay of BALP.

3.7. Estimation of the amount of BALP in human serum

The FI-BI technique was used to estimate BALP in human serum samples. The results obtained from the proposed FI-BI system were compared to those obtained from a commercial ELISA kit based on monoclonal antibody against BALP. The two methods gave a regression equation of $y = 1.76x - 3.83$ with a correlation coefficient (r) of 0.74 at the significance level of 0.001 ($p = 0.001$), when plotting the results obtained by the FI-BI system as y-axis and that of the commercial ELISA kit as x-axis. By average, BALP activities obtained from the FI-BI assay are almost twice higher than those found when using a commercial ELISA kit. This could be due to higher area of solid surfaces of beads as compared to the surface of the wall of micro-well. The actual cause of unequal analytical signals of the two methods is still unknown and further studies will be useful. Nevertheless, higher sensitivity obtained from the FI-BI system should be a great benefit.

In this study, comparison of average BALP activities in the normal group and the osteoporosis group from the FI-BI assay indicates that the levels of BALP in these two sample groups are significantly different. The trends were with that by the commercial ELISA kit. The FI-BI system showed average BALP of 46 and 18 $U\,L^{-1}$ for osteoporosis and normal serum samples, respectively while the ELISA kit showed average BALP of 24 and 15 $U\,L^{-1}$ for the same osteoporosis and normal serum samples, respectively. The significance of the difference of the average BALP activities in normal and osteoporosis groups were calculated in terms of p-value. The p-value of 1.0×10^{-4} (significance level of 0.0001, 99.99% confidence level) was found with the FI-BI assay and p-value of 6.4×10^{-3} (significance level of 0.01, 99% confidence level) was found with ELISA kit. The difference in BALP levels of the two sample groups found when using the FI-BI system is higher than that found when using the ELISA kit which is the consequence of the higher sensitivity of the FI-BI system, as mentioned earlier. The FI-BI assay should provide better differentiation of normal from patient groups.

4. Conclusions

A cost effective FI-BI system for the assay of bone alkaline phosphatase (BALP) in human serum samples was developed. Wheat germ coated beads were employed to isolate BALP form human serum, followed by the enzyme–substrate reaction for detection. The simple FI-BI system can be used to perform online assay of BALP. As compared to the ELISA kit, the proposed system offers an assay run with good analytical characteristics, comparable precision and cross activity, simpler operation with less requirement for a highly trained personnel, less direct contact by the operator to blood sample, and lower cost. Referring to a sample throughput, it should also be noted that although the ELISA 96 well procedure can assay 96 samples in 4 h of one run but the proposed FI-BI system provides much shorter analysis time per run (30 min as compared to 4 h). Therefore, this FI-BI system is useful for a small to medium number of samples. Another advantage of the FI-BI system includes its tendency to better differentiate between groups of people with and without bone disease as compared to the ELISA kit. Therefore, this developed system would have a high potential of being used as an alternative

method to screen and monitor for bone disorders. Further investigation for a higher degree of automation and studies to determine a more precise cut-off value using more samples would be useful.

Acknowledgements

Financial support from The Thailand Research Fund (TRF), Commission on Higher Education (CHE), The Center for Innovation in Chemistry: Postgraduate Education and Research Program in Chemistry (PERCH-CIC), Ministry of Education and The National Research Council of Thailand (NRCT, to PK) are gratefully acknowledged. We thank Dr. Jaroon Jakmunee for some useful contributions.

Appendix A. Supplementary data

Supplementary data associated with this article can be found, in the online version, at doi:10.1016/j.aca.2006.12.056.

REFERENCES

[1] V.O. Van Hoof, M. Martin, P. Blockx, A. Prove, A. Van Oosterom, M.M. Couttenye, M.E. De Broe, L.G. Lepoute, Clin. Chem. 41 (1995) 853.
[2] P. Magnusson, L. Arlesig, E. Paus, S. Di Mauro, M.P. Testa, T. Stigbrand, J.R. Farley, K. Nustad, J.L. Millan, Tumor Biol. 23 (2002) 228.
[3] P. Magnusson, C.A. Sharp, J.R. Farley, Clin. Chim. Acta 325 (2002) 59.
[4] F. Schiele, J. Henny, J. Hitz, Clin. Chem. 29 (1983) 634.
[5] J.R. Farley, C.H. Chesnut, D.J. Baylink, Clin. Chem. 27 (1981) 2002.
[6] D.W. Moss, R. Henderson, in: C.A. Burtis, E.R. Ashwood (Eds.), Enzymes in Tietz Textbook of Clinical Chemistry, second ed., W.B. Saunders Company, Philadelphia, 1994, pp. 830–844.
[7] R.H. Christenson, K. Panigrahi, J.F. Chapman, L.M. Silverman, in: L.A. Kaplan, A.J. Pesce (Eds.), Isoenzymes and isoforms in Clinical Chemistry: Theory, Analysis and Correlation, second ed., C.V. Mosby Company, St. Louis, 1996, pp. 1077–1085.
[8] C. Karmen, P.D. Mayne, A.Y. Foo, S. Parbhoo, S.B. Rosalki, J. Clin. Pathol. 37 (1984) 1.
[9] K. Jung, M. Pergande, S. Klotzek, Clin. Chem. 35 (1989) 1955.
[10] P.M. Crofton, Clin. Chem. 38 (1992) 663.
[11] E. Schoenau, K.H. Herzog, H.J. Boechles, J. Clin. Chem. Clin. Biochem. 24 (1986) 641.
[12] G.M. Lawson, J.A. Katzmann, T.K. Kimlinger, J.F. O'Brien, Clin. Chem. 31 (1985) 381.
[13] W. Withold, U. Schulte, H. Reinauer, Clin. Chem. 42 (1996) 210.
[14] S.B. Rosalki, A.Y. Foo, Clin. Chem. 30 (1984) 1182.
[15] W. Behr, J. Barnert, Clin. Chem. 32 (1986) 1960.
[16] H. Tobiume, S. Kanzaki, S. Hida, T. Ono, T. Moriware, S. Yamauchi, H. Tanaka, Y. Seiko, J. Clin. Endocrinol. Metab. 82 (1997) 2056.
[17] K. Jitmanee, S. Kradtap Hartwell, J. Jakmunee, S. Jayasvasti, J. Ruzicka, K. Grudpan, Talanta 57 (2002) 187.
[18] P. Ampan, S. Lapanantnoppakhun, P. Sooksamiti, J. Jakmunee, S. Kradtap Hartwell, S. Jayasvati, G.D. Christian, K. Grudpan, Talanta 58 (2002) 1327.
[19] S. Kradtap Hartwell, K. Grudpan, G.D. Christian, TrAC 23 (2004) 619.
[20] http:// www.quidel.com/Products/BoneHealth/Clinical/metra_bap_desc.php? section=pro available, 2005, 10 Oct.
[21] J.C. Miller, J.N. Miller, Statistics for Analytical Chemistry, Ellis Horwood, Chichester, 1993.
[22] S.B. Rosaki, Clin. Chem. Acta 226 (1994) 143.

ISSN 0911-775X CODEN: JFIAEA

JOURNAL OF Flow Injection Analysis

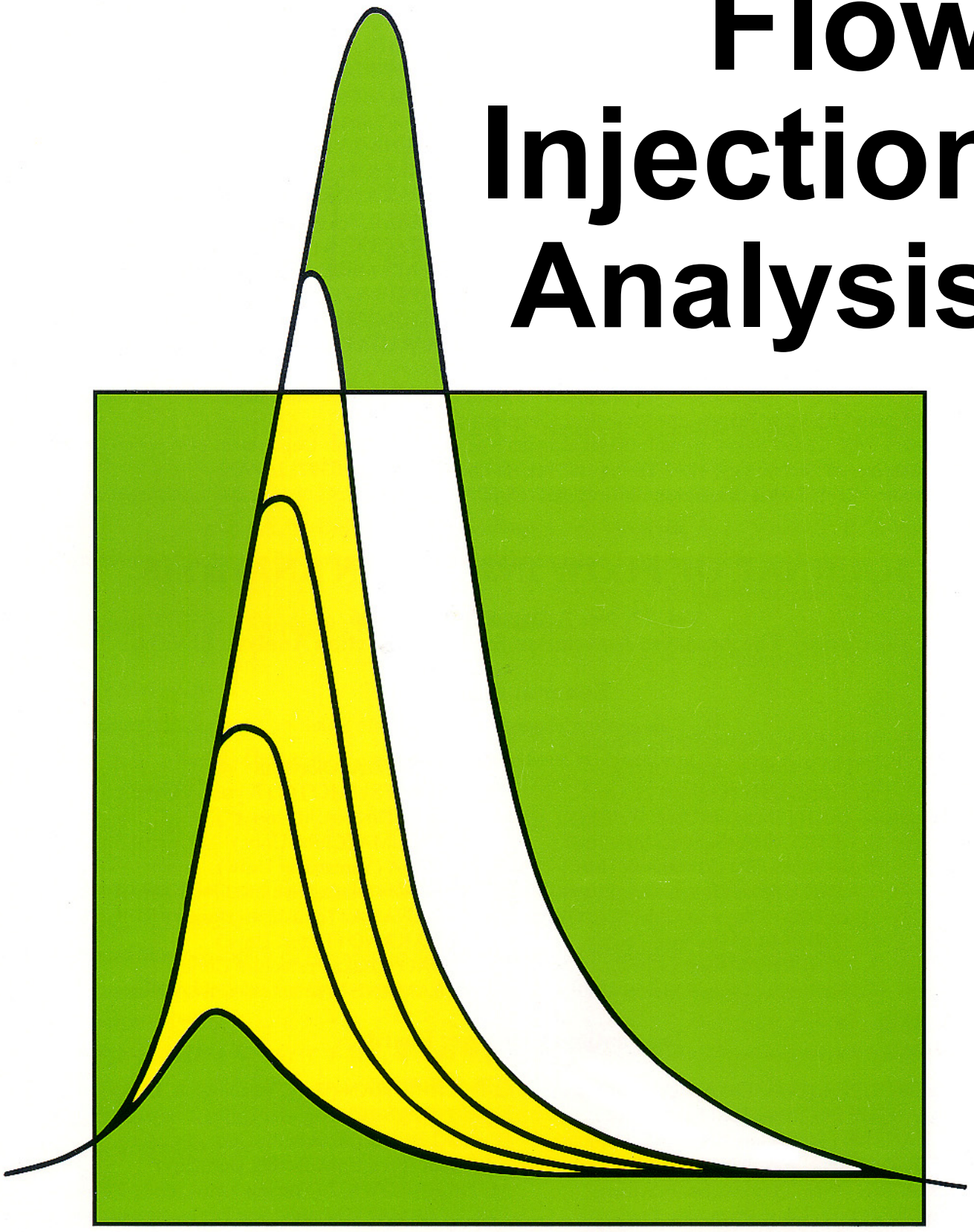

FIA 研究懇談会会誌

J. Flow Injection Anal., Vol. 24, No. 1 (2007) 23–26

Spectrophotometric Flow Injection Analysis of Protein in Urine Using Tetrabromophenolphthalein Ethyl Ester and Triton X-100

Tadao Sakai[1,*], Yoshikazu Kito[1], Norio Teshima[1], Shuji Katoh[2], Kanchana Watla-Iad[3] and Kate Grudpan[3]

[1] Department of Applied Chemistry, Aichi Institute of Technology, 1247 Yachigusa, Yakusa-cho, Toyota 470-0392, Japan
[2] Murakami Memorial Hospital, Asahi University, 3-23 Hashimoto-cho, Gifu 500-8523, Japan
[3] *Department of Chemistry, Chiang Mai University, Chiang Mai 50200, Thailand*

Abstract

A sensitive, rapid and accurate determination of protein in patient urine was carried out by flow injection analysis (FIA) using tetrabromophenolphthalein ethyl ester (TBPE·H) and Triton X-100 at pH 3.0. The detection system was based on the ion association formation between human serum albumin (HSA) and TBPE·H in the micelle formed by Triton X-100. The calibration graph was linear in the range of 0.15 – 12 mg/dL HSA with $R^2 = 0.998$. The 3σ limit of detection of the proposed FIA method was 0.05 mg/dL at 610 nm. The relative standard deviation ($n = 10$) of 3.0 mg/dL HSA was 1.2% and the sample throughput was 30 h^{-1}.

Keywords Protein determination, Urine, Tetrabromophenolphthalein ethyl ester, Flow injection analysis; Ion association formation

1. Introduction

Of proteins, albumin is very important as an active substance in our body and is synthesized in the liver. In the liver disease, the amount of albumin in the blood decreases. And also, protein is excluded as a renal proteinuria in nephropathy and diabetic nephropathy. Especially, the measurement of protein amount excluded in the urine is an important indicator to the diabetes diagnosis. In the clinical laboratory, the test paper impregnating the dyestuff is commonly used for the rapid examination of renal disease. The visible detecting technique using the test paper is simple and easy to deal with, however, the detection of protein is semi-quantitative and the measurable concentrations are classified as follows; (–) < 15 mg/dL, (±) 15 – 30 mg/dL, (+) > 30 mg/dL, (++) > 100 mg/dL, (+++) > 300 mg/dL.

Accordingly, simple and accurate spectrophotometric determinations of urinary albumin and micro-albuminuria assay using bromophenol blue [1,2] have been reported. And, Fujita et al. have reported highly sensitive spectrophotometric methods for urinary protein with dye-metal complexes and micelle media [3–7]. Huang et al. have reported the determination of albumin and globulin with α-, β-, γ-, δ-tetrakis(4-sulfophenyl)porphine [8]. Bromocresol green and bromocresol purple were used for the serum albumin determination [9] and bromothymol blue has been proposed the determination of serum albumin [10]. And also, the chemical equilibrium of protein-dye binding for protein error was studied [11,12] and the interactions of dye and/or complexes with protein were reported [13,14]. On the other hand, Yoshimoto et al. have proposed the visual, simple and sensitive analytical method for the protein detection [15,16]. Recently, simultaneous determination of human albumin, globulin and glucose by near-infrared spectroscopy [17] and fluorescence quenching method [18] of bovine serum albumin by CdS nanoparticles have been reported. And, Hashimoto et al. reported the protein assay with tetrabromophenol blue [19]. However, these methods mentioned above have been performed by the batchwise technique and the procedure needs much time and large reagent consumption.

In the clinical laboratory, the routine and accurate quantification of albumin in urine is very important for a clinical evaluation of patients with renal disease. Flow injection analysis (FIA) developed by Ruzicka and Hansen is a versatile and practical technique [20]. The technology has been widely used in environmental, clinical and pharmaceutical analyses because the method permits automatic, rapid and sensitive analysis compared with the batchwise method. FIA with Coomassie brilliant blue G-250 was used to determine rapidly protein in urine [21] and also, high-sensitivity flow method with micro-flow plunger pumps [22] and capillary stream sensor [23] were demonstrated for the serum albumin determination. However, the sample throughput was only 15 h^{-1}. The albumin in biological fluids was analyzed using FIA-CL technology, however, the derivatization reaction was carried out off-line [24].

We found that an insoluble TPBE·H formed around at pH 3.8 was dissolved in the presence of Triton X-100. In this paper, a simple two channel FIA system using TBPE·H with Triton X-100 is proposed as a rapid and precious sensor of urinary protein.

2. Experimental

2.1. Reagents

All reagents used were of analytical-reagent grade, and deionized water purified by an Advantec GSH-210 apparatus was used throughout.

A TBPE stock solution (1.0×10^{-3} M) was prepared by dissolving 0.07 g of tetrabromophenolphthalein ethyl ester potassium salt (MW: 700, Tokyo Kasei) in 100 mL of ethanol.

A Triton X-100 solution (0.5%) was prepared by dissolving 0.5 g of *t*-octylphenoxypolyethoxyethanol (Sigma Chemical) in 100 mL of water.

A human serum albumin standard (HSA, 100 mg/dL) was prepared by 0.1 g of human serum albumin (MW: 66,000, Seikagaku Kogyo) in 100 mL of water.

Working solutions were prepared by suitable dilution of the stock solutions with water.

Buffer solution was prepared by mixing 0.1 M potassium hydrogen phthalate and 0.1 M hydrochloric acid.

*Corresponding author.
E-mail: tadsakai@ac.aitech.ac.jp

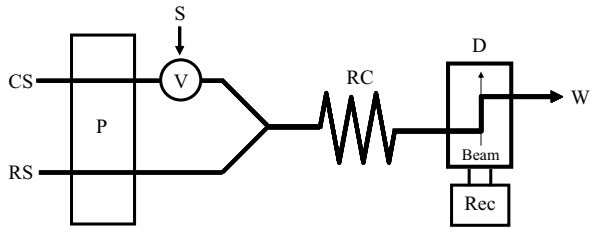

Fig. 1 Schematic diagram of the flow system. CS, water; RS, TBPE·H (1.2×10^{-5} M) + TritonX-100 (0.02%) + buffer (potassium hydrogen phthalate-hydrochloric acid, pH 3); P, pump (0.9 mL/min); V, valve; S, sample (200 μL); RC, reaction coil (ϕ 0.25 mm × 5 m); D, detector (610 nm); Rec, recorder; W, waste.

2.2. Apparatus

A JASCO, Model V-550, double beam spectrophotometer with 10 mm cell and a Horiba, Model F-22, pH meter were used for the batchwise method.

The manifold of the flow injection system is shown in Fig. 1. The dual micro-pump (F·I·A Instruments, Model PD-2000) was used to deliver carrier (CS) and reagent solution (RS). An LED visible spectrophotometer with an interfering filter (610 nm) (F·I·A Instruments, Model KCM-0306) equipped with a micro flow cell was used for the measurement of protein associate.

2.3. Procedures

2.3.1. Batchwise method

To the HSA standard solution, 5 mL of 1.0×10^{-4} M TBPE solution, 5 mL of 0.1% Triton X-100 and 2 mL of buffer solution (pH 3.1) were added in a 25 mL volumetric flask and the mixture was diluted to the mark with water. After mixing, absorbance was measured at 610 nm against water.

2.3.2. FIA method

The two channel flow system as shown in Fig. 1 is assembled. CS (water) and RS (a mixture of 1.2×10^{-5} M TBPE, 0.02% TritonX-100 and buffer (pH3.0)) were pumped at the rate of 0.9 mL/min. An aliquot (200 μl) sample solution is injected into the CS stream by a six-way injection valve. After mixing in the 5 m reaction tube (inner diameter 0.25 mm), absorbance was monitored at 610 nm.

3. Results and discussion

3.1. Batchwise study

3.1.1. Effects of TBPE and Triton X-100 concentrations

TBPE concentration was varied from 1.0×10^{-5} M to 8.0×10^{-5} M and Triton X-100 concentration was varied in the range of 0.005 – 0.1% in the absence of HSA. TBPE (blue) dissolved in ethanol was converted to yellow TBPE·H molecule in an aqueous media below pH 3.5 because the dissociation constant, $pK_{a,TBPE}$, was 4.2 [25]. A yellow TBPE·H was insoluble in water, however, TBPE·H was soluble in the presence of Triton X-100. Absorbance of the reagent blank increased with increase of TBPE concentration. This could be due to that TBPE·H in the micelle produced a dissociated TBPE ion slightly. In this study, 0.02% Triton X-100 and 2.0×10^{-5} M TBPE were chosen.

3.1.2. Effect of pH for ion association formation

The effect of pH on the formation of TBPE-protein associate was investigated. pH was varied from pH 2.9 to 4.2. The 2.0×10^{-5} M TBPE and 0.02% Triton X-100 solutions were used for 2.4 mg/dL HSA. With increasing pH, absorbance of the associate increased, however, absorbance of the reagent blank increased gradually. However, the calibration curve at pH 3.4 gave $y = 0.21x + 0.05$, $R^2 = 0.956$ (y = absorbance, x = HSA concentration in mg/dL, R^2 = correlation coefficient) and that at pH 3.1 gave $y = 0.17x + 0.03$, $R^2 = 0.980$ in the range of 0 – 3.0 mg/dL HSA. Consequently, pH 3.1 was chosen in this study.

Fig. 2 shows absorption spectra at pH 3.1 and 3.8 for various HSA concentrations. At pH 3.1, the reagent blank gave a low absorbance at 610 nm and absorbance of the associate increased in proportion to the HSA concentration. And also, the isosbestic point appeared at 490 nm. The larger absorbance was obtained at pH 3.8, however, the absorbance of the reagent blank became larger and the absorbance of the associate was not proportional to the HSA concentration, because TBPE・H in the micelle dissociated into TBPE anion at higher pH, and the ion associate formation was not stoichiometric.

3.1.3. Binding ratio of protein-TBPE associate

The binding ratio of the protein-TBPE associate was investigated by the continuous variation plots. The result is represented in Fig. 3. According to the continuous variation plots, it can be assumed that the binding number of TBPE to HSA is over 18. And also, it was simulated to obtain a presumed binding number as given below. When 3.6×10^{-7} M HSA was added, the absorbance was 0.417 at 610 nm. Hence, the molar absorptivity

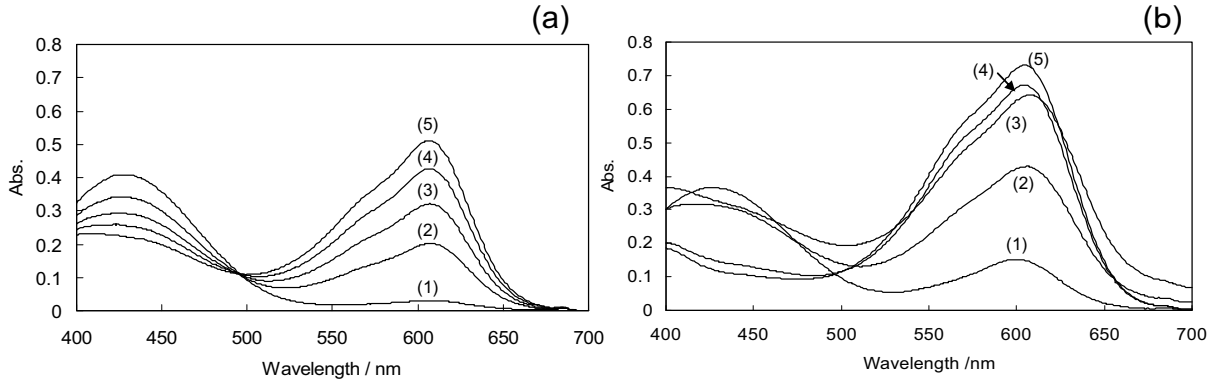

Fig. 2 Absorption spectra at different pH by batchwise method. (a), pH 3.1; (b), pH 3.8. HSA concentrations (mg/dL): (1), 0; (2), 0.8; (3), 1.6; (4), 2.4; (5), 3.2. TBPE·H, 2.0×10^{-5} M; Triton X-100, 0.02%.

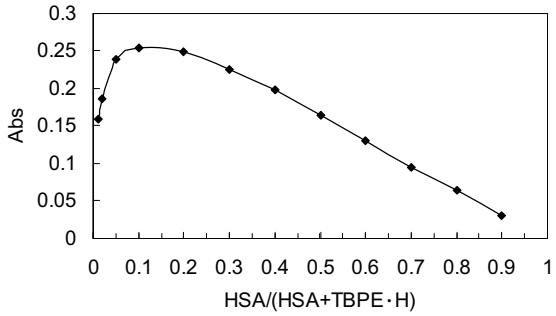

Fig. 3 Continuous variation plot of TBPE-HSA associate. $C_{HSA} + C_{TBPE} = 4\times10^{-5}$ M.

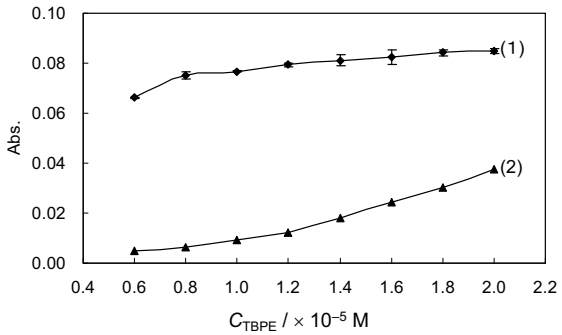

Fig. 4 Effects of TBPE concentration in FI method. (1) HSA (3 mg/dL) and (2) baseline absorbance against water. pH 3.0; Triton X-100, 0.02 %; RC: ϕ 0.25 mm×5 m; flow rate, 0.9 mL/min; sample loop, 200 μL. Error bar denotes standard deviation in tripricate.

for 3.6×10^{-7} M HSA, $\varepsilon_{HSA\cdot(TBPE)x}$ (x denotes the binding number of TBPE), was 1.2×10^{6} L mol^{-1} cm^{-1}. In this study, ε_{TBPE} in the presence of Triton X-100 was 5.7×10^{4} L mol^{-1} cm^{-1}. The ε_{TBPE} multiplied by 21 gives the same value of 1.2×10^{6} L mol^{-1} cm^{-1} as the $\varepsilon_{HSA\cdot(TBPE)x}$. Consequently, we estimated the binding ratio of TBPE to HSA was 21:1. Hence, the chemical equilibrium of the association reaction and its micelle extraction constant ($K_{ex(m)}$) can be expressed as:

$$21(TBPE\cdot H)_m + HSA^{21+} \rightleftharpoons (HSA^{21+}\cdot(TBPE^-)_{21})_m + 21H^+ \quad (1)$$

$$K_{ex(m)} = \frac{[HSA^{21+}\cdot(TBPE^-)_{21}]_m[H^+]^{21}}{[TBPE\cdot H]_m^{21}[HSA^{21+}]} \quad (2)$$

where $[\ ]_m$ is the concentration of chemical species in the micelle. Motomizu et al. have reported micelle extraction constants of ion associate formed between quaternary ammonium salts (quaternary phosphonium salts) and TBPE·H in the presence of Triton X-100 [26,27]. However, in this study, it was difficult to determine the micelle extraction constant of TBPE-HSA because HSA is a large and hydrophilic molecule.

3.1.4. Calibration graph and interference study

A calibration graph with a good linear relationship (R^2 = 0.980) was obtained up to 3.0 mg/dL of HSA. The 3σ limit of detection (LOD) and 10σ limit of quantitation (LOQ) were 0.05 and 0.17 mg/dL, respectively.

Sodium chloride and creatinine concentrations in normal urine are 1000 mg/dL and 100 mg/dL, respectively. The interferences on sodium chloride and creatinine were studied. As the results, sodium chloride did not interfere up to 30 mg/dL and 18 mg/dL creatinine did not give the interference. Accordingly, the coexisting sodium chloride and creatinine in urine did not give the interference on the determination of HSA in this method because the urine sample was diluted with water to 62.5-fold before measurements.

3.2. FIA study

3.2.1. Effect of pH

The effect of pH for 3.0 mg/dL HSA was investigated in the range of pH 2.7 – 3.3. With increasing pH, absorbance increased gradually. However, over pH 3.1, absorbance of the baseline also increased. In this study, pH 3.0 was selected.

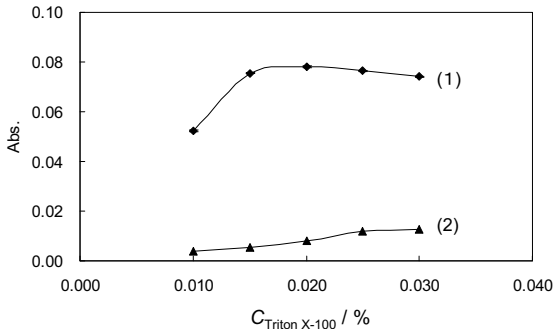

Fig. 5 Effects of Triton X-100 concentration in FI method. (1) HSA (3 mg/dL) against reagent blank and (2) baseline absorbance against water. TBPE, 1.2×10^{-5} M; pH 3.0; RC, ϕ 0.25 mm×5 m; flow rate, 0.9 mL min^{-1}; sample loop, 200 μL. Error bar denotes standard deviation in tripricate.

3.2.2. Effects of TBPE and Triton X-100 concentrations

TBPE·H concentration was varied in the range from 0.6×10^{-5} to 2.0×10^{-5} M (Fig. 4). Over 1.2×10^{-5} M TBPE·H, absorbance increased slightly. However, over 1.4×10^{-5} M TBPE·H, absorbance of the baseline increased drastically. A higher TBPE·H concentration gave the large reagent blank in a similar manner as mentioned in the batchwise study. In this study, 1.2×10^{-5} M TBPE·H was used.

The effect of Triton X-100 concentration was varied from 0.01 to 0.03%. At the 0.01% solution, the absorbance of the associate was very low because the dissolution of TBPE·H into the micelle was not sufficient. Over 0.015%, the largest and constant absorbance was obtained as shown in Fig. 5. The 0.02% concentration was chosen.

3.2.3. Other variables

The reaction coil (tubing of 0.25mm ID) length was varied in the range of 0.5 to 5 m using 3 mg/dL HSA. The constant and largest absorbance was obtained even below 2 m. However, the correlation coefficient (R^2) of the calibration curve was 0.977 at 2 m and R^2 at 5m was 0.998 in the range of 4–8 mg/dL HSA. As a result, a 5-m tubing was chosen.

Table 1 Determination of protein in human patient urine

Sample No.	Test paper[a]	Batchwise method /mg/dL[b]	FIA method /mg/dL[b]
1	++	50.1±2.4	43.2±1.3
2	++	82.3±1.9	83.7±4.5
3	++	58.3±2.3	53.2±1.2
4	++	89.7±2.2	88.0±2.2
5	++	70.6±2.0	66.3±1.5
6	++	89.8±3.0	81.8±0.8
7	++	108.8±1.2	109.7±1.0

a. Semi-quantitation by Albustix purchased from Bayer Medical Ltd., The symbol (++) shows > 100 mg/dL protein
b. Dilution ratio for sample determined was 62.5.

The effect of flow rate was investigated in the range of 0.5 to 1.3 mL min^{-1}. Over 0.7 mL min^{-1}, the constant and largest absorbance was obtained and the baseline became lower.

The sample volume was varied from 50 μL to 300 μL. With increasing the volume, absorbance increased gradually. The 200 μL sample volume was used.

3.2.4. Calibration graph

The calibration graph was linear up to 12 mg/dL of HSA with $R^2 = 0.998$ and the graph passed through the origin: $y = 0.026x$ (y = absorbance, x = HSA concentration in mg/dL). The LOD and LOQ of the proposed FIA method were 0.05 and 0.15 mg/dL, respectively. The sample throughput was 30 h^{-1}. The relative standard deviation ($n = 10$) was 1.2% for 3 mg/dL.

3.2.5. Interferences

Interference by sodium chloride and creatinine was studied on the determination of 3 mg/dL HSA by the proposed FIA method. Over 60 mg/dL sodium chloride, absorbance decreased. However, sodium chloride less than 20 mg/dL did not interfere. And, 10 mg/dL creatinine did not give any interference. Since urine sample was diluted with water to 62.5-fold in this study, the influence from sodium chloride and creatinine could be negligible.

3.3. Application to urinary protein and serum protein analysis

The urinary protein contents in samples collected from nephropathy and diabetic nephropathy patients were determined by a paper test kit (commercially available Albustix by Bayer Medical), batchwise method and the proposed FIA method. Each urine sample was centrifuged at 3000 rpm and the supernatant was diluted with water to 62.5-fold. The results obtained by the three methods are summarized in Table 1. The concentrations by the test paper showed around 100 mg/dL for all samples because the judged concentration range was rough and not accurate as described above. The correlation coefficient (R^2) between batchwise method and FIA method was 0.954, and the slope was 1.03. The experimental t-value was 2.42 and the theoretical t-value was 2.447 for $n = 7$. Accordingly, the proposed FIA using TBPE·H and Triton X-100 was useful by offering some advantages on low reagent blank, rapidity, simplicity, accuracy and less reagent consumption.

In conclusion, two channel flow injection system using TBPE·H dissolved in Triton X-100 was proposed for the determination of urinary protein collected from patients. The calibration range was 0.15 – 12 mg/dL with RSD of 1.2%. The sample throughput was 30 h^{-1}. This could be an alternative method in the clinical laboratory.

Acknowledgement

The author (T.S.) gratefully acknowledges the financial support of this study by Grants-in-Aid for Scientific Research No. 17550087 from Japan Society of the Promotion of Science. This work was partly supported by Grant-in-Aid for Scientific Research No. 18750067 (N.T.) from the Ministry of Education, Culture, Sports, Science and Technology, Japan. K.W. and K.G. acknowledge The Thailand Research Fund (TRF) and The Postgraduate Education and Research Program in Chemistry (PERCH) for financial support.

References

[1] K. H. Schosinsky, M. Vargas, A. L. Esquivel and M. A. Chavarria, *Clin. Chem*., **33**, 223 (1987).
[2] K. Jung, E. Nickel and M. Pergande, *Clin. Chim. Acta*, **187**, 163 (1990).
[3] Y. Fujita, I. Mori and S. Kitano, *Bunseki Kagaku*, **32**, E379 (1983).
[4] Y. Fujita, I. Mori, K. Ikuta, Y. Nakahashi, K. Kato and T. Nakanishi, *Chem. Pharm. Bull*., **37**, 2452 (1989).
[5] Y. Fujita, I. Mori and M. Toyoda, *Anal. Sci*., **7**, 771 (1991).
[6] Y. Fujita, *ICMR Annals*, **20**, 237 (2000).
[7] T. Yamaguchi, E. Amano, S. Kamino, S. Umehara, C. Yanaihara and Y. Fujita, *Anal. Sci*., **21**, 1237 (2005).
[8] C. Z. Huang, J. X. Zhu, K. A. Li and S. Y. Tong, *Anal. Sci*., **13**, 263 (1997).
[9] Y. Suzuki, *Bunseki Kagaku*, **52**, 269 (2003).
[10] Y. Suzuki, *Bunseki Kagaku*, **52**, 939 (2003).
[11] Y. Suzuki, *Bunseki Kagaku*, **42**, 497 (1993).
[12] Y. Suzuki, *Bunseki Kagaku*, **53**, 691 (2004).
[13] Y. J. Wei, K. A. Li and S. Y. Tong, *Talanta*, **43**, 1 (1996).
[14] Y. Fujita, I. Mori, K. Fujita, Y. Nakahashi and T. Nakanishi, *Yakugaku Zasshi*, **107**, 640 (1987).
[15] K. Yoshimoto, E. Kaneko and T. Yotsuyanagi, *Chem. Lett*., **29**, 6 (2000).
[16] K. Yoshimoto, E. Kaneko and T. Yotsuyanagi, *Bunseki Kagaku*, **49**, 363 (2000).
[17] S. Kasemsumran, Y. P. Du, K. Murayama, M. Huehene and Y. Ozaki, *Analyst*, **128**, 1471 (2003).
[18] L. Tan, L. Y. Liu, Q. J. Xie, Y. Y. Zhang and S. Yao, *Anal. Sci*., **20**, 441 (2004).
[19] M. Hashimoto, N. Teshima, T. Sakai and S. Katoh, *Bunseki Kagaku*, **54**, 789 (2005).
[20] J. Ruzicka and E.H. Hansen, *Anal. Chim. Acta*, **78**, 145 (1975).
[21] T. Shuto, M. Koga, I. Tanaka, T. Akiyama and H. Igusu, *Bunseki Kagaku*, **36**, 256 (1987).
[22] T. Korenaga, X. Z. Zhou, M. Izawa, T. Takahashi and T. Moriwaki, *Anal. Chim. Acta*, **261**, 67 (1992).
[23] T. Korenaga, M. Izawa, T. Takahashi and K. K. Stewart, *Bunseki Kagaku*, **40**, 481 (1991).
[24] L.G-Gracia, A.M.G-Campana, F.A. Barrero and L.C. Rodriguez, *Anal. Bioanal Chem*., **377**, 281 (2003).
[25] T. Sakai and N. Ishida, *Bunseki Kagaku*, **27**, 410 (1978).
[26] Y. Hosoi and S. Motomizu, *Bunseki Kagaku*, **38**, 205 (1989).
[27] Y. Hosoi and S. Motomizu, *Bunseki Kagaku*, **38**, 211 (1989).

(Received April 20, 2007)
(Accepted May 7, 2007)

Rodjana Burakham[1]
Supalax Srijaranai[1]
Kate Grudpan[2, 3]

[1]Department of Chemistry, Faculty of Science, Khon Kaen University, Khon Kaen, Thailand
[2]Department of Chemistry, Faculty of Science, Chiang Mai University, Chiang Mai, Thailand
[3]Institute for Science and Technology Research and Development, Chiang Mai University, Chiang Mai, Thailand

Original Paper

High-performance liquid chromatography with sequential injection for online precolumn derivatization of some heavy metals

HPLC was coupled with sequential injection (SI) for simultaneous analyses of some heavy metals, including Co(II), Ni(II), Cu(II), and Fe(II). 2-(5-Nitro-2-pyridylazo)-5-[*N*-propyl-*N*-(3-sulfopropyl)amino]phenol (nitro-PAPS) was employed as a derivatizing reagent for sensitive spectrophotometric detection by online precolumn derivatization. The SI system offers an automated handling of sample and reagent, online precolumn derivatization, and propulsion of derivatives to the HPLC injection loop. The metal–nitro-PAPS complexes were separated on a C_{18}-μBondapak column (3.9×300 mm^2). Using the proposed SI-HPLC system, determination of four metal ions by means of nitro-PAPS complexes was achieved within 13 min in which the parallel of derivatization and separation were processed at the same time. Linear calibration graphs were obtained in the ranges of 0.005–0.250 mg/L for Cu(II), 0.007–1.000 mg/L for Co(II), 0.005–0.075 mg/L for Ni(II), and 0.005–0.100 mg/L for Fe(II). The system provides means for automation with good precision and minimizing error in solution handling with the RSD of less than 6%. The detection limits obtained were 2 μg/L for Cu(II) and Co(II), and 1 μg/L for Ni(II) and Fe(II). The method was successfully applied for the determination of metal ions in various samples, including milk powder for infant, mineral supplements, local wines, and drinking water.

Keywords: HPLC / Metal ions / Nitro-PAPS / Online precolumn derivatization / Sequential injection

Received: May 18, 2007; revised: June 29, 2007; accepted: July 2, 2007

DOI 10.1002/jssc.200700215

1 Introduction

Metal ion analysis is of great importance in various fields, including food, pharmaceutical, medical, and environmental sciences. Numerous analytical techniques have been reported for the determination of heavy metals. The most widely used instruments, *e.g.*, atomic absorption [1–3] and inductively coupled plasma atomic emission spectrometers [4, 5], used for metal determination suffer from both spectral and chemical interferences and involve instrumentation complexity. A common UV–Vis spectrophotometry [6] is often simpler and less expensive than atomic spectroscopic methods but does not allow a multielemental analysis and requires derivatization process for improving the sensitivity and selectivity. HPLC [7–10] and ion chromatography [11] have been widely recognized as versatile methods for multielement and sensitive analyses of metal ions using either pre- or postcolumn derivatization. In a typical postcolumn procedure, a chromogenic reagent is mixed with column eluent in a postcolumn mixer and the derivatives formed are detected. To be useful, postcolumn reactions must be rapid and generate low background signals. Dead volume associated with connecting tubing, detector, and mixing devices must be minimized to avoid unnecessary peak dispersion. The precolumn derivatization procedure ensures that the excess of reagent is completely separated from the chelates and does not actually contribute to the increase in baseline signals at the peak positions of the chelates. This fact indicates that the attainable sensitivity is determined only by the inherent S/N of the detector. The potential of this approach is realized in the RP HPLC partition mode, including the ion-pair type. Ion-pair RP HPLC (IP-RPHPLC)

Correspondence: Dr. Rodjana Burakham, Department of Chemistry, Faculty of Science, Khon Kaen University, Khon Kaen 40002, Thailand
E-mail: rburakham@yahoo.com
Fax: +66-43-202373

Abbreviations: IP-RPHPLC, ion-pair RP HPLC; **Nitro-PAPS,** 2-(5-nitro-2-pyridylazo)-5-[*N*-propyl-*N*-(3-sulfopropyl)amino]phenol; **SI,** sequential injection

offers both sensitivity and selectivity owing to the large degree of flexibility in the separation parameters. Several chelating agents have been successively used as a derivatizing reagent such as 4-(2-pyridylazo)resorcinol (PAR) [10], 5-(2-hydroxy-5-nitrophenylazo)thiorhodamine [12], 2,4-dihydroxybenzylidenethiorhodamine [13], 1-(4-aminobenzyl) ethylenediamine-*N*,*N*,*N*′,*N*(-tetraacetate [14], 2-(5-bromo-2-pyridylazo)-5-(*N*-propyl-*N*-(3-sulfopropylamino)aniline (5-Br-PSAA) [15], and 2-(5-nitro-2-pyridylazo)-5-[*N*-propyl-*N*-(3-sulfopropyl)amino]phenol (nitro-PAPS) [16].

Precolumn derivatization is normally performed offline (batch) because of instrumentation simplicity. But offline manipulation is proved to be laborious, time consuming, especially if a number of samples is to be processed, and may result in low precision. On the other hand, online derivatization offers automation, ease and high sampling rate, providing an attractive alternative [17]. Some developments have involved the coupling of flow injection (FI) [10, 18–20] or sequential injection (SI) [17, 21] with HPLC for online precolumn derivatization. FI involves an inexpensive hardware and a simple operational basis, while SI offers high potential for higher degree in laboratory automation with less reagent consumption.

In this work, attempts were made for coupling IP-RPHPLC with SI for online precolumn derivatization and determination of some heavy metals, including Co(II), Cu(II), Ni(II), and Fe(II). Nitro-PAPS was used as the derivatizing reagent for a sensitive spectrophotometric detection. Application to a variety of samples was investigated. The method would provide simple, low consumption of sample and reagent, and easy operation with higher degree of automation. The chromatographic system could be an alternative for simultaneous analysis of some heavy metals.

2 Materials and methods

2.1 Chemicals and reagents

All the reagents used were of analytical reagent grade. Deionized water was used throughout the experiments. The atomic absorption standard solutions (1000 mg/L) of copper (II) nitrate and nickel (II) nitrate were obtained from Ajax Chemicals (Australia). Stock standard solution (1000 mg/L) of cobalt (II) was prepared using cobalt (II) chloride hexahydrate in water. Stock standard solution (1000 mg/L) of iron (II) was prepared by dissolving iron (II) sulfate heptahydrate in 10^{-4} mol/L hydrochloric acid. Working standards were freshly prepared by diluting the stock solution with water to obtain appropriate concentrations. Nitro-PAPS was obtained from Dojindo Laboratories (Japan). Tetrabutylammonium bromide (TBABr) was purchased from Fluka (Switzerland). ACN was of HPLC grade. All HPLC mobile phases were filtered through 0.45 μm membrane filters and sonicated prior to use.

2.2 Instrumentation

The SI-HPLC system used is schematically depicted in Fig. 1a. The SIA part consists of a 2.5 mL syringe pump (Cavro, USA), a 10-position selection valve VICI with a microelectric actuator (Valco Instruments, USA), and a holding coil (220 × 0.07 cm id PTFE tubing). Instrumentation control was manipulated *via* the FIAlab software (FIAlab Instruments, USA). The HPLC part consists of a Waters 6000A dual pump, a Rheodyne injector with a 50 μL injection loop, and a Waters 484 absorbance detector (Waters, USA) operated at the wavelength of 570 nm. The SI system was connected to the HPLC injection port by means of the 37 × 0.07 cm id PTFE tubing. Separations were performed on a 3.9 × 300 mm^2 C_{18}-μBondapak column with 5 μm particle size (Waters). The CSW 32 software (Waters) was used for data acquisition.

2.3 Procedure

Effective separation of the studied metal–nitro-PAPS complexes was achieved through the IP-RPHPLC mode using the mobile phase containing ACN, buffer and ion pairing agent. The column was equilibrated with the mobile phase being used for 25 column-volumes before start.

The SI-HPLC operation steps were as follows: the manifold lines were washed with water, and all the reagents were filled into the ports of the selection valve. Then, suitable volumes of the reagents were sequentially aspirated and stacked as zones in the holding coil. By flow reversal of the syringe pump, the reaction mixture, metal–nitro-PAPS complexes in this work, was propelled to the HPLC injection loop and injected into the HPLC system. A mobile phase flow rate of 1.0 mL/min was used throughout.

3 Results and discussion

3.1 IP-RPHPLC of metal–nitro-PAPS chelates

To achieve adequate separation for the studied chelates within a minimum elution time, optimization of the HPLC separation was performed by offline derivatization of metal–nitro-PAPS chelates. Nitro-PAPS chelates of Co(II), Ni(II), Cu(II), and Fe(II) were formed by mixing metal ion solutions and the nitro-PAPS solution with the concentration ratio of 1:2 and was manually injected in the HPLC system. It has been known that the composition of mobile phase plays an important role in IP-RPHPLC. The mobile phase components include concentration of buffer, pH, amount of organic modifier, and

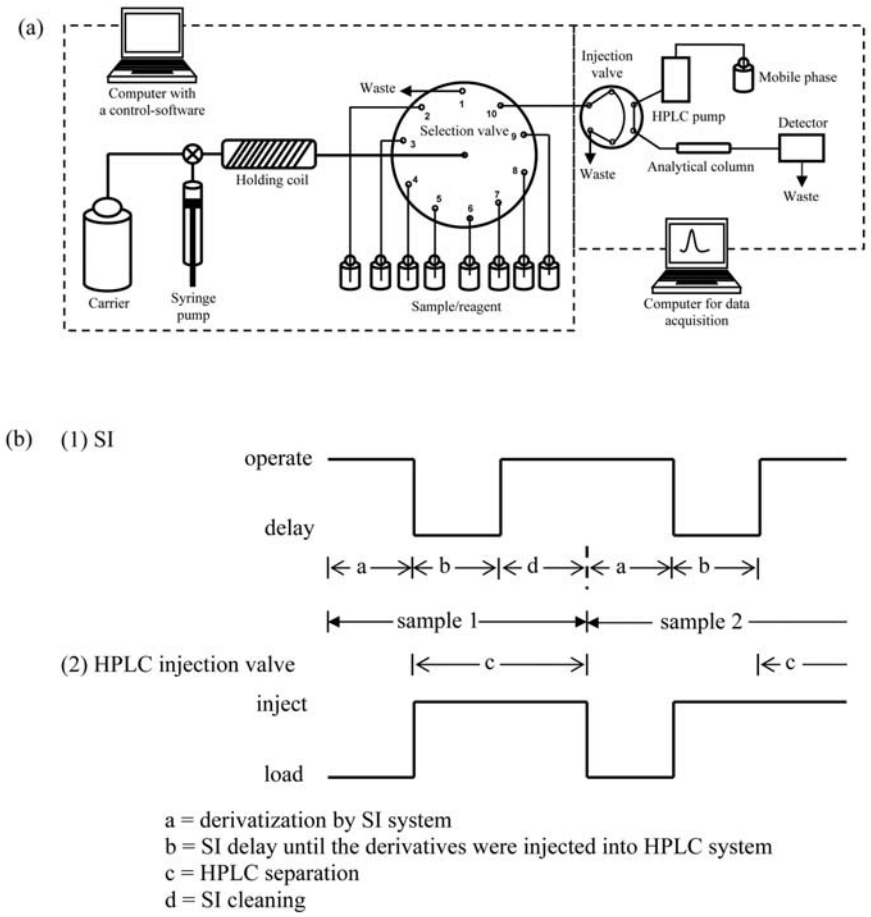

Figure 1. (a) Schematic diagram of the SI-HPLC system, (b) diagram of operational sequence of the SI-HPLC system.

concentration of ion pairing agent. The selectivity of the IP-RPHPLC was susceptible to the content of organic modifier in the mobile phase due to the variation in polarity and hydrophobicity which lead to different strengths and selectivity. The role of buffer is to control the pH of the chromatographic system, while the role of the ion pairing agent is to provide the exchange sites for the target analytes. Therefore, some degrees of variation in the retention behavior and chromatographic selectivity are expected by addition of ion pairing agent in IP-RPHPLC. The mobile phase was selected from our preliminary studies and was found to be 30% ACN in 10.0 mmol/L acetate buffer of pH 5.0 and 3.5 mmol/L TBABr. Separation of four metal–nitro-PAPS chelates and removal of excess nitro-PAPS reagent was achieved within 13 min with the elution order of Cu(II)-nitro-PAPS, Co(II)-nitro-PAPS, excess nitro-PAPS reagent, Ni(II)-nitro-PAPS, and Fe(II)-nitro-PAPS, respectively. The conditions were adopted for the coupling of SI to HPLC.

3.2 Online coupling of SI to HPLC

Using the SI-HPLC system shown in Fig. 1a, the experimental parameters affecting the sensitivity of the determination were considered. First, it must be ensured that the most concentrated part of the reaction mixture will be injected into the separation column. Therefore, after forming derivatives by the SI system, the dispensing volumes of the syringe pump ranging from 240 to 380 µL were optimized and the peak areas were compared. The dispensing volume (at a constant flow rate) determined the time interval between the start of dispensing of the derivative zone by the syringe pump of the SI system and the actual injection into the HPLC system. Second, the sequence orders of aspiration together with the volumes of sample and reagent and the number of flow reversals were examined. The operational sequence in which the sample and reagent were aspirated as small segments gave a higher sensitivity, while the mixing by several flow reversals was unnecessary. The metal–nitro-PAPS derivatives could be formed immediately and the sensitivity was enhanced by mixing during the transportation to the HPLC loop. However, the connection between the SIA part and the HPLC injection loop should be shortened to prevent further dispersion of the product zone. It has been known theoretically that increase in the sample and/or reagent volumes results in increase in the sensitivity but it must be compromised between the volumes

Table 1. The operational sequence of the SI-HPLC system for online derivatization of metal–nitro-PAPS complexes

Sequence	Port no.	Flow rate (μL/s)	Volume (μL)	Description
1	3–9	50	70	Aspiration of sample into HC[a)]
2	2	50	25	Aspiration of nitro-PAPS into HC
3	3–9	50	70	Aspiration of sample into HC
4	2	50	25	Aspiration of nitro-PAPS into HC
5	3–9	50	60	Aspiration of sample into HC
6	10	50	300	Propulsion of metal–nitro-PAPS derivatives to HPLC loop
7	10	–	–	HPLC analysis

a) HC = holding coil.

Table 2. Analytical characteristics of the proposed system

Metal–nitro-PAPS	Linear range (mg/L)	Linear equation	r^2	LOD[a)] (μg/L)
Cu(II)	0.005–0.250	$y = 1652.6x - 72.5$	0.9928	2
Co(II)	0.007–0.100	$y = 2479.5x - 3.2$	0.9968	2
Ni(II)	0.005–0.075	$y = 1607.8x - 1.5$	0.9945	1
Fe(II)	0.005–0.100	$y = 3018.0x - 4.9$	0.9938	1

a) S/N = 3.

of derivative product and the volume of the HPLC injection loop. The derivative should be formed such that it is just enough for injecting into the HPLC loop with adequate sensitivity and precision. In addition, the peak shape of the obtained chromatogram must be considered. On increasing the injection volume, a wider peak will be obtained and leads to overloading of the column. The selected operational sequences as well as the volumes of sample and reagent are summarized in Table 1 and Fig. 1b. Finally, the chemical parameter, the concentration of nitro-PAPS reagent, was varied to increase the sensitivity and minimize the excess of reagent concentration. The optimum results were obtained using a nitro-PAPS concentration of 1×10^{-4} mol/L. The sensitivity determined by the peak areas of all metal complexes remained constant and the peak of excess nitro-PAPS reagent was resolved from the derivative peaks. A typical chromatogram is presented in Fig. 2. Baseline disturbance was observed under an elution time of approximately 3–5 min from the time when the blank solution was injected, and this could be due to the excess of the reagent. Quantification of peak area using peak-to-peak baseline correction was carefully performed.

3.3 Analytical characteristics

Under the selected SI and HPLC conditions, quantitative features of the proposed system were evaluated by examining the linear range, precision, and LOD. Calibration graphs were constructed by plotting the peak area against the concentration of each metal ion. The detection limits were calculated at a signal level of three times

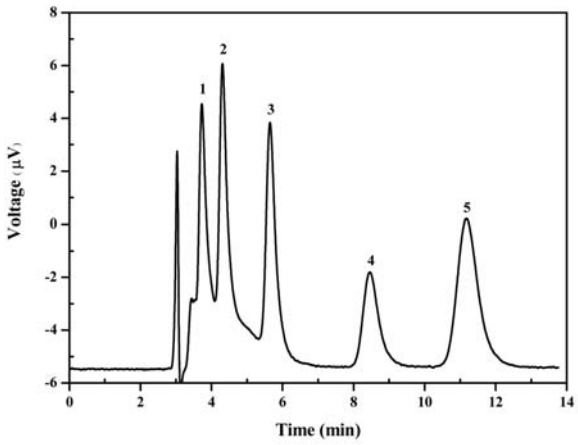

Figure 2. Typical chromatogram of metal–nitro-PAPS complexes: 1, 0.100 mg/L Cu(II); 2, 0.050 mg/L Co(II); 3, excess nitro-PAPS; 4, 0.075 mg/L Ni(II); 5, 0.075 mg/L Fe(II).

the baseline noise (S/N = 3). The equations of the obtained calibration graphs, the linear ranges, and the detection limits are given in Table 2. The RSDs of the peak area and retention time of each analyte were less than 6%. The effects of interferences on the SI-HPLC of metal–nitro-PAPS chelates were studied by adding the metal ions at different concentrations into a mixture of 0.060 mg/L Co(II), 0.010 mg/L Cu(II), Fe(II), and Ni(II). No interference, *i.e.*, no signal change within ±5%, was observed from common ions with the maximum concentrations studied up to 20 mg/L of Na^+, Ca^{2+}, and Cl^-; 25 mg/L of CO_3^{2-}, 30 mg/L of SO_3^{2-}, NO_2^-, and NO_3^-; and 50 mg/L of Cd^{2+}, Pb^{2+}, and Zn^{2+}.

3.4 Analysis of real samples

The applicability of the SI-HPLC system was investigated by determining the metal ions in various samples, including modified milk powder for infants, mineral supplements, local wines, and drinking water. For milk powder and supplement samples, fine powder samples were weighed, dissolved in water, and filtered before determination. For wines and drinking waters, the sam-

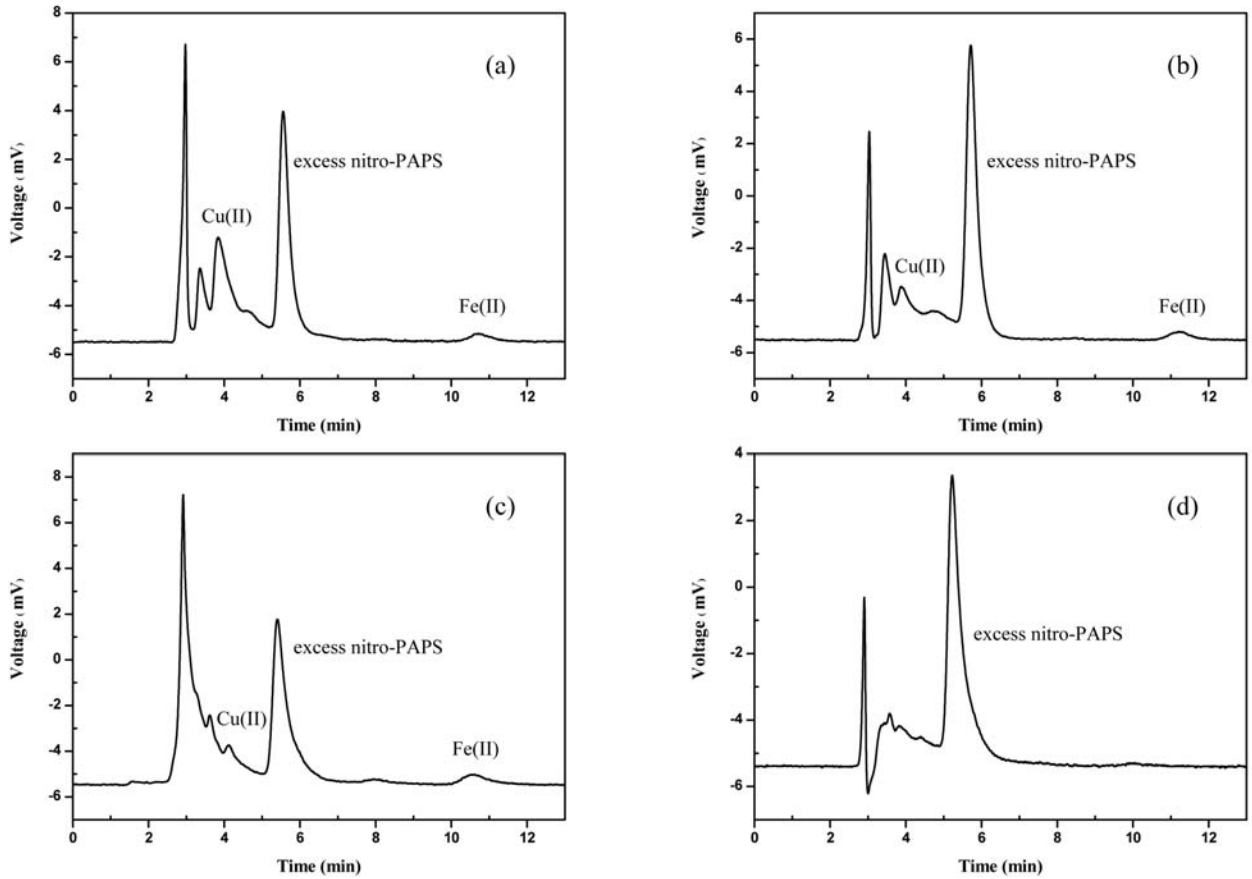

Figure 3. Chromatograms obtained from sample determination: (a) milk, (b) supplement, (c) wine and (d) drinking water.

Table 3. Analysis of real samples and recovery studies

Sample	Cu(II)			Co(II)			Ni(II)			Fe(II)		
	This work[a] (mg/L)	Labeled (mg/L)	Recovery (%)	This work (mg/L)	Labeled (mg/L)	Recovery (%)	This work (mg/L)	Labeled (mg/L)	Recovery (%)	This work[a] (mg/L)	Labeled (mg/L)	Recovery (%)
Milk 1	273.7 ± 2.1	312.0	91	–	–	99	–	–	99	5.8 ± 0.2	7.0	97
Milk 2	314.0 ± 3.6	340.0	95	–	–	98	–	–	96	5.5 ± 0.1	6.0	95
Milk 3	552.5 ± 1.8	580.0	97	–	–	99	–	–	99	7.2 ± 0.1	7.8	99
Supplement 1	1.6 ± 0.4	2.0	93	–	–	96	–	–	98	8.7 ± 0.1	10.0	97
Supplement 2	2.1 ± 0.1	2.5	90	–	–	99	–	–	99	12.9 ± 0.1	15.0	94
Wine 1	1.0 ± 0.2	1.4	102	–	–	94	–	–	105	1.5 ± 0.1	1.8	98
Wine 2	5.2 ± 0.6	6.8	93	–	–	97	–	–	102	1.8 ± 0.1	2.1	93
Wine 3	–	–	95	–	–	95	–	–	98	0.8 ± 0.2	1.0	105
Wine 4	–	–	106	–	–	101	–	–	96	0.2 ± 0.1	0.4	101
Water 1	–	–	93	–	–	99	–	–	99	–	–	98
Water 2	–	–	90	–	–	99	–	–	99	–	–	99

– Not detected.
Supplement 1 ingredients (tab^{-1}): Cu ($CuSO_4$) 2 mg, Fe ($FeSO_4$) 10 mg.
Supplement 2 ingredients (tab^{-1}): Cu ($CuSO_4$) 2.5 mg, Fe (ferrous gluconate) 15 mg.
[a] $n = 3$.

ples were analyzed by the system without any further pretreatment except filtration and dilution. Typical chromatograms of sample determination are shown in Fig. 3. The results, as shown in Table 3, were in agreement with the labeled values (for milk powder and mineral supplement samples) and those obtained by AAS methods (for wines and drinking water), evaluated by *t*-test at 95% confidence level. It was not surprising that some metal ions such as Co(II) and Ni(II) were not detectable in these samples and all metal ions in drinking water samples were lower than the LODs. However, the recoveries, assessed by experiment of known amounts of metal ions (0.020 mg/L each) spiked in the real samples, obtained were satisfactory (90 – 106%).

4 Concluding remarks

Coupling HPLC with SI offers an online precolumn derivatization system for analyses of some heavy metal ions. The derivatives can be formed online and subsequently injected and analyzed in the HPLC system. This leads to possibility in automation. By parallel operation of derivatization and separation, advantages of less consumption of sample/reagent, as well as better analysis time could be gained. It has been demonstrated that HPLC hyphenated with SI could be an alternative for simultaneous analyses of some heavy metal ions in various samples.

We thank the Thailand Research Fund (TRF) and the Commission on Higher Education (CHE). This work was partly supported by the Postgraduate Education and Research Program in Chemistry (PERCH). Thanks are due to Professor T. Sakai for supply of the reagent (Nitro-PAPS) which was under the Frontier Research Project – Materials for the 21st Century (Materials Development for Environment, Energy and Information).

5 References

[1] Lasztity, A., Kelko-Levai, A., Varga, I., Zih-Perenyi, K., Bertalan, E., *Microchem. J.* 2002, *73*, 59 – 63.

[2] Torrence, K., McDaniel, R., Self, D., Chang, M., *Anal. Bioanal. Chem.* 2002, *372*, 723 – 731.

[3] Quaresma, M., Cassella, R., Guardia, M., Santelli, R., *Talanta* 2004, *62*, 807 – 811.

[4] Benkhedda, K., Dimitrova, B., Infante, H., Ivanova, E., Adams, F., *J. Anal. At. Spectrom.* 2003, *18*, 1019 – 1025.

[5] Melaku, S., Dams, R., Moens, L., *Anal. Chim. Acta* 2005, *543*, 117 – 123.

[6] Riganakos, K., Veltsistas, P., *Food Chem.* 2003, *82*, 637 – 643.

[7] Matsumiya, H., Iki, N., Miyano, S., *Talanta* 2004, *62*, 337 – 342.

[8] Li, Z., Yang, G., Wang, B., Jiang, C., Yin, J., *J. Chromatogr. A* 2002, *971*, 243 – 248.

[9] Salar Amoli, H., Porgam, A., Bashiri Sadr, Z., Mohanazadeh, F., *J. Chromatogr. A* 2006, *1118*, 82 – 84.

[10] Srijaranai, S., Chanpaka, S., Kukusamude, C., Grudpan, K., *Talanta* 2006, *68*, 1720 – 1725.

[11] Sarzanini, C., Bruzzoniti, M. C., *Trends Anal. Chem.* 2001, *20*, 304 – 310.

[12] Hu, Q., Yang, X., Huang, Z., Chen, J., Yang, G., *J. Chromatogr. A* 2005, *1094*, 77 – 82.

[13] Dong, X., Han, Y., Hu, Q., Chen, J., Yang, G., *J. Braz. Chem. Soc.* 2006, *17*, 189 – 193.

[14] Saito, S., Danzaka, N., Hoshi, S., *J. Chromatogr. A* 2006, *1104*, 140 – 144.

[15] Gotoh, S., Teshima, N., Sakai, T., Ida, K., Ura, N., *Anal. Chim. Acta* 2003, *499*, 91 – 98.

[16] Teshima, N., Gotoh, S., Ida, K., Sakai, T., *Anal. Chim. Acta* 2006, *557*, 387 – 392.

[17] Zacharis, C. K., Theodoridis, G. A., Voulgaropoulos, A. N., *Talanta* 2006, *69*, 841 – 847.

[18] Dantan, N., Frenzel, W., Kuppers, S., *Chromatographia* 2001, *54*, 187 – 190.

[19] Luque de Castro, M. D., Valcarcel, M., *J. Chromatogr. A* 1992, *600*, 183 – 188.

[20] Hyotylainen, T., Savola, N., Lehtonen, P., Riekkola, M., *Analyst* 2001, *126*, 2124 – 2127.

[21] Zacharis, C. K., Theodoridis, G. A., Volgaropoulos, A. N., *J. Chromatogr. B* 2004, *808*, 169 – 175.

Anal Bioanal Chem (2007) 388:1839–1846
DOI 10.1007/s00216-007-1361-5

ORIGINAL PAPER

Exploiting flow injection system with mini-immunoaffinity chromatographic column for chondroitin sulfate proteoglycans assay

Supaporn Kradtap Hartwell · Kanokphan Pathanon · Duriya Fongmoon · Prachya Kongtawelert · Kate Grudpan

Received: 9 March 2007 / Revised: 8 May 2007 / Accepted: 10 May 2007 / Published online: 20 June 2007

Abstract A flow injection (FI) system with a mini-immunoaffinity chromatographic column was used to perform on-line assays of specific proteoglycans. The 300-μL mini-column contained beads coupled with monoclonal antibodies against the specific sulfation pattern of chondroitin sulfate proteoglycans, which have been reported to be a potential biomarker for cancer. The amount of these proteoglycans present was estimated indirectly from their protein content using the Bradford assay, which is an alternative to a direct carbohydrate assay. The system developed was tested by assaying for chondroitin sulfate proteoglycans in sera from patients with various cancers and comparing the results to those obtained for sera from healthy people. The results indicated that this approach could be used as a cost-effective alternative system for determining the amount of these specific biomarker proteoglycans. The column could be reused at least 90 times, with each run consisting of 200 μL of serum sample diluted twofold; an analysis rate of 30 min per run was achieved, as compared to 4 h for a batch procedure.

Keywords Flow injection · Immunoaffinity · Proteoglycans · Chromatographic column · Chondroitin sulfate · Cancers

S. K. Hartwell (✉) · K. Pathanon · K. Grudpan
Department of Chemistry, Faculty of Science and Institute for Science and Technology Research and Development, Chiang Mai University, Chiang Mai 50200, Thailand
e-mail: kradtas@yahoo.com

D. Fongmoon · P. Kongtawelert
Thailand Excellence Center for Tissue Engineering, Department of Biochemistry, Faculty of Medicine, Chiang Mai University, Chiang Mai 50200, Thailand

Introduction

Some diseases, such as cancers, can be difficult and expensive to diagnose at an early stage, which has led to the study and use of biomarkers by many researchers [1–7]. A good tumor marker should have the following characteristics: it should be cancer-specific; it should not exhibit elevated levels in a normal person; it should be easy to detect during the earliest stages of cancer; the marker signal should increase in strength as the cancer progresses [8–11]. Even though a cancer marker with all of the above characteristics is yet to be found, some tumor biomarkers have still proved useful. Examples of cancer biomarkers currently in use are carcinoembryonic antigen (CEA) [12, 13], prostate-specific antigen (PSA) [14, 15], and alpha fetoprotein (AFP) [16]. Many other new biomarkers are currently being studied [3, 4, 6, 8, 13]. Among them, certain proteoglycans have been studied as biomarkers of liver, joint, and cancer diseases in clinical research [17–20].

There are many modern biochemical techniques that have been used to study such biomarkers; for example, DNA and gene expression technology [2, 21], PCR [1, 13], immunoassay [16], as well as chromatography and mass spectrometry, such as matrix-assisted laser desorption/ionization (MALDI) and surface-enhanced laser desorption/ionization (SELDI) [10, 22, 23]. However, these standard high-performance techniques are simply not available in many rural areas of developing countries since they lack adequate facilities and funding. A simple and low-cost system that minimizes the need for well-trained operators would be very useful since it could be used to provide health care to people living in remote places where poverty and inadequate transportation often prevent access to a modern hospital.

Flow injection (FI) is a cost-effective and well-established technique that utilizes the continuous flow of solutions in a closed system. The chemical reactions and physical interactions of reagents and samples take place on-line, and the resulting product can be monitored simultaneously when coupled with a suitable detector [24–32]. The FI technique has been applied in many study areas, including environmental, food, industrial, and clinical studies [33–40]. Immunoaffinity chromatography has been used for the purification of substances from complex biological matrices [41, 42], and for the removal of small amounts of biological materials from large amounts of contaminating substances [43].

The work presented here was conducted to develop a simple and low-cost system to assay for chondroitin sulfate proteoglycans (proteoglycans that contain the specific sulfation pattern of chondroitin sulfate), which have been reported to be a potential biomarker for ovarian cancer [44–48]. The FI system allowed on-line isolation of the specific proteoglycans from nonspecific ones in a mini-immunoaffinity chromatographic column that was packed with specific monoclonal-antibody-coupled beads. Quantification of the specific proteoglycans was done indirectly by determining the amount of protein in the proteoglycans using a Bradford protein assay [49, 50], which gave a colored complex that could be quantified spectrophotometrically. Serum samples from patients with different types of cancer were studied to evaluate the potential of the proposed system as an alternative approach to assaying for the proteoglycans biomarker of interest. The system may provide an alternative and inexpensive method of on-line operation. This may reduce the need for experienced personnel during batchwise operation or an expensive automated system for the precise timing of incubation/washing steps and the precise manipulation of small volumes of reagents used in more complicated techniques such as a batchwise ELISA procedure.

Materials and methods

Reagents and apparatus

All chemicals used were of analytical grade unless specified otherwise. Monoclonal antibodies against the specific sulfation pattern of chondroitin sulfate were prepared in the laboratory. This is an IgM that can bind to A-1 shark proteoglycans. Its specificity was checked by ELISA, using an A-1 shark-coated well plate, peroxidase-conjugated mouse anti-IgM, and *O*-phenylenediamine substrate. The antibodies were coupled onto Sepharose 4B beads (Pharmacia Biotech, Piscataway, NJ, USA) through cyanogen-bromine (CNBr) activation. Bovine serum albumin (BSA, Sigma, St. Louis, MO, USA) was used as a standard protein.

Instruments used in this work include a B 5050 incubator (Heraeus, Hanau, Germany), an RS-60 tube rotator (BioSan, Riga, Latvia), a Mettler HK 160 autobalance (Mettler Instruments A.G., Greifensee, Switzerland), a 5301 concentrator (Eppendorf, Hamburg, Germany), a FOC-1 lyophilyzer (Martin Christ, Osterode, Germany), a Gast 0211-V45M-0230CX pump (Benton Harbor, MI, USA), a Mini-PROTEIN II electrophoresis cell and a model 200/2.0 Mini Trans-Blot electrophoretic and power supply (Bio-Rad, Hercules, CA, USA), a Vortex-Genie k-550-GE (Springfield, MA, USA), a UV-VIS spectrophotometer (UV 1200, Shimadzu, Kyoto, Japan), a pH meter (Beckman Coulter, Fullerton, CA, USA), a model 400 peristaltic pump (Watson–Marlow Alitea Co., Ltd., Stockholm, Sweden), a six-port bulkhead-mounted injection valve and four-way switching valve (Upchurch Scientific, Oak Harbor, WA, USA), a Spectronic 21 (Milton Roy Company, Ivyland, PA, USA) with a flow-through cell (Hellma, Plainview, NY, USA), BDS software for integration (BarSpec Ltd., Rehovot, Israel), and a Titertek Multiscan MCC/340 microplate reader (Labsystems Flow Laboratories, VA, USA).

Flow injection mini-immunoaffinity chromatographic column system

The flow manifold used in this work is represented diagrammatically in Fig. 1. The 0.1 M Tris-HCl buffer containing 0.15 M NaCl, pH 7.4, was pumped by a peristaltic pump to equilibrate the column for 2 min. Another peristaltic pump was used to pump the Bradford dye reagent (Bio-Rad) diluted in 30% v/v ethanol. Serum sample solution was injected into the column via a six-port injection valve with a 200-μL sample loop. 0.1 M acetate buffer with 0.5 M NaCl, pH 2.0, was used as the eluting buffer.

Results and discussion

The reagents and the beads

The monoclonal antibody used in this study is called WF6, which has been proved, as described in the international patent No. WO 2005/118645 A1 and previous reports [51, 52], to selectively bind to the specific sulfation pattern of chondroitin sulfate containing chondroitin-6-sulfate (CS-C). It was raised in mice and produced from serum-free media for hybridoma cell cultures.

Purification of monoclonal antibody using a thiophilic-gel (T-gel) column (Pierce Biotechnology, Rockford, IL, USA) was carried out according to the manufacturer's

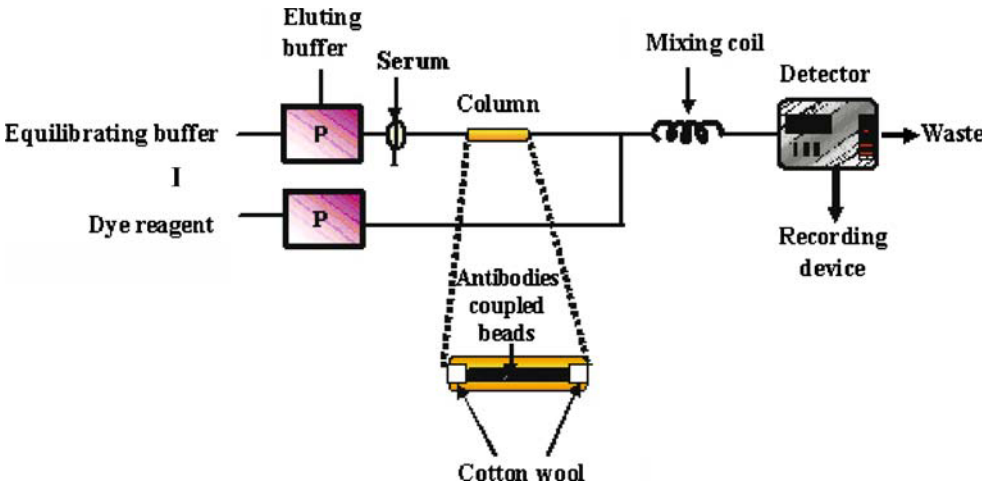

Fig. 1 Diagram of the FI system with a mini-immunoaffinity chromatographic column used to assay for specific proteoglycans. *P*, a peristaltic pump; *I*, six-port injection valve; *S*, sample; equilibrating buffer: 0.1 M Tris-HCl containing 0.15 M NaCl; eluting buffer: 0.1 M acetate buffer containing 0.5 M NaCl; dye reagent: Bradford. Pump tubing was Tygon® tubing with 1/16″ ID; all other tubing was made of Teflon with 1/32″ ID

instructions [53, 54]. Thiophilic adsorption is based on the ability of immunoglobulins to bind to an immobilized ligand that contains a sulfone group. Sodium phosphate buffer solutions with and without potassium sulfate were used to elute unbound and bound proteins, respectively. At a low salt concentration, i.e., without potassium sulfate added to the buffer, the disulfide bonds were broken and the bound proteins were released. The molecular weight of the monoclonal antibody from the bound fraction was identified using electrophoresis, and its specific activity was confirmed by ELISA prior to use.

Coupling of antibodies onto the beads was based on the standard CNBr method, as suggested by the manufacturer of Sepharose 4B (Phamacia Biotech) [55–58]. Sepharose 4B gel was first activated with cyanogen bromine (CNBr). At a high pH of 11–12, CNBr reacts with the –OH groups on the agarose beads to form reactive electrophilic cyanogen ester groups on the bead surfaces. This cyanogen ester reacted with the nucleophilic groups, e.g., $–NH_2$, –SH and –OH of the antibodies in the coupling buffer (0.1 M $NaHCO_3$, 0.5 M NaCl, pH 8.3). After washing away the excess antibodies, the remaining reactive cyanogen ester groups were blocked to prevent nonspecific binding by incubating beads in 0.2 M glycine, pH 8.0, for 2 h at 25 °C. Finally the beads were washed in 0.1 M acetate buffer containing 0.5 M NaCl, pH 4.0, followed by 0.1 M Tris-HCl buffer containing 0.5 M NaCl, pH 8.0. Antibody-coupled beads were maintained at 4 °C before use.

Separation of specific proteoglycans in the FI system

The target chondroitin sulfate proteoglycans in serum were isolated from other nonspecific proteoglycans by means of the FI system with the mini-immunoaffinity chromatographic column. The affinity column was packed with beads coupled with monoclonal antibody. When the serum samples were passed through the affinity column, nonspecific proteoglycans and other serum proteins were not retained by the antibody-coupled beads and were thus eluted out first with the equilibrating buffer (0.1 M Tris-HCl containing 0.15 M NaCl, pH 7.4). They formed a colored complex when mixed with the Bradford reagent, and gave a first peak (unbound peak) at 590 nm when detected with a Spectronic 21. After the baseline became constant, indicating that the nonspecific proteoglycans and other serum proteins had been removed, the eluting buffer (0.1 M acetate buffer containing 0.5 M NaCl, pH 2.0) was introduced to elute the specific proteoglycans, resulting in a second peak (the bound peak). The profile of the separation of proteoglycans into two groups, nonspecific and specific, is illustrated in Fig. 2, where A is the unbound peak and B is the bound peak, respectively. The column was cleaned with

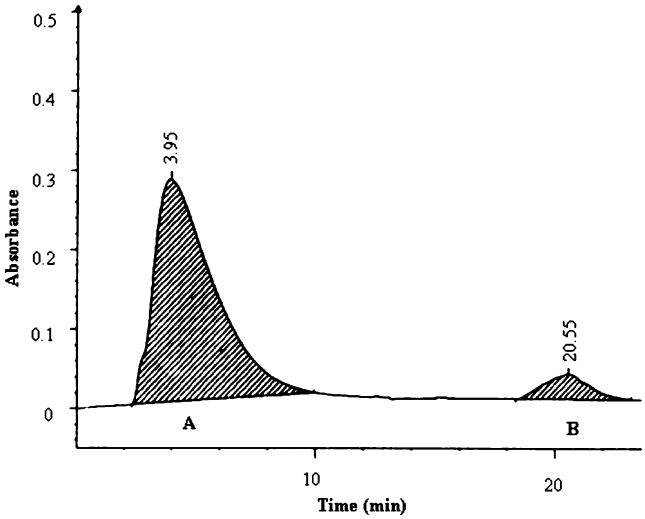

Fig. 2 Absorbance profile of the amount of protein in proteoglycans obtained using a Bradford dye assay after separating the specific proteoglycans (peak B) from the nonspecific proteoglycans (peak A) in normal serum sample using the FI system with a mini-immunoaffinity chromatographic column. Peak areas were integrated and the bound peak (peak B) percentage was calculated based on the total peak area (sum of the areas of peaks A and B)

approximately five times the column volume of the equilibrating buffer before the next sample analysis was started.

Using electrophoresis [59] and Western blotting [60, 61] techniques, the bound portion that was thought to contain the proteoglycans of interest was investigated to estimate the range of molecular weights of these proteoglycans and to confirm their specific activity, and then compare these properties to those of the unbound portion. The results showed that the amount of proteoglycans associated with the bound peak of cancer serum was greater than that associated with the bound peak from normal serum (seen at 70 kDa MW protein, results not shown). The unbound peak also contained specific proteoglycans but the amount associated with this peak was smaller than the amounts associated with the bound peaks in both the normal and cancer sera. The specific proteoglycans detected in the unbound peak may be proteoglycans that were hindered by other proteins or proteoglycans in serum and thus did not bind to the beads. Only the levels of specific proteoglycans associated with the bound peaks were used when analyzing serum samples.

Indirect estimation of the amount of specific proteoglycans from the amount of protein

The proportion of the total proteoglycans that were chondroitin sulfate proteoglycans was calculated based on a comparison of the protein content in the proteoglycans. Protein content was determined using the peak areas obtained from the Bradford protein assay, since this assay is much simpler to perform than a direct carbohydrate assay.

A possible limitation of this indirect protein assay is that the free chondroitin sulfate chains or fragments might not be detected. However, these fragments should not be found in serum in significant quantities due to the covalent nature of the bond between the protein core and the glycans. Even if free chondroitin sulfate is produced during the enzyme reactions and released into the serum, it should be bound to other serum proteins. In addition, the WF6 antibody exhibits specificity toward the pattern of chondroitin sulfate [51, 52], so other serum proteins without chondroitin sulfate should not interfere with an assay for the specific proteoglycans.

The performance of the proposed system was evaluated by determining the amount of protein in the specific proteoglycans in sera from patients with various cancers as compared to those from healthy people. It was assumed that the sum of the areas under peaks A and B (see Fig. 2) corresponds to the total protein. The amount of protein in the specific proteoglycans was estimated from the ratio of the area under peak B to the sum of the areas under peaks A and B. The ratio was converted into milligrams (mg) via a calibration plot constructed from a series of BSA standards that formed colored products when they react with Bradford reagent. BSA was chosen as the standard protein since it is widely available.

Optimization of the FI mini-immunoaffinity chromatographic column system

There are a few parameters of the FI mini-immunoaffinity chromatographic column system that need to be optimized. These include the concentrations of Bradford reagent and the solvent, the flow rate, the gel volume, the sample dilution ratio, the length of the mixing coil, and the pH of the buffer solutions. Optimization was performed using pooled serum samples from nine healthy people. This was to ensure an adequate number of samples for the optimization process.

It was observed that the Bradford dye could stick to the flow line and the wall of the flow-through cell when only water was used as a solvent. This caused the baseline to drift upwards over time, which made it difficult to integrate the peak area. Although the Bradford reagent is soluble in methanol [62], ethanol (which is less toxic) was tried as a solvent to eliminate the problem of the dye sticking to the tubing wall. The concentration of aqueous ethanol was varied from 10 to 40% (v/v), and a concentration of 30% (v/v) was chosen in order to conserve the reagent as much as possible while effectively preventing the colored Bradford reagent from sticking to the tubing wall.

The concentration of the Bradford reagent was also studied in order to save reagent. Various dilutions of the Bradford reagent with 30% (v/v) ethanol (1:10, 1:25, 1:50 and 1:100) were tried, and the 1:25 ratio was ultimately chosen.

The flow rate of the buffer solution greatly affected the performance of the system. When the flow rate was too high it led to a high back-pressure that caused leakage. When the flow rate was too low it increased the analysis time and lowered the sample throughput. Flow rates of 0.5, 1.0, 2.0, and 3.0 mL/min were investigated. A flow rate for the buffer and the Bradford reagent solution of 1.0 mL/min was selected.

The gel volume used also affected the results. Packing too much gel into the column caused high back-pressure, while too little gel led to the ineffective isolation of proteoglycans. The gel volume was varied by repacking the column with different volumes of gel. The optimum amount of gel, 300 μL, was chosen after testing the system with 200, 300, 400, and 500 μL of gel.

The highest concentration of sample that could be studied was related to the capacity of the column (i.e., the amount of gel used). However, if the sample concentration was too high, the specific proteoglycans would pass through the column without retention and would be considered to be nonspecific proteoglycans. To prevent such a false negative result, all samples introduced into the

column need to be diluted to the same dilution factor. In this study, dilution factors of 1:8, 1:4, and 1:2 were investigated and compared to the results obtained using the undiluted sample. A dilution factor of 1:2 was selected since it gave the best sensitivity.

The mixing coil is also an important part of this system. A coil that is too short will not provide enough time for the reaction to occur, while a coil that is too long will increase the analysis time and the dispersion of the product. The effect of varying the length of the mixing coil of 1/32″ ID (lengths of 25, 50, 100, 150 and 200 cm were studied) was evaluated, and a length of 150 cm was eventually chosen.

A poor choice of buffer solution pH would cause ineffective retention and separation of the proteoglycans, and could also damage the solid matrix. The effects of varying the pH of the equilibrating buffer (pH values of 6.5, 7.4, and 8.5 were tested) and the pH of the eluting buffer (2.0, 3.0 and 4.0 were tested) were investigated. pH values of 7.4 and 2.0, respectively, were selected, since these led to the best performance during the separation process and enabled the column to be reused.

These optimized parameters were employed during assays of chondroitin sulfate proteoglycans in serum samples taken from healthy people and cancer patients.

Performance of the system

Using the selected set of conditions described above, the same pooled serum sample from nine healthy people was analyzed 11 times consecutively. The average level of protein in the specific proteoglycans calculated from the 11 measurements was 1.87 mg in 100 mg total protein. The repeatability, expressed as %RSD, was calculated from the relative peak area of the bound proteoglycans, and was found to be 2.3. The lifetime of the column was estimated by performing the analysis with the same column over and over again until there was a significant reduction in the signal, as determined by the RSD of the system. Again, the same pooled serum was used in this study. The same column could be used more than 90 times without a significant reduction in signal. This indicates that the system gives satisfactory reproducibility. Each analytical run took about 30 min, including the washing time between each sample run. The sample volume of the twofold-diluted serum needed for each run was 200 μL.

Application of the system

The applicability of the FI system with the mini-immunoaffinity chromatographic column developed here to real-world samples was evaluated by using it to assay for chondroitin sulfate proteoglycans in serum samples from cancer patients (provided by hospitals). All serum samples were diluted twofold with 0.1M Tris-HCl, pH 7.4, prior to injection into the system.

These serum samples were catagorized into six groups, namely: 1) normal; 2) CEA or sera that had tested positive when screened for cervical cancer using the carcinoembryonic antigen tumor marker; 3) PSA or serum that had tested positive when screened for prostate cancer using the prostate specific antigen tumor marker; 4) prostate or sera from patients who were diagnosed of having prostate cancer; 5) cervix or sera from patients diagnosed with cervical cancer, and; 6) ovary or sera from patients diagnosed with ovarian cancer.

The relative amount of protein in the specific proteoglycans per 100 mg total protein was plotted for each sample from each group, as shown in Fig. 3. The average (and the standard deviation of this value) relative amount of monoclonal antibody specific proteoglycans was calculated for each sample group, and the results were compared with those for the normal samples using the *t*-test (statistical tests performed using Origin 7.0). It was found that the levels of the specific proteoglycans from the normal group were significantly lower than those of the other groups, with $P < 0.05$ (P values in all cases were no higher than 0.0005, or a confidence of level of at least 99.95%).

Various cutoff values were trialed when plotting the receiver operator characteristic (ROC) curve. The resulting curve showed that a relative amount of protein in specific proteoglycans of 2 mg per 100 mg total protein was the most suitable cutoff value. The numbers of true and false responses obtained for each cancer group when this cutoff value was used are summarized in Table 1. Among all

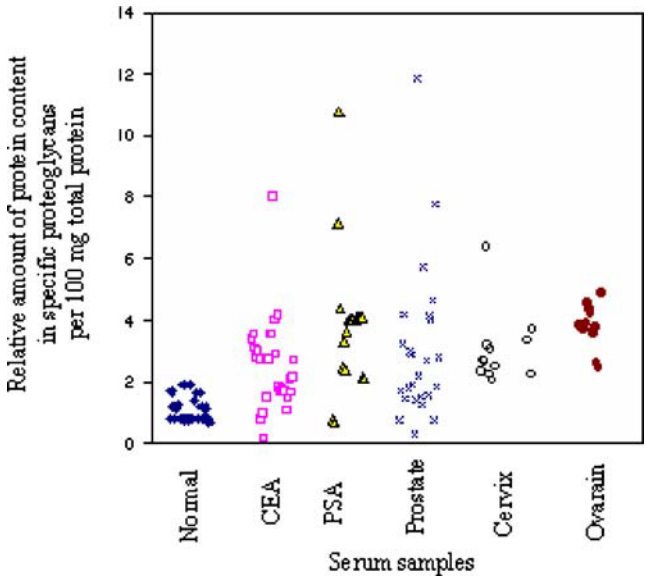

Fig. 3 Comparison of the amount of specific proteoglycans (based on the protein content) in sera from patients with different types of cancer

Table 1 Summary of the numbers of true and false responses and the sensitivity and specificity of the system obtained when 2 mg protein in specific proteoglycans per 100 mg total protein is chosen as a cutoff value

Sample group	No. of samples	Avg. % protein in specific proteoglycans*	TP*	FN*	TN*	FP*	SV*	SP*	Prob. positive*
Normal	25	1.26±0.64	-	-	25	0	-	1.00	-
CEA	27	2.64±1.48	16	11			0.59		1.00
PSA	21	3.18±2.53	13	8			0.62		1.00
Prostate	25	3.01±2.52	13	12			0.56		1.00
Cervix	12	3.03±1.17	12	0			1.00		1.00
Ovarian	14	3.79±0.66	14	0			1.00		1.00

* *Avg. % protein in specific proteoglycans* is the average relative amount of protein in specific proteoglycans per 100 mg total protein, calculated based on the area of the bound peak and using BSA as a standard protein

TP is true positive or the number of diseased patients that test positive

FN is false negative or the number of diseased patients that test negative

TN is true negative or the number of nondiseased patients that test negative

FP is false positive or the number of nondiseased patients that test positive

The same TN, FP, and SP were used for all cancer cases because they are based on the same normal group.

SV is sensitivity or $\frac{\text{number of diseased patients with positive test}}{\text{number of diseased patients}} = \frac{TP}{TP+FN}$

SP is specificity or $\frac{\text{number of nondiseased patients with negative test}}{\text{number of nondiseased patients}} = \frac{TN}{TN+FP}$

$\text{Prob. positive is probability of disease if the test is positive} = \frac{TP}{TP+FP}$

groups, the ovarian cancer group showed the highest average amount of specific chondroitin sulfate proteoglycans. The test showed very good sensitivity and specificity for the ovarian and cervical cancer groups, while lower sensitivities were obtained for other groups. The CEA, PSA and prostate groups showed high percentages of false negative results, which indicate that assays for this particular proteoglycan biomarker may not be suited to these three sample groups. The ROC plot also revealed that the ovarian group yielded higher sensitivity and specificity for all cutoff values than the other cancer groups. These results agree with previously reported studies which found that an elevated amount of chondroitin sulfate proteoglycans is associated with the existence of cancer and other disorders of the ovary [44–48]. The same trends were seen in a preliminary study performed by our group using batchwise competitive ELISA with A-1 shark, which showed that the average amount of chondroitin sulfate proteoglycans in samples from people with ovarian cancer was significantly higher than it was in samples from healthy people. However, the results in Fig. 3 also show that the levels of these specific proteoglycans obtained for various cancers overlap. Therefore, it would be necessary to consider the level of some other complementary biomarker in addition to the level of these specific proteoglycans in order to predict the specific type of cancer. In addition, a larger number of samples would be needed for an in-depth evaluation of the method and to determine a more precise cutoff value. A future study with increased numbers of samples from both the normal and each of the cancer groups is planned in order to validate the reliability of this method for routine analysis.

Nevertheless, this preliminary study illustrates the ability of the proposed system to assay for the amount of specific proteoglycans, which is a candidate biomarker for ovarian cancer. The results obtained here show the same trends as seen in the results of previous reports [44–48]. The proposed simple semi-automatic system showed good performance and yielded results that agree with those obtained using the more complicated batchwise ELISA process. The main advantages of this system are its relatively low cost, its relatively short analysis time per run, and the reduced need for highly trained personnel to perform the test in a batchwise procedure. This system would be beneficial in cases where a batch of a small-to-medium number of samples need to be tested, as well as in situations where modern medical facilities are not available.

Conclusion

A FI system with a mini-immunoaffinity chromatographic column was untilized to assay for chondroitin sulfate proteoglycans, a candidate biomarker for ovarian cancer. This approach involves indirectly quantitating the specific proteoglycans using the Bradford protein assay. The performance of the system developed here was evaluated by performing assays of chondroitin sulfate proteoglycans in human serum samples. The column could be reused over 90 times, even when the assays involved blood matrices.

The flow system offers a semi-automated capability in which the analyte can be isolated and monitored on-line. This economical system has the potential to be developed further for use as an alternative routine screening test for some proteoglycan-based biomarkers.

Acknowledgements We acknowledge the Thailand Research Fund (TRF), the Commission on Higher Education (CHE), the National Research Council of Thailand (Drugs and Chemicals Project), and the Center for Innovation in Chemistry:Postgraduate Education and Research in Chemistry(PERCH-CIC) for their support. We also thank Prof. Robert Kennedy, Prof. Jonathan Sweedler, Dr. Pises Pisespongsa, M.D., Dr. Jaroon Jakmunee, and Dr. Somchai Lapanantnoppakhun for their valuable comments.

References

1. Kelleher TB, Mehta SH, Bhaskar R, Sulkowski M, Astemborski J, Thomas DL, Moore RE, Afdhal NH (2005) J Hepatol 43:78–84
2. Mengel M, Kreipe H, von Wasielewski R (2003) Appl Immunohistochem Mol Morphol 11:261–268
3. Wu Y, Han B, Sheng H, Lin M, Moore PA, Zhang J, Wu J (2003) Int J Cancer 105:724–732
4. Wang K, Liu N, Radulovich N, Wigle DA, Johnston MR, Shepherd FA, Minden MD, Tsao M (2002) Oncogene 21:7598–7604
5. Gan Y, Wientjes G, Au JL (1998) Clin Cancer Res 4:2949–2955
6. Liu N, Gao F, Han Z, Xu X, Underhill CB, Zhang L (2001) Cancer Res 61:5207–5214
7. Arican M, Carter SD, Bennett D (1996) Br Vet J 152:411–423
8. Bharti A, Ma PC, Maulik G, Singh R, Khan E, Skarin AT, Salgia R (2004) Anticancer Res 24:1031–1038
9. Celis JE, Gromov P, Cabezon T, Moreira JMA, Ambartsumian N, Sandelin K, Rank F, Gromova I (2004) Mol Cell Proteomics 3:327–344
10. Shiwa M, Nishimura Y, Wakatabe R, Fukawa A, Arikuni H, Ota H, Kato Y, Yamori T (2003) Biochem Biophy Res Com 309:18–25
11. Lamberts SWJ, Hofland LJ, Nobels FRE (2001) Front Neuroendocrinol 22:309–339
12. Duffy MJ, van Dalen A, Haglund C, Hansson L, Klapdor R, Lamerz R, Nilsson O, Sturgeon C, Topolcan O (2003) Eur J Cancer 39:718–727
13. Sakakura C, Takemura M, Hagiwara A, Shimomura K, Miyagawa K, Nakashima S, Yoshikawa T, Takagi T, Kin S, Nakase Y, Fujiyama J, Hayasizaki Y, Okazaki Y, Yamagishi H (2004) Br J Cancer 90:665–671
14. Pauler DK, Finkelstein DM (2002) Stat Med 21:3897–3911
15. Saffran DC, Reiter RE, Jakobovits A, Witte ON (1999) Cancer Metastasis Rev 18:437–449
16. Beneduce L, Castaldi F, Marino M, Tono N, Gatta A, Pontisso P, Fassina G (2004) Int J Biol Markers 19:155–159
17. Kongtawelert P, Brooks PM, Ghosh P (1989) J Rheumatol 16:1454–1459
18. Paradis V (2005) J Hepatol 43:913–914
19. Hook M, Kjellen L, Johansson S (1984) Annu Rev Biochem 53:847–869
20. Horai T, Nakamura N, Tateishi R, Hattori S (1981) Cancer 48:2016–2021
21. Sugita M, Geraci M, Gao B, Powell RL, Hirsch FR, Johnson G, Lapadat R, Gabrielson E, Bremnes R, Bunn PA, Franklin WA (2002) Cancer Res 62:3971–3979
22. Ball G, Mian S, Holding F, Allibone RO, Lowe J, Ali S, Li G, McCardle S, Ellis IO, Creaser C, Rees RC (2002) Bioinformatics 18:395–404
23. Qu Y, Adam B, Yasui Y, Ward MD, Cazares LH, Schellhammer PF, Feng Z, Semmes OJ, Wright GL (2002) Clin Chem 48:1835–1843
24. Grudpan K (2004) Talanta 64:1084–1090
25. Hartwell SK, Christian GD, Grudpan K (2004) TrAC 23:619–623
26. Cankur O, Korkmaz D, Ataman OY (2005) Talanta 66:789–793
27. Quintás G, Armenta S, Morales-Noé A, Garrigues S, dela Guardia M (2003) Anal Chim Acta 480:11–21
28. Grudpan K, Nacapricha D, Wattanakanjana Y (1991) Anal Chim Acta 246:325–328
29. Sant'Ana OD, Wagener ALR, Santelli RE, Cassella RJ (2002) Talanta 56:673–680
30. Grudpan K, Jakmunee J, Sooksamiti P (1998) Lab Robot Autom 10:25–31
31. Dressler VL, Pozebon D, Curtius AJ (1998) Spectrochim Acta 53B:1527–1539
32. Sooksamiti P, Geckeis H, Grudpan K (1996) Analyst 121:1413–1417
33. Sakai T, Tanaka S, Teshima N, Yasuda S, Ura N (2002) Talanta 58:1271–1278
34. Khampha W, Yakovleva J, Isarangkul D, Wiyakrutta S, Meevootisom V, Emnéus J (2004) Anal Chim Acta 518:127–135
35. Myint A, Zhang Q, Liu L, Cui H (2004) Anal Chim Acta 517:119–124
36. LeThanh H, Lendl B (2000) Anal Chim Acta 422:63–69
37. Catalá Icardo M, Giménez Romero D, García Mateo JV, Martínez Calatayud J (2000) Anal Chim Acta 407:187–192
38. Hartwell SK, Srisawang B, Kongtawelert P, Christian GD, Grudpan K (2005) Talanta 65:1149–1161
39. Yamamoto K, Ohgaru T, Torimura M, Kinoshita H, Kano K, Ikeda T (2000) Anal Chim Acta 406:201–207
40. Narinesingh D, Ngo TT (2002) Anal Chim Acta 453:53–61
41. Battersby JE, Vanderlaan M, Jones AJS (1999) J Chromatogr B 728:21–33
42. Nishino T, Nishino T, Tsushima K (1981) FEBS Lett 131:369–372
43. Palombo G, Verdoliva A, Fassina G (1998) J Chromatogr B 715:137–145
44. Meng N, Nakashima N, Nagasaka T, Fukatsu T, Nara Y, Yoshida K, Kawaguchi T, Takeuchi J (1994) Pathol Int 44:205–212
45. Isogai Z, Shinomura T, Yamakawa N, Takeuchi J, Tsuji T, Heinegard D, Kimata K (1996) Cancer Res 56:3902–3908
46. Nash MA, Deavers MT, Freedman RS (2002) Clin Cancer Res 8:1754–1760
47. Kokenyesi R (2001) J Cell Biochem 83:259–270
48. Pothacharoen P, Siriaunkgul S, Ong-Chai S, Supabandhu J, Kumja P, Wanaphirak C, Sugahara K, Hardingham T, Kongtawelert P (2006) J Biochem 140:517–524
49. Darbre A (1987) Practical protein chemistry: a handbook. Wiley, Chichester, UK, pp 294–295
50. Bradford MM (1976) Anal Biochem 72:248–254
51. Kongtawelert P, Hardingham T, Ong-Chai S, Sugahara K (2005) Antibody specific for a chondroitin sulfate epitope (Int. Pub. No. WO2005/118645 A1). World Intellectual Property Organization, Geneva
52. Pothacharoen P, Teekachunhatean S, Louthrenoo W, Yingsung W, Ong-Chai S, Hardingham T, Kongtawelert P (2006) Osteoarthr Cartil 14:299–301
53. Pierce Biotechnology (2006) Instructions for T-gel adsorbent. http://www.piercenet.com/files/0406as4.pdf. Cited 2 Nov 2005
54. Porath J, Maisano F, Belew M (1985) FEBS Lett 185:306–310
55. Janson J, Rydn L (1989) Protein purification: principles, high-resolution methods and applications. Wiley-VCH, New York
56. Jurado LA, Jarrett HW (2003) J Chromatogr A 984:9–17
57. Porath J, Aspberg K, Drevin H, Axen R (1973) J Chromatogr A 86:53–56

58. Pharmacia Biotech (2002) Instructions for EAH Sepharose 4B, 71-7097-00 Edition AC. Pharmacia Biotech, Piscataway, NJ
59. Hoefer Scientific Instruments (1994) Protein electrophoresis: applications guide. Hoefer Scientific Instruments, San Francisco, CA
60. Roche Diagnostics GmbH (2004) BM chromogenic Western blotting kit (AP, mouse/rabbit). http://www.roche-applied-science.com/pack-insert/1647644a.pdf. Cited 2 Nov 2005
61. Bio-Rad (2005) Mini Trans-Blot electrophoretic transfer cell: instruction manual (catalog numbers 170-3930, 170-3935). Bio-Rad, Hercules, CA. http://www.bio-rad.com/cmc_upload/0/000/013/280/M1703930E.pdf. Cited 29 May 2007
62. Bio-Rad (2005) Protein Assay Manual Bio-Rad, Hercules, CA. http://www.fhcrc.org/science/labs/hahn/methods/biochem_meth/biorad_assay.pdf. Cited 29 May 2007

ANALYTICA CHIMICA ACTA 604 (2007) 139–146

available at www.sciencedirect.com

ScienceDirect

journal homepage: www.elsevier.com/locate/aca

Successive determination of urinary protein and glucose using spectrophotometric sequential injection method

Kanchana Watla-iad[a,b], *Tadao Sakai*[a,*], *Norio Teshima*[a], *Shuji Katoh*[c], *Kate Grudpan*[b]

[a] *Department of Applied Chemistry, Aichi Institute of Technology, 1247 Yachigusa, Yakusa-cho, Toyota 470-0392, Japan*

[b] *Department of Chemistry, Chiang Mai University, Chiang Mai 50200, Thailand*

[c] *Murakami Memorial Hospital, Asahi University, Hashimoto-cho, Gifu 500-8523, Japan*

ARTICLE INFO

Article history:
Received 15 August 2007
Received in revised form
5 October 2007
Accepted 8 October 2007
Published on line 13 October 2007

Keywords:
Sequential injection
Spectrophotometry
Successive determination
Urinary protein and glucose
Ion association with tetrabromophenolphthalein ethyl ester
Catalytic reaction
Screening for diabetic

ABSTRACT

A new sequential injection (SI) system with spectrophotometric detections has been developed for successive determination of protein and glucose. The protein assay is based on ion-association of protein with tetrabromophenolphthalein ethyl ester (TBPE) in the presence of Triton X-100 at pH 3.2. The blue product is monitored for absorbance at 607 nm. For glucose, hydrogen peroxide, generated by the oxidation of glucose in the presence of glucose oxidase immobilized on glass beads packed in a minicolumn, is monitored using iron-catalyzed oxidation reaction of *p*-anisidine to form a red colored product (520 nm). The SI procedure takes advantage in performing the protein assay during the incubation period for glucose oxidation. Linear ranges were up to 10 mg dL^{-1} human serum albumin (HSA) with a limit of detection (LOD) (3σ) of 0.3 mg dL^{-1}, and up to 12.5 mg dL^{-1} glucose with LOD of 0.08 mg dL^{-1}. R.S.D.s ($n = 11$) were 2.7% and 2.5% (for 1 mg dL^{-1} and 5 mg dL^{-1} HSA) and 1.4% (9 mg dL^{-1} glucose). Sample throughput for the whole assay of both protein and glucose is 6 h^{-1}. The automated system has been demonstrated for the successive assay of protein and glucose in urine samples taken from diabetic disease patients, with good agreement with the other methods. This developed SI system is an alternative automation for screening for diabetic diagnosis.

1. Introduction

Proteins synthesized in the liver are building blocks for all body parts. Usually, most proteins are too big to pass through kidneys' filters into urine unless the kidneys are damaged. Therefore, appearance of proteins in urine is an important indicator to proteinuria. Over 30% of patients who started undergoing artificial dialysis in Japan in 2000 were the result diabetic nephropathy [1], and diabetes is closely related to kidney failure. Hence, urinary glucose, which also is an important indicator to diabetes, should be monitored for diagnosis of renal disease.

For semi-quantitative assay of protein and glucose in the clinical laboratory [2], a strip of specially treated paper with dyestuff is commonly used for convenient and rapid examination. The color appearance on the urine test paper relates to

* *Corresponding author*. Tel.: +81 565 48 8121; fax: +81 565 48 0076.
E-mail address: tadsakai@aitech.ac.jp (T. Sakai).
0003-2670/$ – see front matter © 2007 Elsevier B.V. All rights reserved.
doi:10.1016/j.aca.2007.10.010

the amount of abnormal values in urine. However, it does not offer accurate analytical values and the determinable range is rough. Therefore, simultaneous and automated protein and glucose quantification in clinical diagnosis requires a method that is more accurate for screening.

Protein dye-binding assays are simple, rapid and becoming increasingly popular for the clinical determination of the total protein. Bromophenol blue was proposed for a simple spectrophotometric determination of urinary albumin [3,4]. Fujita et al. reported highly sensitive spectrophotometric methods for urinary protein with dye-metal complexes and micelle media [5–9]. Simple and rapid analytical methods with bromochlorophenol blue were proposed for protein detection [10,11]. However, the methods mentioned above are manual and consume large amounts of reagents.

Flow injection analysis proposed by Ruzicka and Hansen is a versatile and convenient technology for clinical and pharmaceutical analysis [12]. A highly sensitive flow injection method was proposed for the determination of proteins using Coomassie Brilliant Blue G-250 (CBB) [13]. Zaia et al. found that total protein obtained by using the Bradford method was not statistically different ($p > 0.05$) from the results obtained by the Biuret standard method [14]. However, a short linear range for the calibration graph was offered by this method.

Sakai et al. have reported that tetrabromophenolphthalein ethyl ester (TBPE) anion has a larger molar absorptivity (10^5 L mol^{-1} cm^{-1}), comparing with bromophenol blue and bromocresol green [15]. Fortunately, it was found that TBPEH dissolved in the micelle formed by adding Triton X-100. Consequently, it is possible to use TBPEH as a chromogenic reagent for the protein–TBPE associate formation. In a previous paper [16], TBPEH in the micelle was applied to the FIA procedure for the protein determination at less than 1 mg dL^{-1} level.

Glucose can be determined using *o*-toluidine by batchwise [17] and/or on-line procedure [18], but it requires heating. Glucose oxidase is widely used for quantitative analysis of glucose in body fluids [19,20] due to selectivity, but it is a tedious method.

Flow injection determination of glucose using glucose oxidase (GOD) immobilized on controlled porosity glass (CPG) was reported [21–23]. Hydrogen peroxide generated by the oxidation of glucose in the presence of GOD was monitored using an iron-catalyzed oxidative coupling of 4-aminoantipyrine with *N*,*N*-dimethylaniline [23]. While FIA shows some advantages for practical analyses, because of the continuous flow of the reagents it still consumes relatively high amounts of reagents, resulting in higher amount of laboratory waste in comparison to the second generation, sequential injection analysis (SIA).

We recently found that vanadium acted as a catalyst for the oxidation of *p*-anisidine by bromate [24]. Furthermore, preliminary experiments in this paper reveal that iron has a catalytic effect on the oxidation of *p*-anisidine by hydrogen peroxide and that this catalytic reaction is useful for an alternative indicator reaction of glucose. As a result, we propose here a new automated sequential injection method for successive determination of protein with TBPE and glucose based on the new catalytic reaction by iron in urinary samples. This should be useful to diagnostic screening for diabetic disease.

2. Experimental

2.1. Reagents

All chemicals used were of analytical-reagent grade and were used without further purification. The DI water used throughout the experiments was purified by an Advantec GSH-210 apparatus.

Stock standard solutions were of human serum albumin (HSA) (100 mg dL^{-1}) using MW: 66,000, Seikagaku Kogyo and glucose (180 mg dL^{-1}) prepared by dissolving D-(+)-glucose (Nakarai Chemicals Co., Osaka) in water with standing for at least 12 h before use, to ensure mutarotation equilibrium. Working standard solutions were obtained by mixing the HSA and glucose stock solutions for appropriate concentrations.

Stock solutions of TBPE (1.0×10^{-3} M) and Triton X-100 (0.5%, w/v) were prepared by dissolving tetrabromophenolphthalein ethyl ester potassium salt (MW: 700, Tokyo Kasei, Tokyo) in ethanol and *t*-octylphenoxypolyethoxyethanol (Sigma Chemical) in water, respectively.

A *p*-anisidine solution (0.1 M) was prepared by dissolving *p*-anisidine (Wako Pure Chemical Co., Japan) in water.

An iron(II) stock solution (0.1 M) was obtained by dissolving iron(II) sulphate (MW: 278.01, Wako Pure Chemical Co.) in 0.005 M sulfuric acid.

Buffer solutions were prepared by adding acetic acid in 0.5 M sodium acetate solution to adjust pH values to be 3.2 and 4.5 for protein and glucose assay, respectively.

Controlled porosity glass beads (200–400 mesh size, 182 Å mean pore size) were obtained from Sigma Chemical Company. Glucose oxidase (E.C.1.1.3.4) from *Aspergillus sp.* (200 U mg^{-1}) was obtained from Roche Diagnostics, USA. A working solution of glucose oxidase was obtained by dissolving the enzyme in phosphate buffer (4 °C, pH 7.0) and with suitable dilution. Aqueous aminoalkylating agent (10%) was prepared by adding 5.2 mL of 3-aminopropyltriethoxysilane (99%, Acros organics) to 50 mL of water and the pH was carefully adjusted to 3.45 with hydrochloric acid. The cross-linking agent (2.5%) was prepared by adding 2.5 mL of glutaraldehyde (50%, Kanto Kagaku Co., Japan) to 50 mL of water.

2.2. Apparatus

A schematic diagram of the SI system for successive analysis of protein and glucose in urine samples is shown in Fig. 1. The flow lines were of Teflon tubings (0.5 mm inner diameter). Flows of the carrier and reagent were controlled by a syringe pump (FIAlab instruments, USA) and a 10-port selection valve (C25-3180EMH, Valco instruments Co. Inc.). The enzymatic column was immersed in circulating thermostated water bath at 37 °C (Thermo minder SM-05, Taitec, Japan). Absorbance was monitored at 607 nm for protein determination and at 520 nm for glucose analysis. The detection unit consisted of a tungsten halogen light source (LS-1, FIAlab Instruments, USA) and a spectrometer (USB2000, Ocean Optics, USA) and fiber optic cables (P200-2-UV/Vis, FIAlab instruments, USA) and Z-cell (home made, path length 10 mm). The FIAlab software was used to control the system and some signal processing. Peak evaluation was made by using the Origin software with man-

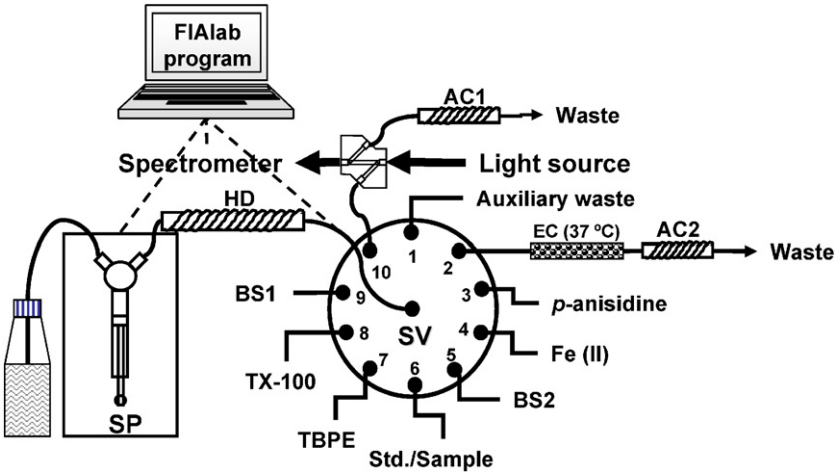

Fig. 1 – Manifold of the SI system for successive determination of protein and glucose in urine samples. HD: holding coil, EC: enzyme column (4.5 cm × 2 mm), AC: auxiliary coil, SV: 10-port selection valve, SP: syringe pump, BS1: 0.5 M acetate buffer pH 3.2, BS2: 0.5 M acetate buffer pH 4.5, TX-100: 0.1% Triton X-100, TBPE: 1×10^{-4} M tetrabromophenolphthalein ethyl ester, Fe(II): 5×10^{-3} M iron(II), *p*-anisidine: 0.1 M *p*-anisidine.

ual operation for each peak: peak area for protein while peak height for glucose.

2.3. *Procedure*

2.3.1. *Immobilization of enzyme on glass beads*

The immobilization of enzyme was performed by following procedures described in previous reports [21–23]. A 5 g amount of CPG was boiled in 300 mL of 5% nitric acid for 30 min. The CPG was washed with water and dried in an oven at 95 °C for 12 h. After that, 10% of 3-aminopropyltriethoxysilane solution (pH 3.45) was added to the dried glass beads with a ratio of 20 mL to 1.0 g of the glass. The mixture was left at 75 °C in a water bath for 2.5 h. The chemically modified alkylamino glass was washed and dried in an oven at 115 °C for 8 h. After that, the alkylamino glass (1 g) was added to 5 mL of an aqueous glutaraldehyde solution (2.5%) and was kept under reduced pressure for 30 min and then kept under atmospheric pressure for 2 h. The activated glass beads were washed with water. Glucose oxidase (100 mg) was dissolved in a cold phosphate buffer (0.1 M, pH 7.0, 4 °C) and added to the activated glass beads. The mixture was kept at 4 °C for 2.5 h. The immobilized enzyme derivative was washed with cold phosphate buffer and cold water to remove unlinked enzymes that remained

Table 1 – Operation sequence of SI system for successive determination of protein and glucose (see full protocol in ESI)

No.	Operation sequence of the SI method	Remark
1	Aspiration of buffer and glucose solution	Incubation of glucose
2	Aspiration of 0.5 M acetate buffer pH 4.5	
3	Aspiration of stand/sample solution	
4	Aspiration of 0.5 M acetate buffer pH 4.5	
5	Dispensation of all reagents to the enzymatic column	
6	Aspiration of 0.5 M acetate buffer pH 3.2	Determination of protein
7	Aspiration of 0.1% Triton X-100	
8	Aspiration of 1×10^{-4} M TBPE	
9	Aspiration of 0.5 M acetate buffer pH 3.2	
10	Flow several process for mixing	
11	Aspiration of protein standard/sample	
12	Flow reversal process for mixing	
13	Monitoring of product	
14	Cleaning the holding coil and flow cell	Cleaning the system
15	Aspiration of 0.5 M acetate buffer pH 4.5	Determination of glucose
16	Aspiration of 5×10^{-3} M iron(II)	
17	Aspiration of 0.1 M *p*-anisidine	
18	Aspiration of 0.5 M acetate buffer pH 4.5	
19	Flow reversal for mixing	
20	Aspiration of peroxide solution from the enzymatic column	
21	Flow reversal for mixing of reagents	
22	Monitoring of product	
23	Washing the holding coil, flow cell and enzymatic column	Cleaning the system

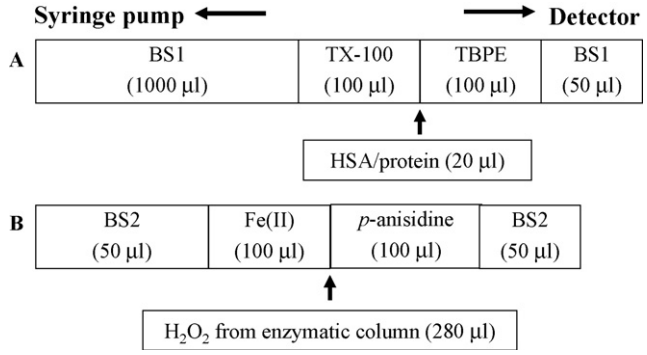

Fig. 2 – The sequence of reagents for protein and glucose determination. The concentrations of all reagents are defined in Fig. 1. (A) for protein determination, (B) for glucose determination.

on the glass beads. The immobilized glass beads were packed into a Teflon tube (4.5 cm × 2 mm). The two ends of the column were plugged with cotton filters and stored at 4 °C in water. The activity of enzyme can be kept for at least 1 month.

2.3.2. *Procedure for the successive determination of protein and glucose*

Using the manifold shown in Fig. 1, the system was filled with water as a carrier. The enzymatic column was controlled at 37 °C (temperature in human body). The home made Z-cell (10 mm path length) was connected to port#10 of a selection valve with 5 cm tubing to minimize dispersion of product zone. The auxiliary coils 1 and 2 were set to protect from waste and air flow to the flow cell and the enzymatic column, respectively. Sequences for SI operation are summarized and illustrated in Table 1 and Fig. 2.

To start the glucose determination process, 20 μL of 0.5 M acetate buffer solution of pH 4.5 (BS2), 280 μL of glucose standard solution or sample and 50 μL of 0.5 M acetate buffer solution (pH 4.5) were dispensed to the enzymatic column through port#2 for incubation during the protein analysis process. The protein determination started with aspirating the following into the holding coil (Fig. 2A): 1000 μL of 0.5 M acetate buffer solution of pH 3.2, 100 μL of 0.1% Triton X-100, 100 μL of 1×10^{-4} M TBPE and 50 μL of 0.5 M acetate buffer solution of pH 3.2. Flow reversal was made to promote mixing of the reagents via the flow cell port of the selection valve. Then, the standard human serum albumin (HSA) or sample solution was inserted into the micelle mixture solution. The blue color product zone that occurred after the second-flow reversal process was transferred to detection unit for absorbance monitoring at 607 nm. At the end of this process, the system was washed with water. Then, the glucose determination step restarted again by aspirating 0.5 M acetate buffer (pH 4.5), 5×10^{-3} M iron(II) and 0.1 M *p*-anisidine solutions as the sequence in Fig. 2B. Flow reversal was made before inserting the peroxide produced from the enzymatic column into the center of mixture. The red product formed was then transported to the detector.

3. Results and discussion

3.1. *Detection reactions*

For protein, as proposed by Sakai et al. for the micelle extraction of TBPE-protein into Triton X-100 at pH 3.0 [16], the color development occurs according to the following Eqs. (1) and (2).

$$\underset{\text{Yellow}}{\text{TBPE}\cdot\text{H}} + \underset{\text{colorless}}{\text{TX-100}} \rightleftharpoons \underset{\text{Yellow}}{(\text{TBPE}\cdot\text{H})_m} \quad (1)$$

The protein in acid solution (HSA^{x+}) would be associated into the micelle:

$$x\underset{\text{Yellow}}{(\text{TBPE}\cdot\text{H})_m} + \text{HSA}^{x+} \rightleftharpoons \underset{\text{Blue}}{(\text{HSA}^{x+}\cdot(\text{TBPE}^-)_x)_m} + x\text{H}^+ \quad (2)$$

The maximum absorption wavelength of the TBPE–protein associate was found to be at 607 nm.

The detection reactions for glucose determination by the enzymatic method are as follows:

$$\text{D-glucose} + \text{H}_2\text{O} + \text{O}_2 \xrightarrow{\text{GOD}} \text{D-glucono-1, 4-lactone} + \text{H}_2\text{O}_2 \quad (3)$$

$$\text{H}_2\text{O}_2 + p\text{-anisidine} \xrightarrow{\text{Fe(II)}} \text{Red color product} + \text{H}_2\text{O} \quad (4)$$

GOD promotes the oxidation of D-glucose by molecular oxygen to D-glucono-1,4-lactone [25]. Hydrogen peroxide is produced simultaneously. The hydrogen peroxide obtained from the oxidation of glucose oxidizes *p*-anisidine to a red color compound in the presence of iron(II) used as a catalyst.

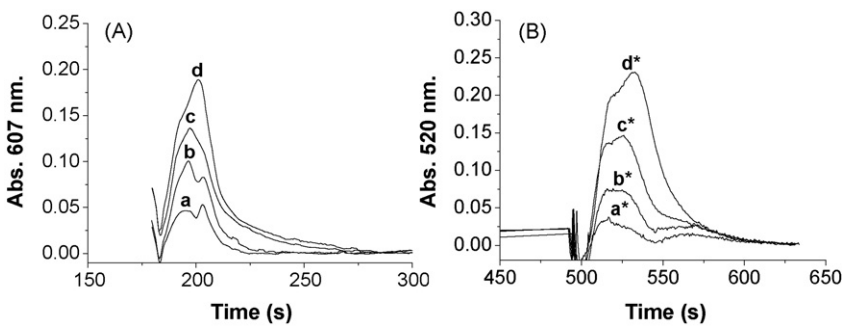

Fig. 3 – Peak profiles due to (A) protein, HSA: (a) blank, (b) 0.5 mg dL^{-1}, (c) 1.0 mg dL^{-1}, (d) 2.0 mg dL^{-1}; (B) glucose: (a*) blank, (b*) 1.8 mg dL^{-1}, (c*) 5.4 mg dL^{-1}, (d*) 12.6 mg dL^{-1}.